

**A STUDY OF THE DECAY OF BROMINE ISOTOPES**

**SIDDHARTHA RAY**

A Study of the decay of Bromine Isotopes

A thesis submitted to the Faculty of Graduate Studies and Research in partial fulfillment of the requirements for the degree of Master of Science.

August, 1968

Siddhartha Ray  
Foster Radiation Laboratory  
McGill University  
Montreal

## ABSTRACT

The decays of  $\text{Br}^{75}$  and  $\text{Br}^{74}$  to  $\text{Se}^{75}$  and  $\text{Se}^{74}$  respectively. The gamma spectra were studied with a 25 c.c. Ge(Li) detector while the beta rays were measured with a 5 mm Si(Li) detector. In the positron decay of  $\text{Br}^{75}$ , Fermi-Kurie plots revealed five prominent beta branches with endpoint energies 1.72, 1.59, 1.45, 1.34 and 1.13 MeV. Only the branch with the endpoint energy 1.72 MeV has been reported before. Following the decay of  $\text{Br}^{75}$ , seven gamma rays with energies 111.8, 140.9, 286.5, 292.9, 377.3, 427.9 and 431.6 keV were observed. Only the 286.5 keV line has been reported previously. Different gamma-gamma and gamma-beta coincidence measurements have led to the construction of the most probable decay scheme. For the coincidence experiments, a fast-slow system was set up using standard ORTEC modules. It was observed that  $\text{Br}^{74}$  positron decays to two excited states in  $\text{Se}^{74}$  with relative branching ratios 3:1. Two gamma rays at energies 633.9 and 732.1 keV were observed. The latter was observed for the first time. The results were discussed in terms of recent nuclear models for anomalous coupling nuclei in this mass region. A 107 keV isomeric transition was observed. Its origin was determined and its multipolarity measured.

ACKNOWLEDGEMENTS

I must thank Dr, S.K.Mark, who suggested and directed this research, thfar his constant help, guidance and encouragement in this work. He is also to be thanked for his help in the design of the "Mini-chamber" and the drafting of this thesis.

I must also thank Dr. J.N.Me, who actively participated in this research and wrote several essential programs for the analysis of the experimental data. He also assisted in the preparation of many of the drawings for this thesis.

Mr. S.Muszynski helped me in the initial stages of the experiment. Thanks are also due to Mr. K.S.Kuchela, who wrote a program for the PDP-8 computer which simplified the data analysis considerably. He was always at hand whenever there was any problem with the PDP-8 computer.

The financial assistance from the laboratory is also acknowledged.

CONTENTS

	Page
Abstract	i
Acknowledgements	ii
List of Illustrations	v
Chapter I-Introduction	1
Chapter II - Instruments and their Calibrations	5
2.1 The Ge(Li) detectors and their efficiency	5
2.2 The Si(Li) detectors and the "Mini-chamber"	17
2.3 Electronics	22
Chapter III- Gamma ray measurements on the decay of Br <sup>75</sup>	28
3.1 History	28
3.2 Source preparation	28
3.3 The Gamma rays	33
3.4 Coincidence measurements	43
Chapter IV - Beta rays from Br <sup>75</sup>	56
4.1 History	56
4.2 Target preparation	57
4.3 Positron spectrum from Br <sup>75</sup>	58
4.4 Beta-gamma coincidence studies	61
Chapter V - Construction of the decay scheme of Br <sup>75</sup>	64
5.1 A summary of previous works	64
5.2 Construction of the decay scheme	66

	Page
Chapter VI - Spins, Parities and Theoretical Discussions	79
6.1 Spins and Parities of the levels of Se <sup>75</sup>	79
6.2 Theoretical Discussions	85
Chapter VII- The 107 keV gamma ray	88
7.1 Introduction	88
7.2 Study of production threshold and yield	89
7.3 Study of (p,2n) reaction on natural Selenium	92
7.4 Conversion Electrons from the 107 keV level	94
Chapter VIII - Gamma rays from Br <sup>74</sup>	99
8.1 Introduction	99
8.2 History of previous works	99
8.3 Gamma rays from the decay of Br <sup>74</sup>	100
Chapter IX - Summary	105
Appendix	108
Bibliography	114

List of Illustrations

Figure No	Page
2.1	13
2.2	13
2.3	14
2.4	15
2.5	16
2.6	23
2.7	24
2.8	27
3.1	32
3.2	36
3.3	37
3.4	38
3.5	39
3.6	40
3.7	41
3.8	42
3.9	48
3.10	49
3.11	50
3.12	51
3.13	52
3.14	53
3.15	54

Figure No.	Page
3.16	55
4.1	60
4.2	63
5.1	65
5.2	75
5.3	76
5.4	77
5.5	78
6.1	84
7.1	91
7.2	98
8.1	104
A.1	113

CHAPTER I  
-----

Introduction  
-----

It has long been known that low-lying anomalous coupling states in medium odd mass nuclei cannot be explained by the simple nuclear shell model. Anomalous coupling occurs in nuclei with  $Z$  or  $N = 43, 45$  or  $47$ . Odd mass nuclei in this region have their protons or neutrons filling the  $1g_{9/2}$  shell and often exhibit low-lying states with spins and parities of  $\frac{5}{2}^+$ ,  $\frac{7}{2}^+$  and  $\frac{9}{2}^+$ . They can be explained on the basis of the multi-particle configuration  $(1g_{9/2})^{3,5,7}$ . (Goldhaber et al, 1951). This approach, however, encounters serious difficulties in explaining the ordering of these states. On the basis of this formalism, the state with the spin  $\frac{9}{2}^+$  should lie lower in energy than the other two with spins  $\frac{5}{2}^+$  and  $\frac{7}{2}^+$ , and this is often contrary to the experimental observations. Using the BCS theory which takes into account the strong pairing effects of the nucleons, Kisslinger et al (Kisslinger et al, 1963) have performed calculations on these nuclei. The different states of the nuclei were treated as different modes of couplings between a vibrating even-even core and a  $1g_{9/2}$ -shell quasi-particle. The core was assumed to be in  $0, 1, 2, 3$  etc. quadrupole phonon states. This model also predicts the lowest positive parity state to be a  $\frac{9}{2}^+$ , corresponding to a single  $1g_{9/2}$ -quasi-particle

coupled to the core in a 0 phonon state. The next group of positive parity states should come about 500 keV higher with spins  $\frac{5}{2}^+ \leq J \leq \frac{13}{2}^+$ , resulting from the coupling of the one  $2^+$  phonon core to the  $1g_{9/2}$ -quasi-particle. In their calculations there is no way in which the phonon multiplet levels can be pulled below the  $\frac{9}{2}^+$  state.

Calculations by Ikegami and Sano (Ikegami et al, 1966) have improved upon Kisslinger and Sorensen's method by taking into account all positive parity single quasi-particle states instead of the  $1g_{9/2}$ -shell only. This pulled the phonon multiplets closer to the  $\frac{9}{2}^+$  state. Talmi and Kisslinger have shown that in the shell model the state with spin  $J=j-1$  and seniority three of the  $j^3$  configuration is particularly lowered by the residual interactions. Although this is an attractive suggestion for the explanation of the low-lying  $\frac{7}{2}^+$  states, this does not account for the low-lying  $\frac{5}{2}^+$  states. Moreover, the energy of this  $(g_{9/2})^3 \frac{7}{2}^+$  state would still be too high. Goswami et al (Goswami et al, 1966) have shown that this close occurrence of quasi-particles and phonon levels can be explained by taking into account three quasi-particle interactions in Kisslinger and Sorensen's formalism.

$\text{Se}^{75}$  is a typical nucleus in this region lying in the beginning of the  $1g_{9/2}$  shell. Its study would be of great interest from both theoretical and experimental points of view. The ground state spin has been measured to be  $\frac{5}{2}^+$  (Lindgreen, 1964). The only other available information

about this nucleus is that it has a strong 285 keV gamma transition. An attempt was made to determine the positions of the excited states and the corresponding spins and parities with the hope that this added information would facilitate theoretical studies in this extremely interesting region.

The excited levels of  $\text{Se}^{75}$  were populated through the positron decay of the ground state of  $\text{Br}^{75}$ . The gamma rays emitted subsequent to this positron decay were studied with a 25 c.c. Ge(Li) detector. Gamma-gamma coincidence experiments were performed using NaI(Tl) and Ge(Li) detectors. The positron spectrum was studied with Si(Li) detectors and Fermi-Kurie plots were constructed. Beta-gamma coincidence experiments were also carried out. For beta spectrometry and beta-gamma coincidence measurements, a special chamber for housing the Si(Li) detectors were designed and constructed. This chamber, christened the "Mini-chamber", will be described in Chapter II in great details.

Gamma ray intensity measurements yielded the gamma and beta branching ratios and the  $\log (ft)$  values of the beta transitions. These enabled the construction of the level scheme of  $\text{Se}^{75}$  and also the assignment of tentative spins and parities to the different levels.

While studying the decay of  $\text{Br}^{75}$ , an isomeric state of 107 keV with a half life of  $4.6 \pm 0.5$  mins. was

observed. This state was identified by means of threshold and yield measurements to be first excited state of  $\text{Br}^{77}$ , which has already been reported. Internal conversion coefficient measurements were done for this line and the multipolarity of the electromagnetic transition was identified.

The gamma rays from the decay of  $\text{Br}^{74}$  were also studied. Two gamma rays of energies 633.9 and 732.1 keV were observed with a half life of  $42 \pm 4$  mins. The first gamma ray has been observed previously, but the 732.1 keV line has not been reported before. The relative intensities of the two gamma rays were also determined.

CHAPTER II  
-----Instruments and their Calibrations  
-----2.1 The Ge(Li) Detectors and their efficiency  
-----

In the past few years, great efforts have been directed towards the development of semiconductor radiation detectors (Goulding, 1966; Mayer, 1966). These detectors, employing direct collection of ionization in the semiconductor material, possess one striking fundamental advantage over other radiation detectors such as scintillation counters. In single crystal semiconductors such as Germanium and Silicon, the average energy required to produce an electron-hole pair is about 3 eV, which is about 35 times smaller than (Houdayer, 1968) the amount of energy required to produce one photoelectron in a good NaI(Tl) scintillation detector. Consequently, the statistical fluctuations in the number of charges produced by a radiation in a semiconductor detector is much smaller, hence, better energy resolution.

There are two types of semiconductor detectors currently used in nuclear spectroscopic studies; the Lithium drifted Silicon Si(Li) detector and the Lithium drifted Germanium Ge(Li) detector. Because of its small photoelectric absorption cross-section, the silicon detector is good for

low energy ( $< 50$  keV) gamma rays and charged particle (electron and positron) detection. On the other hand, the germanium detector has a larger photoelectric absorption cross-section and hence it is more suited for gamma ray studies. Because of the small amount of energy required to liberate an electron-hole pair in semiconductor detectors they must be operated at low temperatures (normally at liquid nitrogen temperature  $77^{\circ}$  K) to minimize the thermal noise in the detector.

In the present work, two Ge(Li) detectors have been used for gamma ray studies. The first one was supplied by the RCA Victor Company (Model SJGG-2-40) with a depletion depth of 2 mm. This detector was used in preliminary studies. The detailed characteristics of this have been described in great lengths by Lessard (Lessard, 1966). The other detector, which was acquired last year, is a co-axial Ge(Li) detector. It was supplied by the Nuclear Diode Corporation of Chicago (Model L-247). The detector is mounted on the cold finger of a liquid nitrogen cryostat in an upright geometry. The nominal volume of the detector is 25 c.c. and the cross-sectional shape is trapezoidal with an area of  $10.8 \text{ cm}^2$ . The active area is  $9.6 \text{ cm}^2$  and the length is 26 mm. The top view of the detector is shown in Fig. 2.1 while the side view is shown in Fig. 2.2. The whole detector is vacuum encapsulated in an aluminium can of wall thickness 20 mil. The intrinsic side of the detector is facing up and is 16

1 mm from the cap. The advantage of having the intrinsic side facing up is that this side of the detector has a very thin ( $\sim 20$  microns) dead layer of germanium so that low energy gamma rays would have minimum attenuation when they enter the detector from the top, while the other sides of the detector have a dead layer of germanium of about 400 microns, which has a sizeable attenuation on low energy gamma rays. When the detector is in operation, it is under a voltage bias of -2000 volts for charge collection. Since the detector is only 16 mm below the aluminium cap, a teflon bar 9 mm wide and 5 mm thick has been inserted between the detector and the cap to prevent electrical breakdown.

The charges collected in the detector are fed into a low-noise charge sensitive pre-amplifier (Tennelec model TC 135L). The entire detector assembly, including the pre-amplifier, gives an energy resolution at full-width-half-maximum (FWHM) of 2.9 keV on the 1.33 MeV  $\text{Co}^{60}$  gamma ray and of 2.0 keV on the 122 keV  $\text{Co}^{57}$  gamma ray.

When a gamma ray enters a detector, it may pass through the detector without losing any of its energy or lose part of its energy via Compton scattering or be absorbed completely by photoelectric effect. The second type of event gives a continuous pulse height distribution, while the last type of event results in a well defined peak in the pulse height spectrum.

Before the detector may be of great use in

gamma ray measurements, its photoelectric (or photopeak) efficiency for gamma rays of different energies must be known. The efficiency calibration of the 2 mm detector at different geometries has already been done in this laboratory (Lessard, 1966). The calibration curves are shown in Fig. 2.3. However there is no calibration for the 25 c.c. detector and this must be carried out before the detector can be used for gamma ray intensity measurements.

Different source-detector geometries which were used in later experiments have been used to obtain these curves. There are two different methods by which these can be done. One method is to use the known efficiencies of a standard NaI(Tl) detector. It requires the recording of different gamma ray spectra by both the Ge(Li) detector at the desired geometry and the NaI(Tl) detector at a fixed geometry. The efficiency of NaI(Tl) detectors is accurately known for different geometries and so by comparing the gamma ray spectra obtained in the two detectors we can construct the efficiency against the energy calibration curve for the Ge(Li) detector. This method is used only when the strengths of the gamma ray sources used for calibration are not known.

The second method utilises gamma ray sources whose strengths are already calibrated. The NaI(Tl) detector is no longer necessary as a comparison standard and in a way makes calculations much easier. The procedure consists

of calculating the number of disintegrations per second of the standard source at a particular geometry with respect to the detector and then computing the area under the photopeak for the particular gamma ray desired. The ratio of these two quantities gives the photopeak efficiency of the detector at that particular gamma ray energy and geometry.

The standard sources used are listed below in Table 2.1. They were obtained from New England Nuclear Corporation, Boston.

Table 2.1

Standard Gamma Ray Sources

Sources	Mode of decay	Photopeak energies
1. Co <sup>57</sup>	Electron capture	1. 122 keV 2. 136 keV
2. Co <sup>60</sup>	Electron decay	1. 1.17 MeV 2. 1.33 MeV
3. Mn <sup>54</sup>	Electron capture	1. 835 keV
4. Cs <sup>137</sup>	Electron decay	1. 662 keV
5. Na <sup>22</sup>	Electron capture & Positron decay	1. 511 keV 2. 1.27 MeV
6. Ba <sup>133</sup>	Electron capture	1. 53 keV 2. 81 keV

-----  
 Table 2.1 (contd.)  
 -----

Source	Mode of decay	Photopeak energies
-----		
6. Ba <sup>133</sup>	(contd.)	3. 160 keV
		4. 223 keV
		5. 277 keV
		6. 303 keV
		7. 356 keV
		8. 384 keV
-----		

Both Mn<sup>54</sup> and Cs<sup>137</sup> have one gamma ray each. So for either of these two sources, all that is to be done is to calculate the total number of disintegrations per second at the time of the measurement and then compare it with the area of the photopeak.

Na<sup>22</sup> decays to Ne<sup>22</sup> by both positron decay and electron capture, the former contributing to 90% of the decay. The 511 keV line comes from the fact that every positron when annihilated gives rise to two 511 keV gamma rays. So the total number of 511 keV gamma rays emitted is twice the number of 90% of the disintegrations taking place per second. For the 1.27 MeV line the calculations are straightforward.

Both  $\text{Co}^{57}$  and  $\text{Co}^{60}$  have complicated decay schemes but all the branching ratios are well known (Lederer, et al, 1967) and the contribution to each gamma ray can be calculated.

$\text{Ba}^{133}$  is one of the most useful standard sources for efficiency calibration in the range 30-400 keV. (Gurfinkel et al, 1967).  $\text{Ba}^{133}$  nucleus decays via electron capture to the excited states of  $\text{Cs}^{133}$ . The depopulation of the  $\text{Cs}^{133}$  energy levels to the ground state via different cascades gives rise to nine different gamma rays. In addition to these, there are two relatively intense  $K\alpha_1$  and  $K\beta_1$  X-rays emitted following the electron capture process. The relative intensities as well as the number of photons per 100 disintegrations for each of the gamma rays are presented in Table 2.2. The 81 keV peak is actually composed of the 79.6 and the 81.1 keV gamma rays which were not resolved. So in the Table we have in all eight gamma rays.

Table 2.2\*

-----  
 Relative Strengths of Gamma Rays from a Ba<sup>133</sup> source  
 -----

\*( Table taken from Gurfinkel et al,1967)

Photon energy keV	Intensity Relative to 356 keV	Intensity Absolute photons per 100 disint.
30.8 ± 0.18	129.0 ± 9.0	66.7 ± 8.7
35.2 ± 0.18	33.9 ± 2.3	17.5 ± 2.4
53.4 ± 0.25	3.7 ± 0.09	1.9 ± 0.22
81.1 ± 0.26	64.7 ± 4.2	33.5 ± 4.3
160.5 ± 0.27	1.2 ± 0.05	0.62 ± 0.074
223.2 ± 0.45	0.8 ± 0.042	0.41 ± 0.051
276.5 ± 0.32	11.6 ± 0.17	6.0 ± 0.67
303.0 ± 0.63	29.7 ± 0.29	15.3 ± 0.17
356.3 ± 0.48	100	51.7 ± 5.7
384.1 ± 0.42	14.1 ± 0.26	7.3 ± 0.82

-----

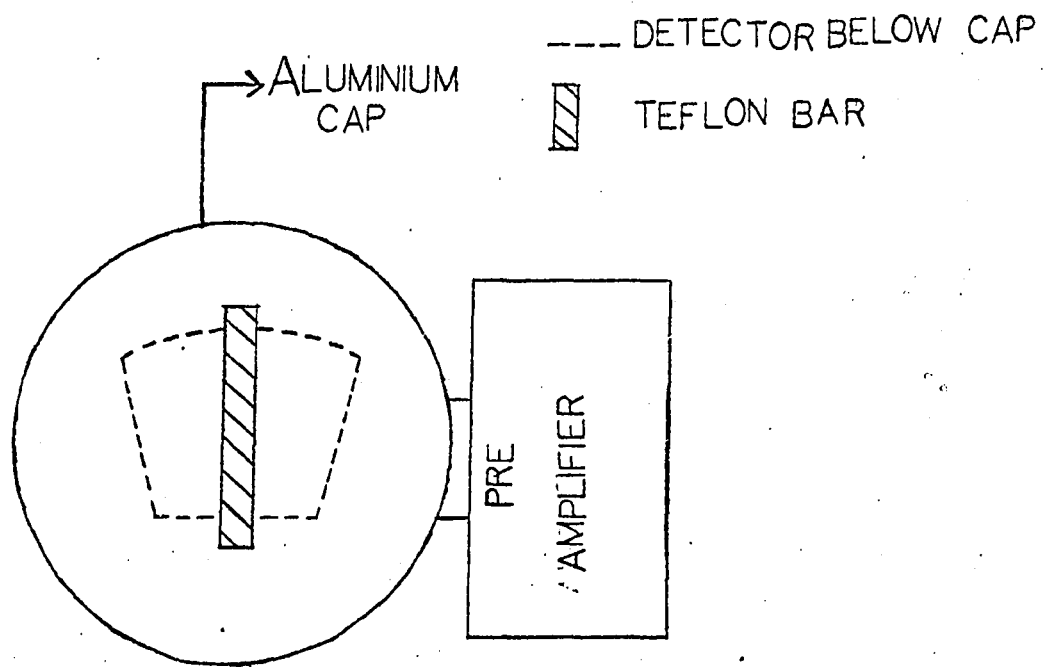
Errors could have been introduced by the uncertainty in the reproducibility of the source-detector geometry. However the standard sources used are all encapsulated in standard containers. To keep the geometry fixed a suspender was attached rigidly to the side of the

Figure 2.1- Top view of the 25 c.c. co-axial  
Ge(Li) detector

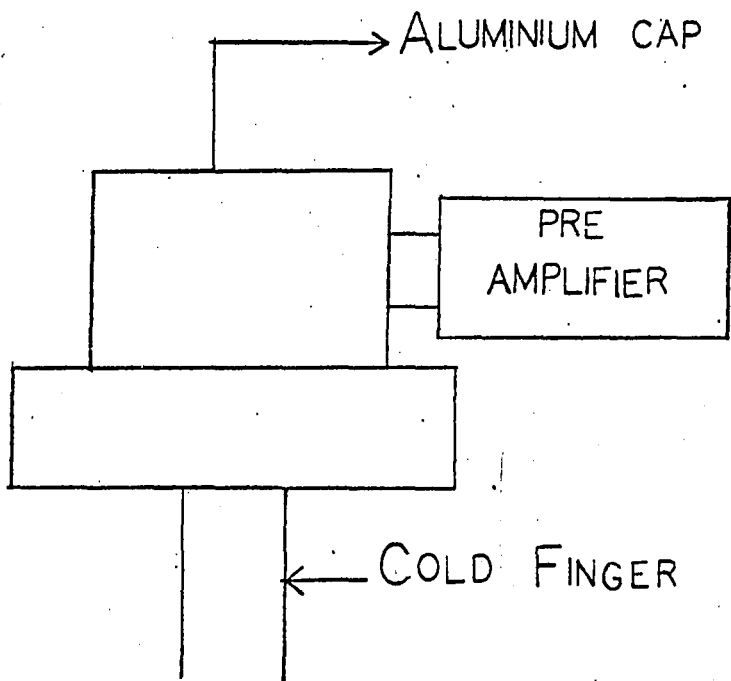
Figure 2.2- Side view of the 25 c.c. co-axial  
Ge(Li) detector

FIGURE 2.1

FIGURE 2.2



2.1



2.2

Figure 2.3- Relative Photoefficiency of the  
2 mm (SJGG-2-40) Ge(Li) detector

FIGURE 2.3

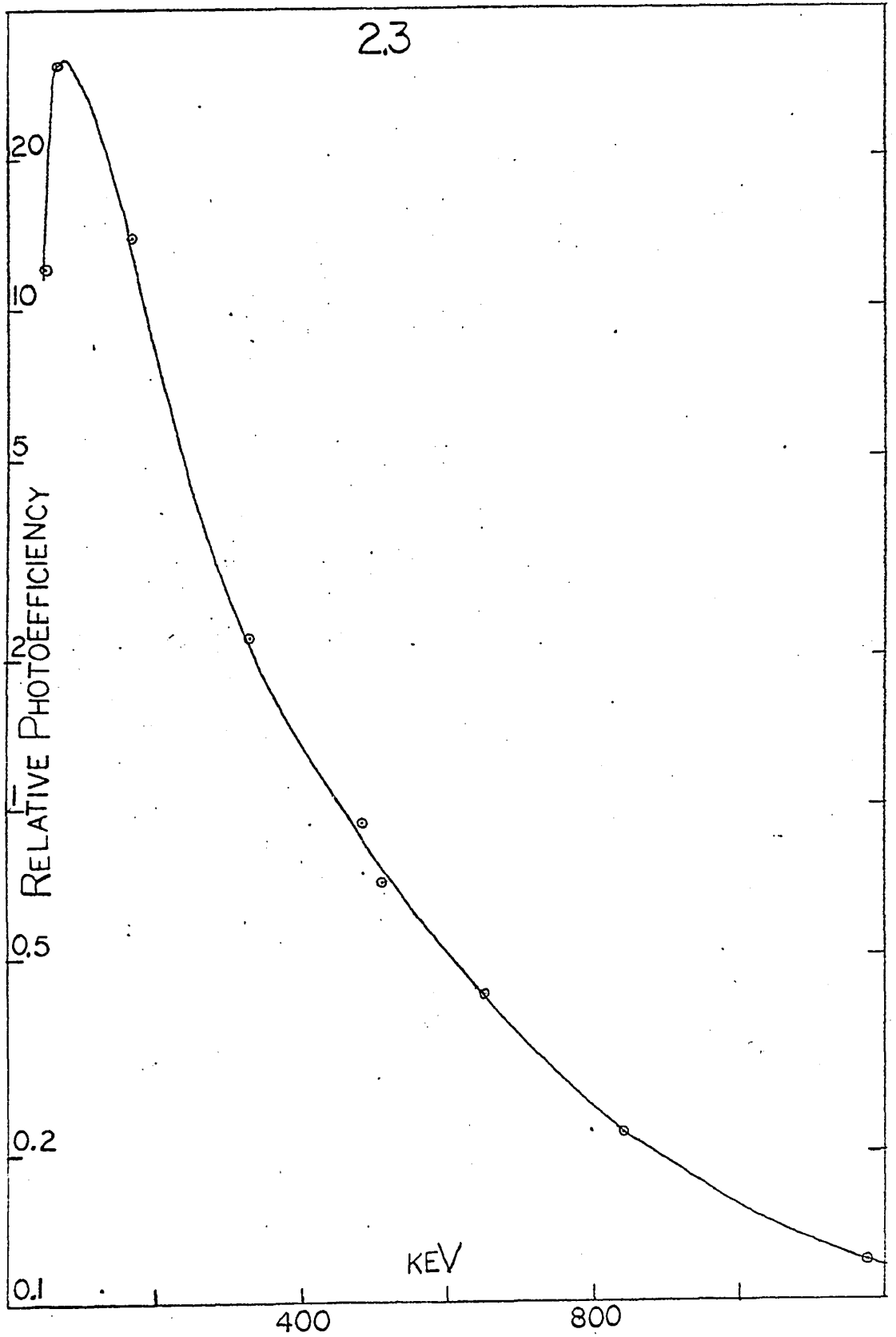


Figure 2.4- Absolute Photoefficiency of the  
25 c.c. (L-247) Ge(Li) detector  
Source placed vertically above the  
detector.

A.- Source-Capsule distance = 1 cm.

B.- Source-Capsule distance = 20 cm.

FIGURE 2.4

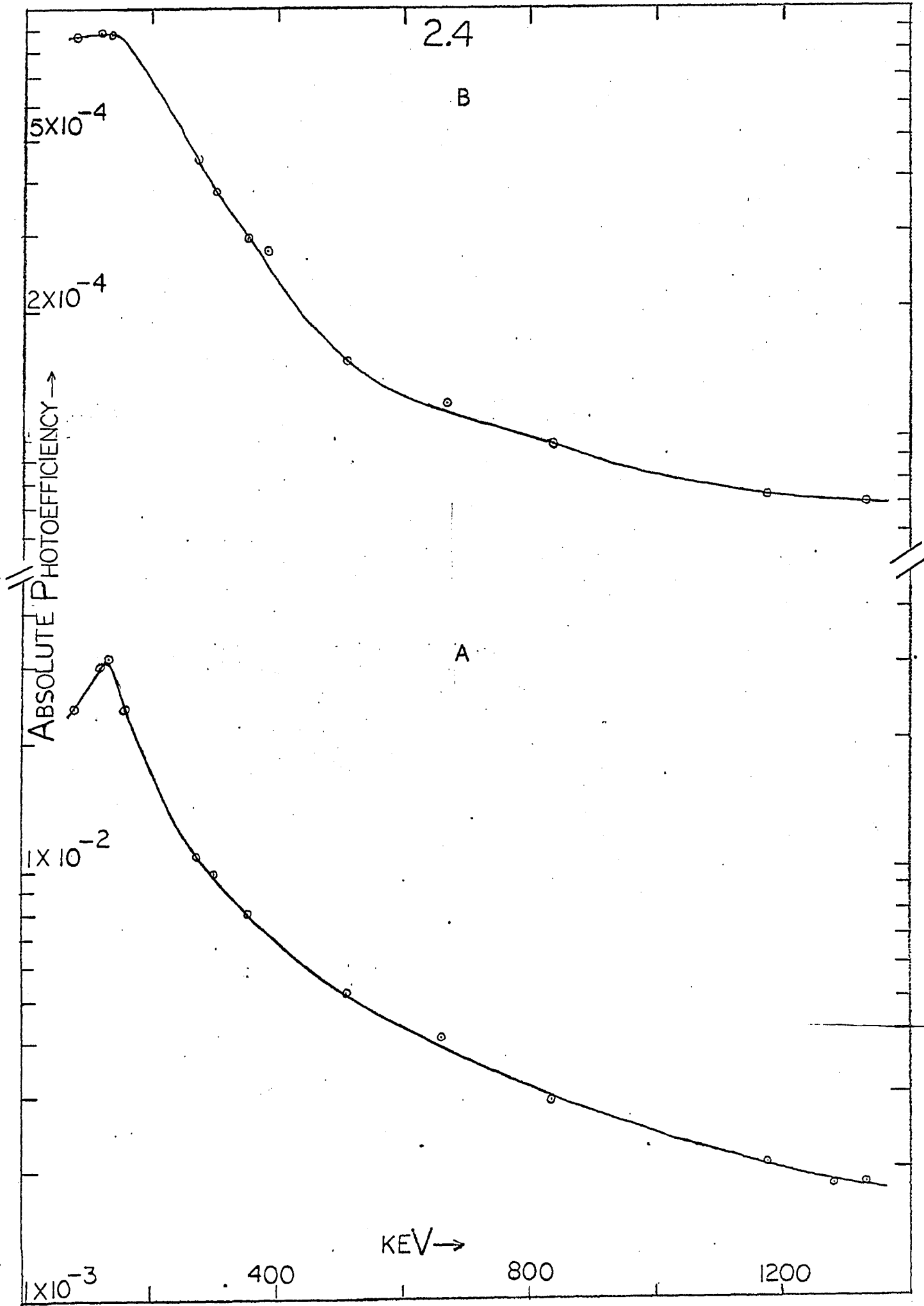
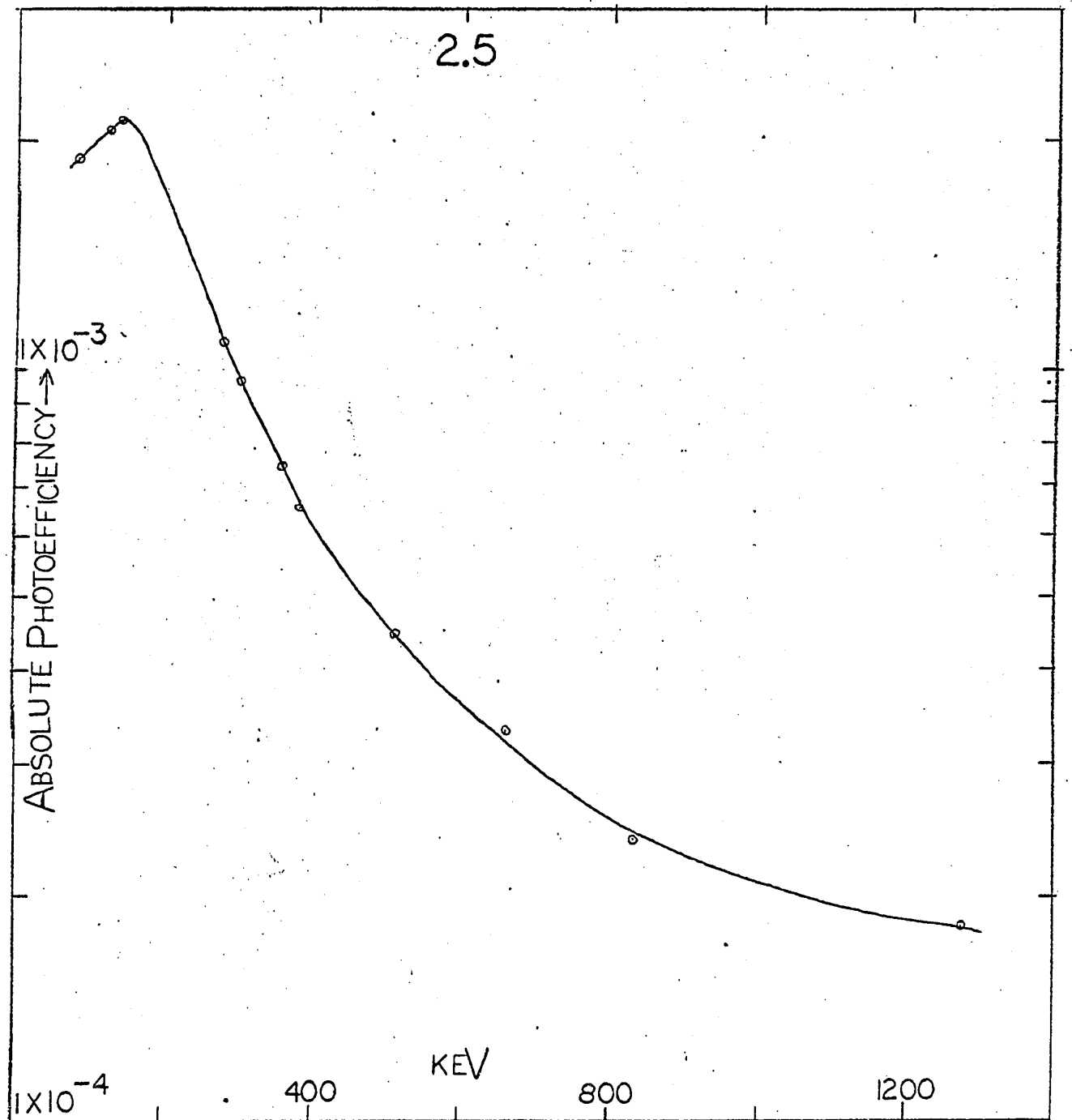


Figure 2.5- Absolute Photoefficiency of the  
25 c.c. (L-247) Ge(Li) detector.  
Source facing the curved surface  
of the detector at a distance of  
11 cm. from the axis. ( This is  
the geometry used in the internal  
conversion coefficient measurement)

FIGURE 2.5



Ge(Li) detector and the standard sources were always placed at a marked fixed position. In any event it is believed that the error introduced in this way is much less than that by the inherent uncertainty ( $\sim 10\%$ ) in the strengths of the standard sources. Thus the results of the photopeak efficiency calibration are at best accurate to about 10%.

The efficiencies were determined for three different distances and configurations with respect to the detector. The calibration curves are shown in Figs. 2.4 and 2.5.

## 2.2 The Si(Li) detectors and the "Mini-chamber"

Si(Li) detectors were used for electron and positron measurements. These were supplied by the SIMTEC Ltd. Montreal. For studying the positron spectrum, a 5 mm Si(Li) detector (SIMTEC model K14) was used. It can stop beta particles of energies upto 2.3 MeV. For the work described here, this detector is thick enough to stop the most energetic electrons and positrons encountered. Although the Si(Li) detectors have usually negligible photopeak and moderate Compton scattering efficiencies for gamma rays, the photoefficiency increases with the increase of the volume of the detector. For the 5 mm detector, the photoefficiency for lower energy ( $\leq 100$  keV) gamma rays is sufficiently high to interfere a great deal with the accuracy of low

energy electron measurements. Since the electrons produced by internal conversion in nuclear electromagnetic transitions are of low energies, the 5 mm detector is not suitable for their measurements, particularly if the source emits low energy gamma rays. For this reason, a 1 mm Si(Li) detector (SIMTEC model K11) was used for internal conversion electron measurements.

For the best performance, the detector should be operated in vacuum and cooled to liquid nitrogen temperature., exactly like Ge(Li) detectors which are used for gamma ray detection. However gamma ray detectors are encapsulated in small evacuated casings while at the same time being cooled with the help of a highly conducting metal, the so called "cold finger", running deep inside a liquid nitrogen tank. The gamma rays are placed outside the capsule which is usually made of thin aluminium. This is possible only because the gamma rays suffer negligible attenuation while passing through the thin aluminium window. However charged particles have far less penetrating power than gamma rays and hence very thin aluminium windows would attenuate the charged particles considerably, especially if the energy is low. For this reason, the charged particle source as well as the detector have to be kept inside the same vacuum chamber with no windows between them, while at the same time maintaining the detector at liquid nitrogen temperature throughout the experiment. It is with this purpose that the

"Mini-chamber" was designed and constructed. Provisions were also made for utilising this chamber for beta-gamma coincidence experiments and internal conversion coefficient measurements.

Figs. 2.6 and 2.7 show the horizontal and the vertical cross-sections of the mini-chamber respectively. The mini-chamber essentially consists of two portions- the source compartment (1) and the detector compartment (2) which are connected through a vacuum gate (3). The source compartment is made of a brass tube of 12 cm. length and 10.5 cm. diameter. One end of it is closed with a brass flange (4) in the shape of a cup. This cup has an opening of 8 cm. and a depth of 5.5 cm. The bottom of this cup is 15 mil. thick. It protrudes into the source compartment so that a 7.6 cm. by a 7.6 cm. NaI(Tl) detector can be inserted into this opening such that the detector and the source are just separated by a thin brass window. The other side of the source compartment, as already described, is attached to the detector compartment through a vacuum gate. The source can be placed at the centre of the bottom of the cup inside the source compartment. For inserting sources, there is an opening (5) of diameter 9 cm. in the source compartment with a transparent plexiglass cover (6), so that when the source is in vacuum it can be viewed from outside. When the vacuum gate is opened to allow the detector in the detector compartment to face the source, it is necessary to prevent

any light from getting inside the chamber as the Si(Li) detector is sensitive to light. For this purpose, an aluminium cap is provided to cover the plexiglass viewing window. The entire chamber is evacuated through the pumping section (10).

The detector compartment essentially consists of three concentric cylinders. The innermost cylinder (C) is made of stainless steel, and has a length of 17.5 cm, and a diameter of 5 cm. It serves as the liquid nitrogen tank for the detector and its outer wall is silver plated. This cylinder is placed inside another stainless steel cylinder (B). These two cylinders are thermally insulated from one another and supported by teflon rings (7a & 7b). The inner wall of cylinder B is also silver plated for better heat insulation. The two cylinders B and C are fixed with respect to one another and form a thermally insulated detector assembly. The Si(Li) detector (D) is mounted on the end of cylinder C. The detector assembly slides along a triple 'O' ring vacuum seal inside the outermost cylinder A. This cylinder A is made of brass and has a diameter of 9 cm, and a length of 7.5 cm. The signal lead from the detector D is connected to a pressurized BNC connector (8) on the side of the cylinder B.

To operate the mini-chamber, the source chamber is connected to the detector chamber by lifting the vacuum gate. The whole chamber is then evacuated with the help of

a mechanical pump. The ultimate pressure obtained is less than  $10\mu$ . Liquid nitrogen is then poured into the tank (cylinder C). The silver plated surface of the two inner cylinders and the vacuum in the space between them provide an effective thermal insulation to the liquid nitrogen tank. There is a leverage mechanism by which the detector assembly can be pulled away from or pushed in towards the source as may be required. During an experiment, high geometrical efficiency is needed and as such the detector must be as close to the source as possible. When a new source is to be inserted, the detector is withdrawn and the gate is closed. Air is then allowed to enter the source compartment and the old source replaced by a new one. Since the vacuum gate is closed, the detector is maintained in vacuum. After insertion of the new source, the source compartment is pumped down again. When the pressure is low enough the vacuum gate is opened and the experiment is resumed. For fine adjustments of the source-detector distance, there is an adjustable ring stopper (9) installed at the end of the outer cylinder A. This ring stopper determines the distance through which the detector assembly may be pushed towards the source by catching another ring mounted on the outside of the cylinder B. The mini-chamber is fixed to an iron plate base and is mounted horizontally at present.

This chamber is not only useful for beta ray measurements, it can also be used for conversion coefficient

measurements and beta-gamma coincidence experiments. The thin brass window of the source compartment has negligible attenuation to gamma rays so that a gamma detector can be placed right outside this window.

In view of the 25 c.c. Ge(Li) detector we now have, the mini-chamber must be modified for use in a vertical configuration. In this position, the source would face the full active surface of the Germanium detector instead of facing the curved surface which has a much reduced efficiency. Moreover, the detector can then be brought far closer to the source than is possible with the present arrangement resulting in a great improvement of experimental geometry. This would enable more accurate measurements of internal conversion coefficients.

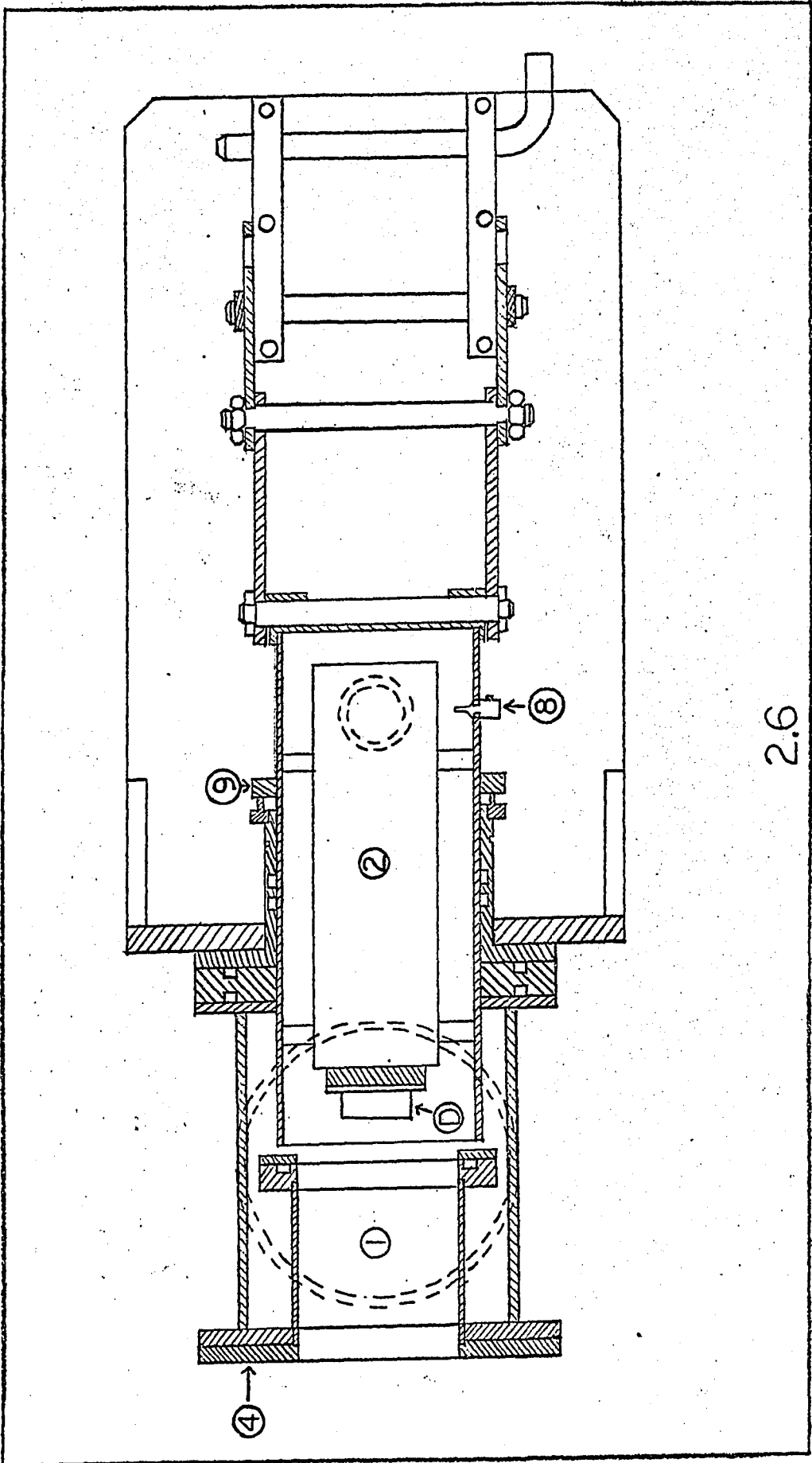
The main modification is to extend the aperture of the cup so that the Ge(Li) detector assembly (diameter 7.6 cm.) can slide up against the thin brass window. The whole mini-chamber should be mounted vertically on a rigid support. At the bottom of the support there should be a platform on which the cryostat (on wheels) for the Ge(Li) detector can be rolled up. This platform can then be raised to a proper height in order to put the gamma detector at an advantageous distance from the source.

### 2.3 Electronics

The electronics used in this work is mainly a

Figure 2.6- Horizontal Cross-section of the  
Mini-chamber. (For explanation of  
symbols, see description).

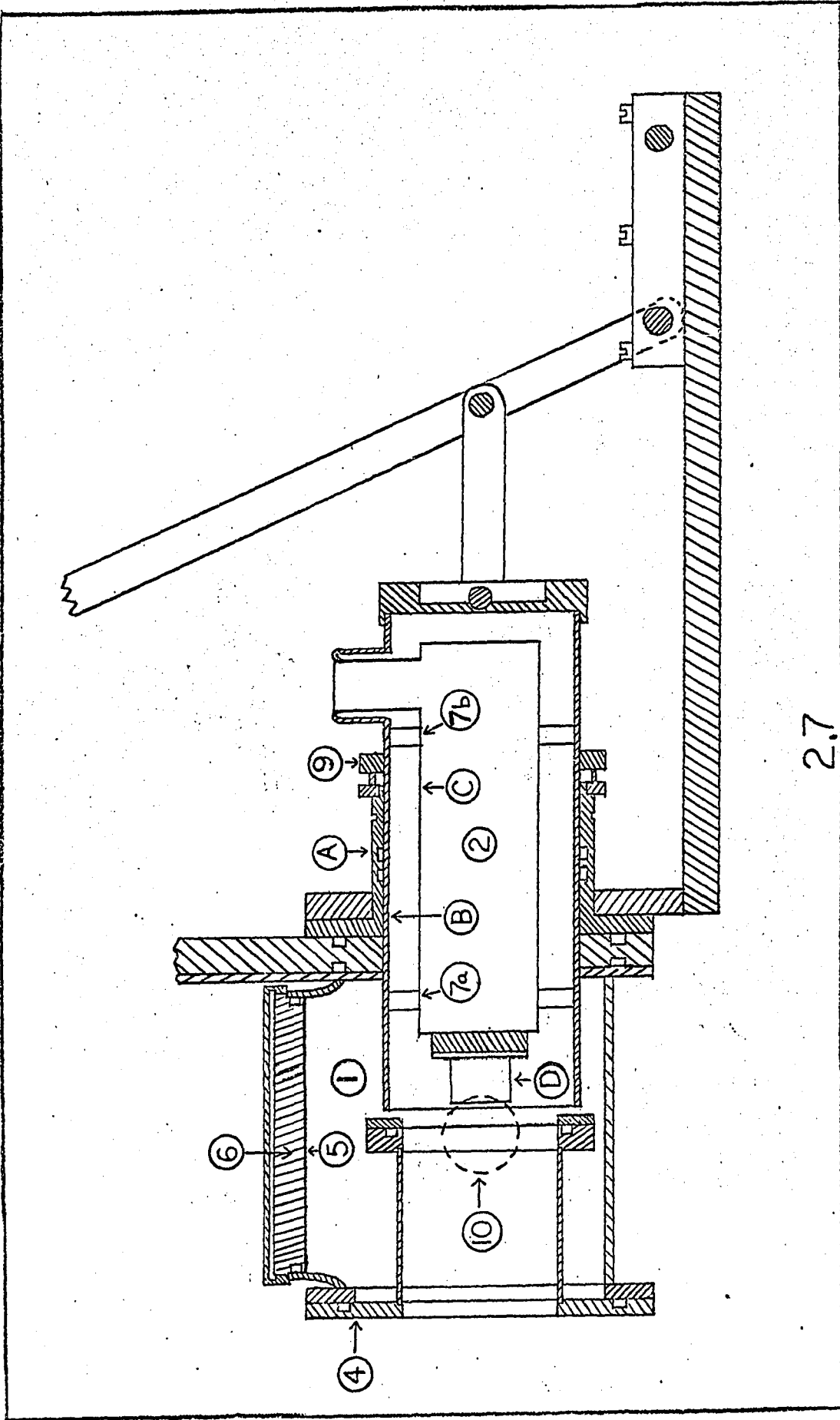
FIGURE 2.6



2.6

Figure 2.7- Vertical Cross-section of the  
Mini-chamber. (For explanation of  
symbols, see description).

FIGURE : 227



2.7

general fast-slow coincidence set up as shown in Fig. 2.8. The building blocks of the set up are the commercially available standard AEC-NIM modules purchased from ORTEC and Canberra Industries Corporations. It basically consists of two coincidence systems; the fast coincidence system with a resolving time in the nanosecond ( $1 \text{ ns.} = 10^{-9} \text{ sec.}$ ) range and the slow coincidence system with a resolving time in the microsecond ( $1 \text{ } \mu\text{s.} = 10^{-6} \text{ sec.}$ ) range. The former insures the time simultaneity of the two radiations detected and the latter makes sure they have the selected energies.

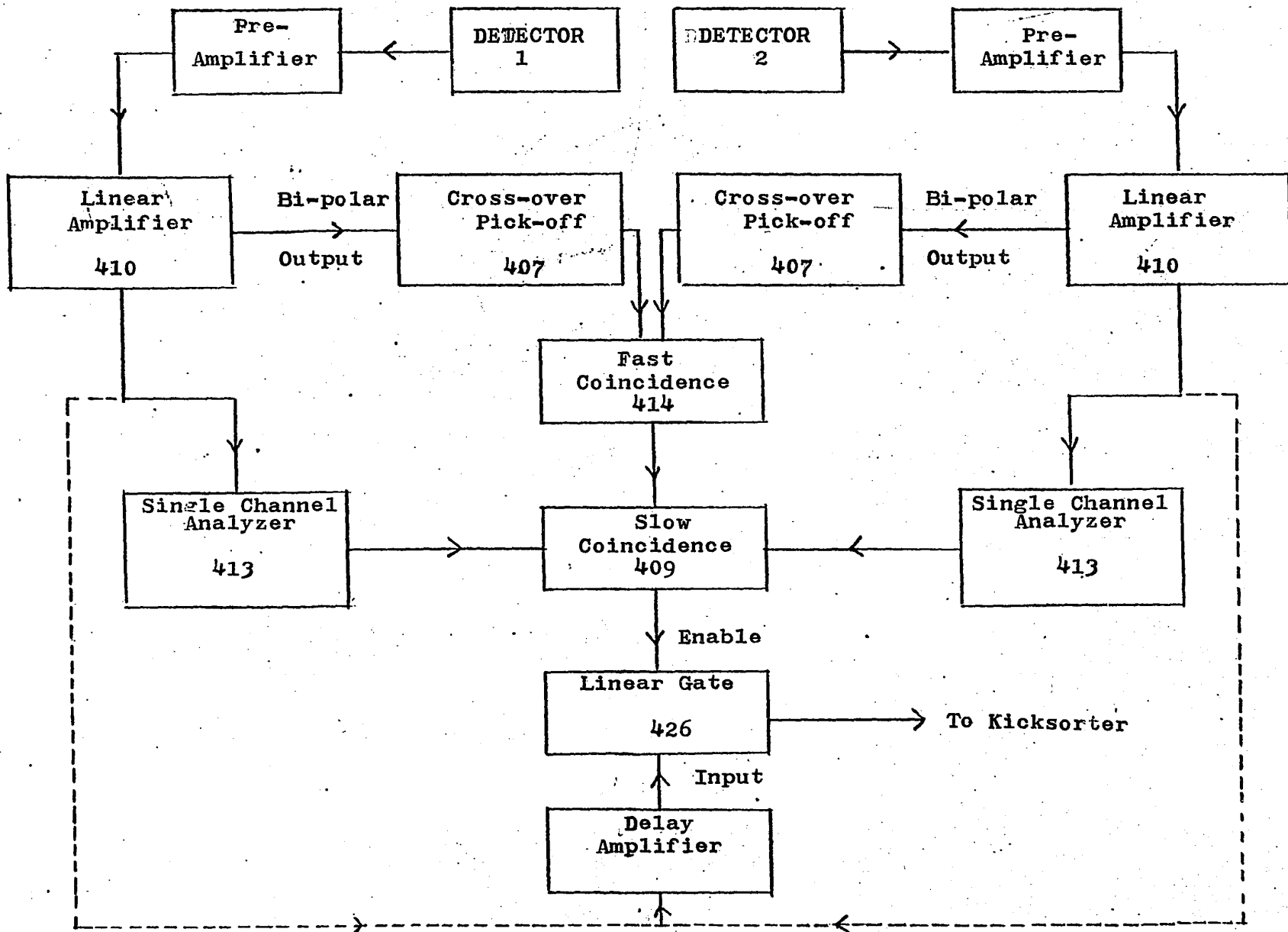
When a pair of coincident radiations strike the two detectors respectively, the two signal pulses from the detectors are fed into the respective pre-amplifiers and then to the linear amplifiers. These amplifiers shape the input signals with appropriate integration and differentiation time constants so that they have the best timing and signal to noise characteristics. The linear amplifiers provide both unipolar and bipolar pulse outputs. The bipolar pulses are fed into the two cross-over pick-off units which send out standard sharp pulses at the time when the signal pulses cross the zero base line. These outputs are then fed into the fast coincidence unit which gives an output when the input pulses arrive within a preset resolving time. The cross-over units have built in variable delay time for their outputs so that signals coming from the detectors having different time characteristics may be

put in coincidence. The unipolar outputs from the linear amplifiers are fed to the two single channel analyzers respectively. This enables the energy selection of the radiations measured by the two detectors. The outputs from the single channel analyzers together with that from the fast coincidence unit are fed to the slow coincidence unit. The logic signal output from the slow coincidence unit indicates that the time and energy characteristics of the two radiations detected. This logic signal is used to operate the linear gate for the pulses from either one of the linear amplifiers. The radiation energy analog pulses from the linear gate are fed into a pulse height analysis system,

The pulse height analysis system used here consists of an analog-digital converter (ADC, Nuclear Data Corporation, model ND-161F) interfaced with an on-line computer PDP-8. The system operates like a 4096 channel pulse height analyzer. It has a pulse height resolution of less than 0.1%. The use of this system facilitates the analysis of complicated gamma ray spectra because it has a teletype for data input and output, a large screen display incorporated with a light pen and capable of continuous display even when data accumulation is in progress, and many soft wares for computer programming are available. The details of the system may be found elsewhere (Kuchela, 1968).

Figure 2.8- Block Diagram of the fast-slow coincidence unit. The numbers in the blocks indicate ORTEC module numbers.

FIGURE 2.8



CHAPTER III  
-----

Gamma ray measurements on the decay of Br<sup>75</sup>  
-----

3.1 History  
-----

The 1.7 hour half life of Br<sup>75</sup> was first reported by Woodward et al (Woodward et al, 1948). Lobkowicz et al (Lobkowicz et al, 1961) studied the (p,n) reaction on As<sup>75</sup> by investigating the characteristics of the gamma rays emitted by the product nucleus and performing different coincidence experiments. The gamma spectrum was recorded by a 5 cm. by 5 cm. NaI(Tl) crystal. They observed gamma rays with energies 110, 135, 285, 385, 505, 615, 640 and 880 keV and a group of gamma rays between 420 and 440 keV. They did not investigate the origin of these gamma rays by measuring their half lives. Baskova et al (Baskova et al, 1962) obtained Br<sup>75</sup> by bombarding Se<sup>74</sup> enriched to 41% with deuterons. The gamma ray spectrum was investigated with a luminescent gamma spectrometer with a 100 channel analyzer. They claimed to observe two gamma rays; a strong one at 285 keV and a weak one at 620 keV. They measured the half life of the 285 keV line to be 100 + 5 mins.

3.2 Source preparation  
-----

Br<sup>75</sup> was produced in the McGill synchro-

cyclotron via the  $\text{Se}^{76}(\text{p},2\text{n})\text{Br}^{75}$  reaction. The threshold for (p,2n) reaction on  $\text{Se}^{76}$  was calculated to be 14 MeV using the semi-empirical mass formula (Seeger,1961) while that for the (p,3n) reaction was calculated to be 24.5 MeV. The following criteria are to be satisfied in choosing a proper proton energy for bombardment:

- i) The energy should be so chosen as to give a large enough cross-section for the desired reaction.
- ii) The energy must not be such that (p,3n) reactions are produced.

The energy of the internal beam is calibrated against the radius of the cyclotron and this calibration is accurate only to  $\pm 2$  MeV. So the energy of bombardment was chosen to be 20 MeV. This would give a high yield for the (p,2n) reaction without producing any product via the (p,3n) reaction.

Other reactions which could contribute unwanted activities are :-

- i)  $\text{Se}^{76}(\text{p},\text{n})\text{Br}^{76}$  reaction. The gamma rays subsequent to the decay of  $\text{Br}^{76}$  are well known and they have an extremely long half life of 16.1 hour. These lines can be easily identified and separated from those of  $\text{Br}^{75}$  by half life study.
- ii) The (p,t) reaction produces  $\text{Se}^{74}$  and the (p,2p) reaction produces  $\text{As}^{75}$ ; both are stable isotopes and so emit no subsequent gamma rays.

iii) Both the (p,d) and the (p,pn) reactions produce  $\text{Se}^{75}$ .

It has a half life of 120.4 days and is therefore no problem in this case.

iv) The  $(\text{p},\text{He}^3)$  and the  $(\text{p},\text{He}^4)$  reactions produce  $\text{As}^{74}$  and  $\text{As}^{73}$  with half lives 17.9 days and 80.3 days respectively and therefore gamma rays from them could be identified.

v) Impurities:- An enriched isotope of  $\text{Se}^{76}$  procured from the Oak Ridge National Laboratories was used for producing  $\text{Br}^{75}$ . Isotopic analysis done by the supplier gives the following breakdown:-

Se	Amount %
74	< 0.2
76	86.1 $\pm$ 0.1
77	2.0 $\pm$ 0.1
77	
78	4.4 $\pm$ 0.1
80	5.9 $\pm$ 0.1
82	1.6 $\pm$ 0.1

A spectrographic analysis also performed by the suppliers showed that the source material contained not more than 0.05% of any other element as impurities. So the relevant activities under this category are:-

a)  $\text{Se}^{77}(\text{p},2\text{n})\text{Br}^{76}$  reaction produces long lived gamma rays all of which are well known.

b)  $\text{Se}^{78}(\text{p},2\text{n})\text{Br}^{77}$  reaction is important. Although the

ground state has a half life of 57 hours it has a known isomeric state at 108 keV with a half life of 4.2 mins.

This will be discussed later on.

c)  $^{80}\text{Se} (p,2n)\text{Br}^{79}$  produces a stable isotope and thus presents no problems.

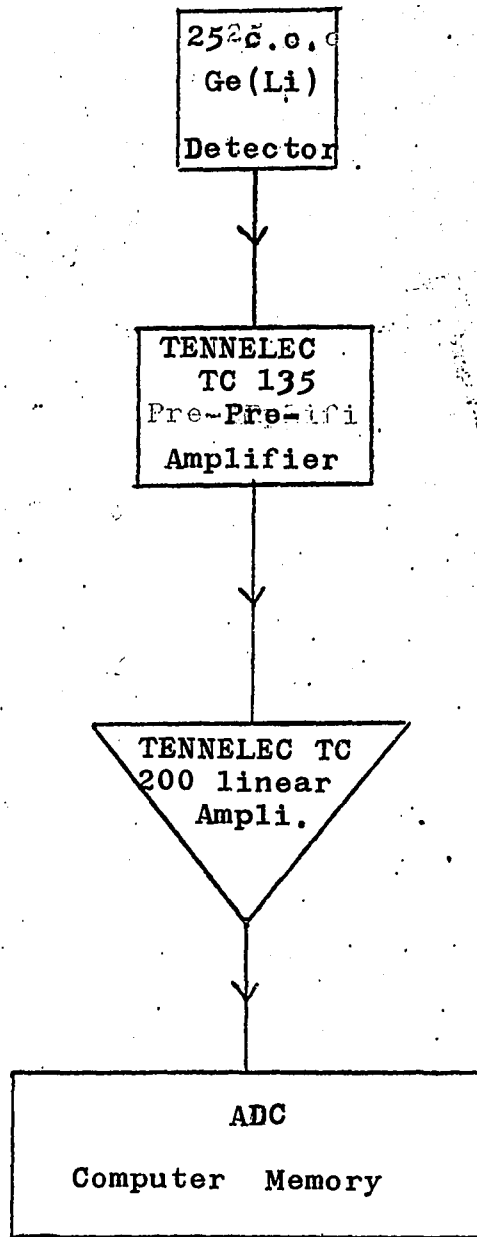
(p,n) reactions on these impurities produce isotopes all of which have been discussed above.

To identify the gamma rays from  $^{76}\text{Se} (p,2n)\text{Br}^{75}$ , half life measurements were performed. The target was prepared in coarse powder form - the same form in which the isotope was obtained. For each target about 1 mg. of isotope was wrapped up in a small aluminium foil which in turn could be attached to the target holder for internal bombardment in the cyclotron. After bombardment, which lasted normally for a period of 20 secs. at an average proton beam current of 1  $\mu\text{A}$ , the powder was transferred to another thin aluminium wrapping so that the high background activity due to the active aluminium was eliminated. The radioactive source inside the inactive aluminium (about 1 mil. thick) was then placed at a suitable distance from the detector for counting.

The set up for pure gamma ray spectrometry is shown in Fig. 3.1. The 25 c.c. Ge(Li) detector was connected to a Tennelec TC 135LFET pre-amplifier and then to a TC 200 linear amplifier. The energy analog signals were fed into the Nuclear Data ADC and then recorded in the memory of the

Figure 3.1- Set up for gamma ray spectroscopy  
with the 25 c.c. Ge(Li) detector

FIGURE 3.1



PDP-8 computer which served as a 1024 or 2048 channel kicksorter.

Initially the half life study was made with the 2 mm Ge(Li) detector connected to a Tennelec TC 130 FET pre-amplifier and then to the TC 200 linear amplifier. The output pulses were fed to a TMC model 401C kicksorter - a 400 channel pulse height analyzer.

### 3.3 The Gamma rays

At first the gamma rays from Br<sup>76</sup> produced via Se<sup>76</sup> (p,n)Br<sup>76</sup> reaction by bombarding Se<sup>76</sup> at 12 MeV were studied in order to identify the gamma rays properly in the subsequent study of the decay of Br<sup>75</sup>. Br<sup>75</sup> was then produced by (p,2n) reaction on Se<sup>76</sup> and gamma rays were examined with the 2 mm Ge(Li) detector. The spectrum is shown in Fig.3.2. The gamma rays observed have approximate energies 110, 142, 285, 377, 430 and 511 keV.

The half lives of the lines were plotted as shown in Figs. 3.3 and 3.4. All the lines except the one at 110 keV showed a half life of  $106 \pm 5$  mins. The 110 keV line exhibited two half lives, viz., the  $106 \pm 5$  mins. and a short  $4.6 \pm 0.5$  mins. To check the reason for this double half life the 1024 channel analyzer was used with the 2 mm detector and a resolution of 2.5 keV FWHM for the Co<sup>57</sup> (122 & 136 keV) lines was obtained. It was observed that the 110 keV line split up into two lines ( see Fig. 3.5)- one

at 107 keV and the other at 111 keV. The lower energy line has the shorter half life and hence cannot be identified as one coming from an isomeric state of  $\text{Se}^{75}$  as otherwise it would have the half life of the long lived parent.

Since the target mainly contains  $\text{Se}^{76}$  and at the chosen bombarding energy there is no known reaction which could produce a gamma ray line at 107 keV with the observed half life, the next question is could this line originate from an isomeric state in  $\text{Br}^{75}$ ? It is possible that this isomeric state first gamma decays to the ground state of  $\text{Br}^{75}$  which then positron decays to the different levels of  $\text{Se}^{75}$ . Furthermore since  $\text{Br}^{77}$  has an isomeric state at 108 keV with a half life of 4.2 mins. nuclear systematics indicate that  $\text{Br}^{75}$  which has two neutrons less, could also have, though not necessarily, an isomeric state. This possibility cannot be ruled out at present and all that can be said now is that this state does not belong to  $\text{Se}^{75}$ . Details concerning its identification will be given in Chapter VII.

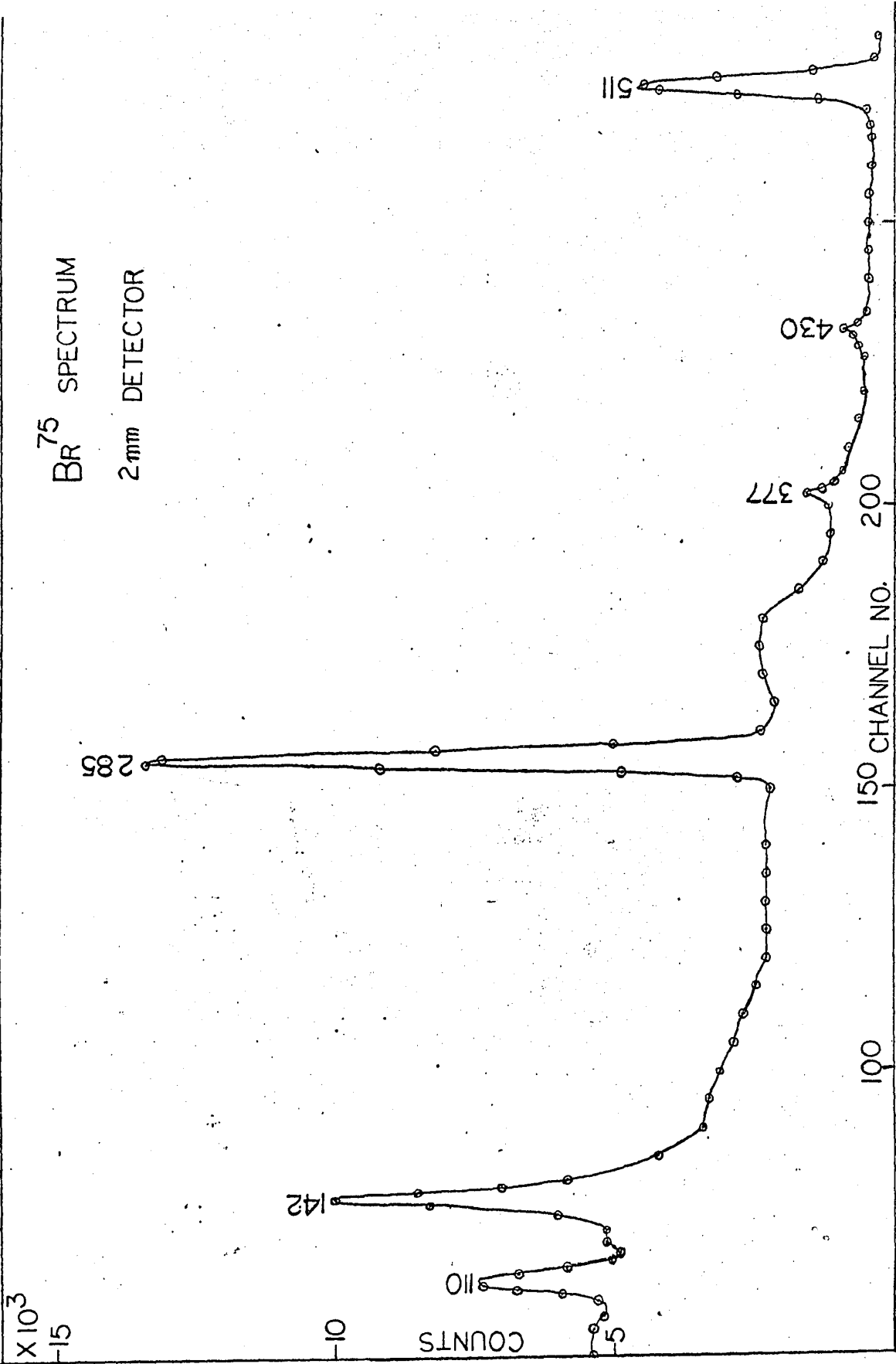
The newly acquired 25 c.c. Ge(Li) detector was used next. The resolution obtained was 2.0 keV FWHM for  $\text{Co}^{57}$  (122 & 136 keV) lines and 2.9 keV FWHM for  $\text{Co}^{60}$  (1.17 & 1.33 MeV) lines. Again the gamma rays from  $\text{Br}^{76}$  by means of the (p,n) reaction were studied first and then the study of  $\text{Br}^{75}$  was taken up. Gamma rays of energies 111.8, 140.9, 286.5, 292.9, 377.3, 427.9, 431.6 and 511.1 keV were observed. The spectrum is presented in Fig. 3.6. With the

'improved detection efficiency and resolution the 285 and the 430 keV lines were identified as doublets as illustrated in Figs. 3.7 & 3.8. To measure the energies of the observed gamma rays accurately, energy calibrations were made by re recording the gamma ray spectra of the six standard sources  $\text{Co}^{57}$ ,  $\text{Co}^{60}$ ,  $\text{Na}^{22}$ ,  $\text{Ba}^{133}$ ,  $\text{Mn}^{54}$  and  $\text{Cs}^{137}$  and finding a linear relationship between the energies of the photopeak and the corresponding channel numbers by the method of least-squares fit. This relation was then utilised to find out the energies corresponding to the photopeaks of the different gamma rays observed. Using the efficiency calibration curves the relative intensities of these gamma rays have been determined and are shown in Table 3.1.

It will be noticed that all the observed gamma rays from  $\text{Br}^{75}$  are below the 511 keV line. A search for higher energy gamma rays was made using the 25 c.c. Ge(Li) detector and all the gamma rays found were long lived and could be identified as coming from  $\text{Br}^{76}$  which was also produced via the (p,n) reaction although the cross-section is comparatively small. Both Lobkowitz et al (Lobkowitz et al, 1961) and Baskova et al (Baskova et al, 1962) reported of observing a gamma ray in the region of 610 keV. A very careful search has been made for it but no line in that region was observed. The gamma ray observed by them could very well be coming from the impurities or other isotopes in their sources.

Figure 3.2- Gamma spectrum of  $\text{Er}^{75}$  measured  
with the 2 mm  $\text{Ge}(\text{Li})$  detector.  
All energies are in keV.

FIGURE 3.2



3.2

Figure 3.3- Curve showing two half lives of  
the 110 keV line. The half lives  
are  $106 \pm 5$  min. and  $4.6 \pm 0.5$  min.

FIGURE 3.3

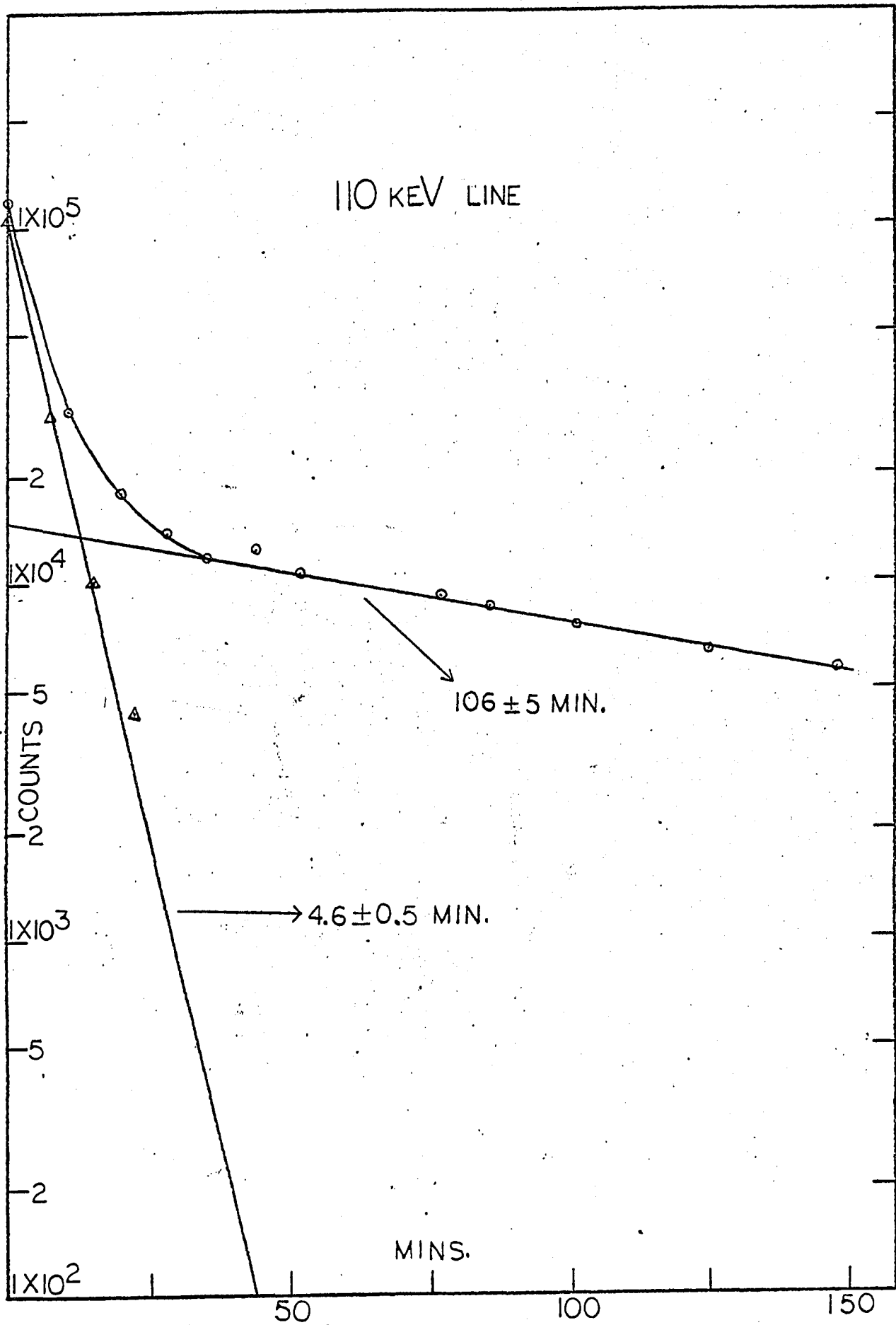


Figure 3.4- Half life curves of the 142, 285,  
and the 377 keV lines. The half  
life in each case is  $106 \pm 5$  min.

FIGURE 3.4

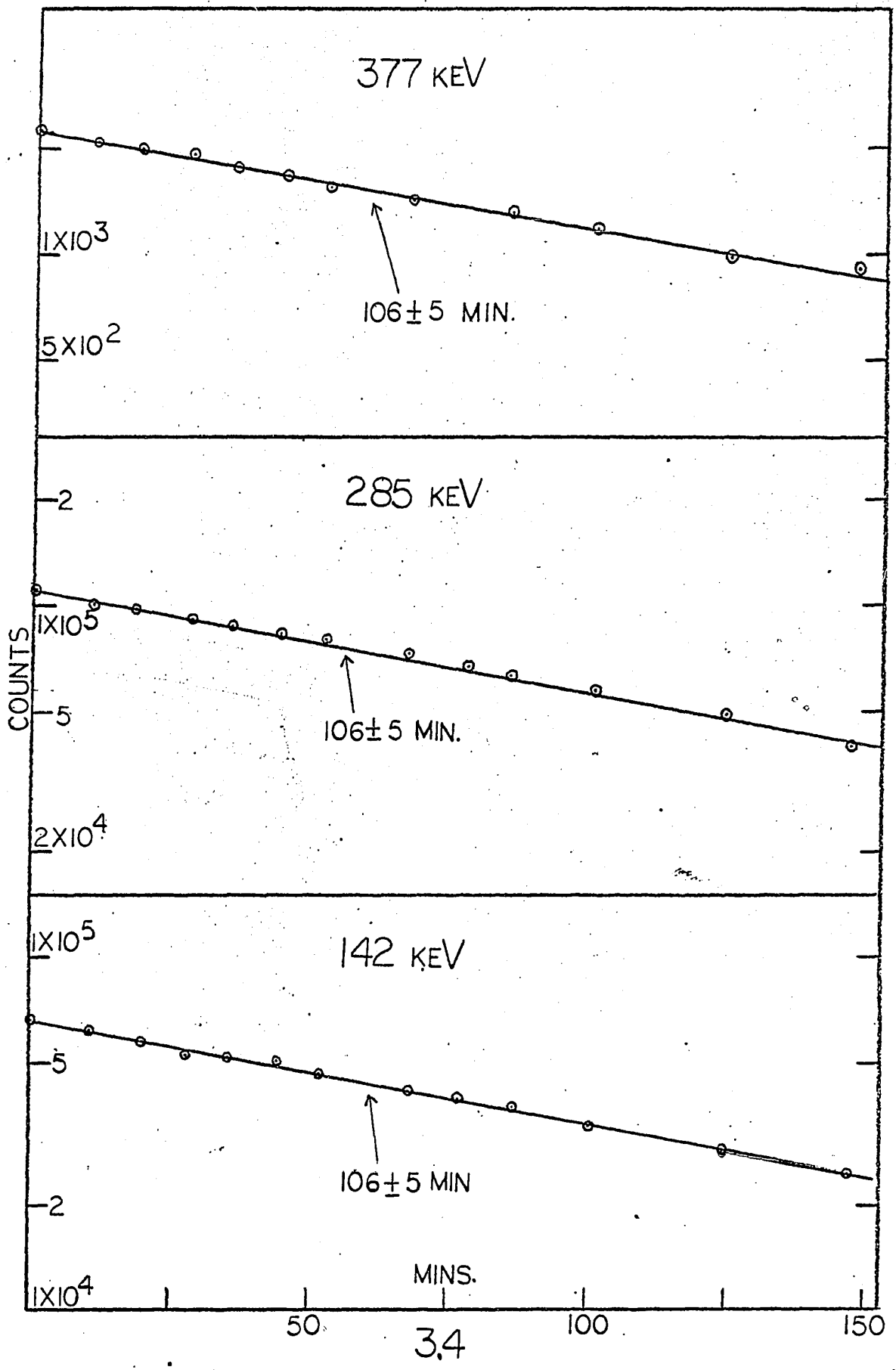
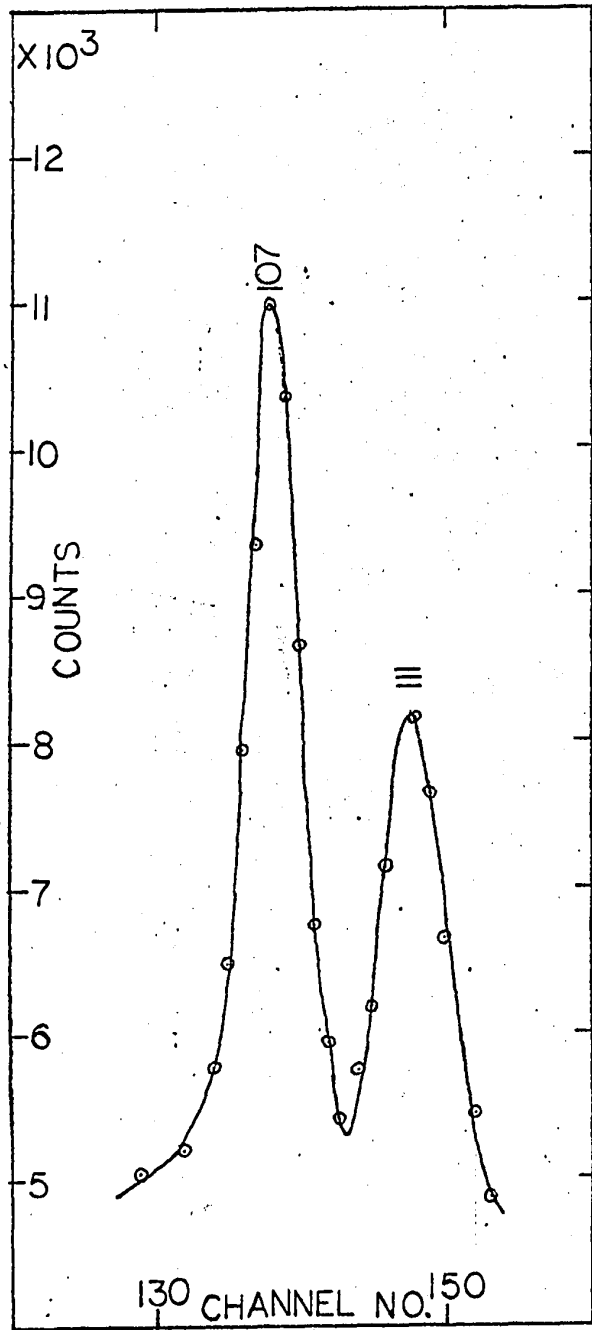


Figure 3.5- The 107 and the 111 keV lines  
resolved from one another.

FIGURE 3.5



3.5

Figure 3.6- Gamma spectrum of Br<sup>75</sup> measured  
with the 25 c.c. Ge(Li) detector.  
All energies are in keV.

FIGURE 3.6

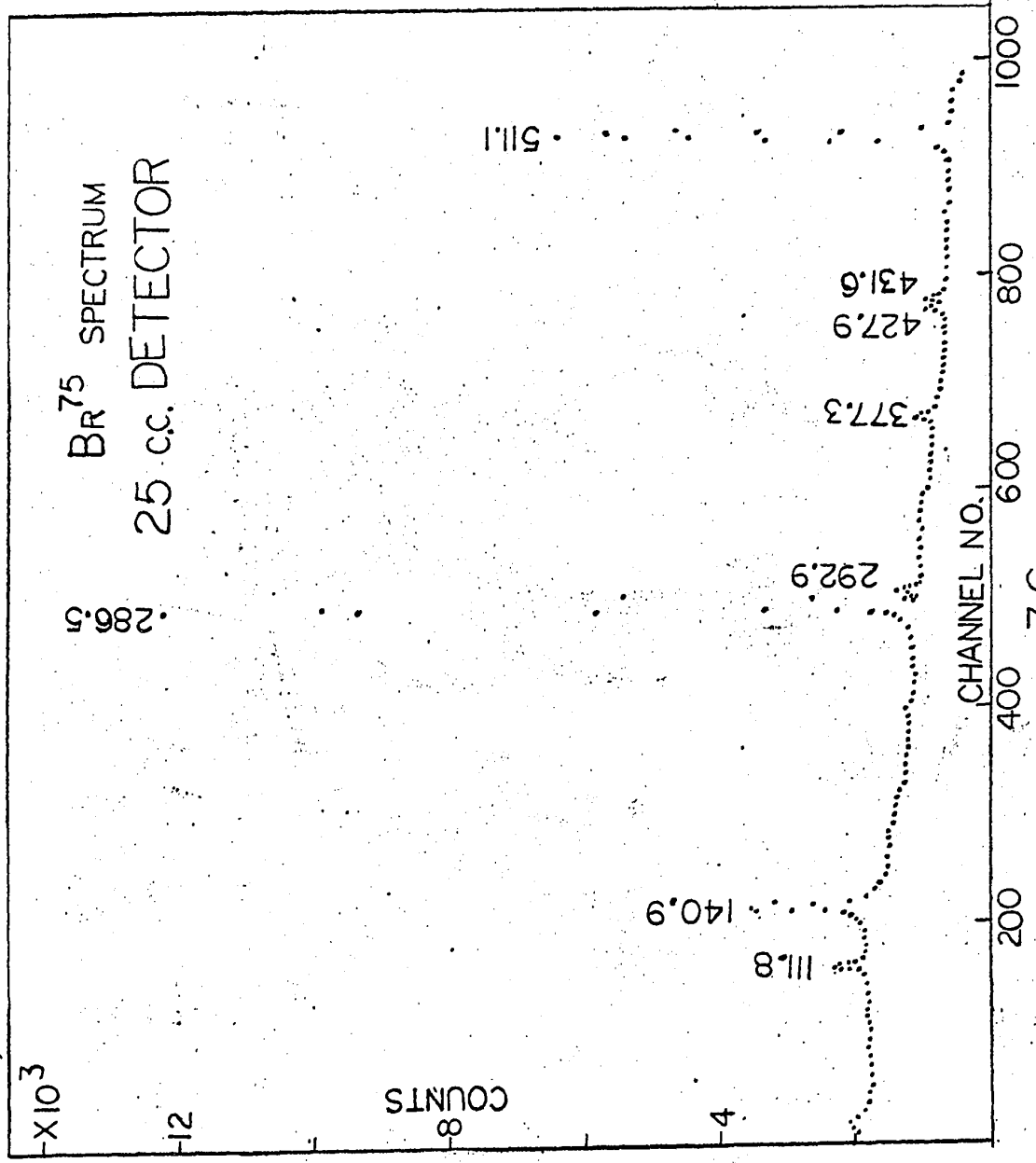


Figure 3.7- An expanded view of the doublet  
of lines at 286.5 and 292.9 keV.

FIGURE 3.7

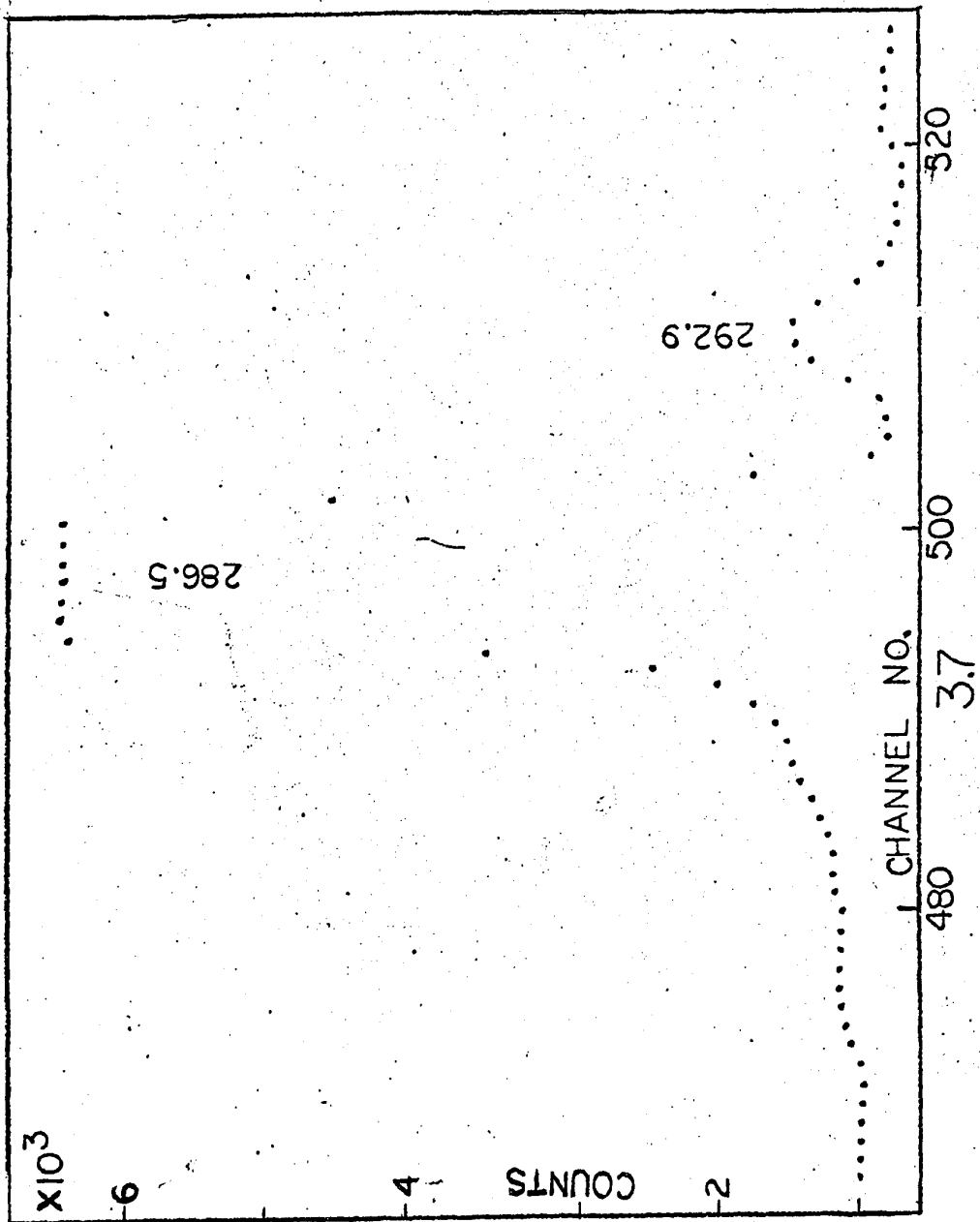


Figure 3.8- An expanded view of the doublet  
of lines at 427.9 and 431.6 keV.

FIGURE 3.8

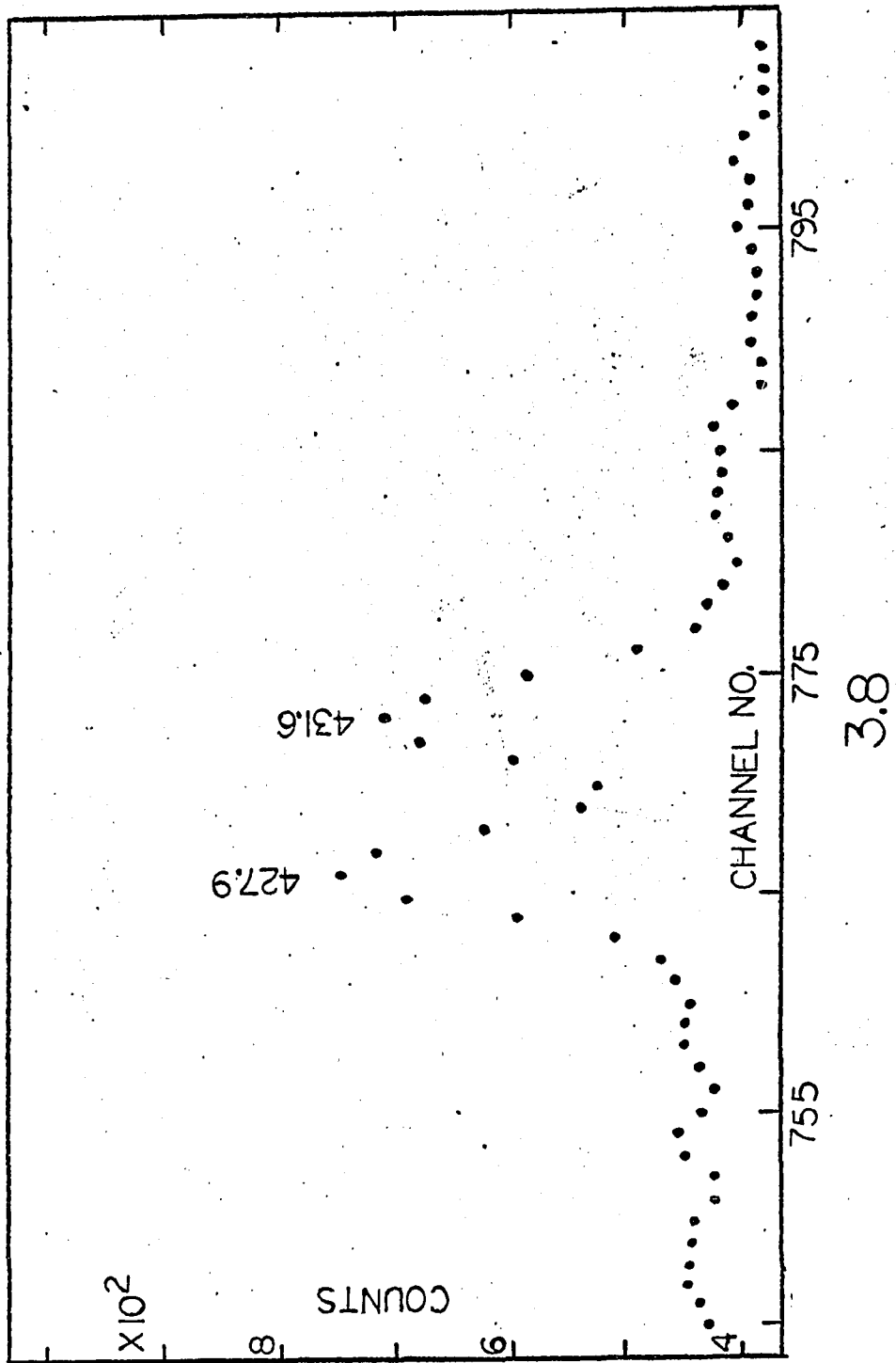


Table 3.1

## Gamma rays and their intensities

Energies in keV	Relative Intensities %
111.8	1.7
140.9	4.7
286.5	80.0
292.9	2.8
377.3	3.2
427.9	3.8
431.6	3.8

Energies are measured accurate to  $\pm 0.25$  keV.

## 3.4 Coincidence measurements

After having found all the gamma rays emitted following the decay of  $\text{Br}^{75}$ , the next task is to establish the sequence in which they are emitted. To do this gamma-gamma coincidence experiments were performed. The 25 c.c. detector was used as one of the radiation detectors. The other counter was a 7.6 cm by 7.6 cm NaI(Tl) Harshaw integral line scintillation crystal. In spite of its poor

energy resolution, the NaI(Tl) detector was used because it has a much higher photopeak efficiency than that of Ge(Li) detectors. This is important for gamma-gamma coincidence experiments. The charge output from the Ge(Li) detector is fed into a Tennelec TC 135L pre-amplifier and that from the photomultiplier in the NaI(Tl) counter is fed into a home made charge-sensitive pre-amplifier. The circuit details of this pre-amplifier are shown in Fig. 3.9. The operation of this circuit is as follows:-

Transistors  $Q_1$  and  $Q_2$  form the input stage cascade amplifier and transistors  $Q_3$  and  $Q_4$  form a White emitter follower stage. The White emitter follower output is negative-feed-back through C to the input and positive-feed-back through  $C_1$  to the load of the cascade amplifier. The two stages form an operational amplifier. The positive feed-back is to increase the amplifier gain and the negative feed-back capacitance is for charge collection. The voltage pulse output of the operational amplifier is differentiated by the  $0.005 \mu\text{f}$  capacitance and the  $10\text{K}$  resistor.  $Q_5$  is the emitter follower and  $Q_6$  and  $Q_7$  form the complementary emitter follower as the output stage. The output pulse has a decay time of  $50 \mu\text{s}$ .

The pulses from the two detectors pre-amplifiers are then fed into the fast-slow coincidence system described in the previous chapter. The fast coincidence system was set to have a resolving time of  $60 \text{ ns}$ .

Initially all the gamma rays measured by the Ge(Li) detector that are in coincidence with the 511 keV positron annihilation gamma ray in the NaI(Tl) counter were observed. All the lines in the original spectrum appeared in this spectrum, except the short lived 107 keV line, which further supports the conclusion that it does not originate from  $\text{Se}^{75}$  unless it comes from an isomeric state and in which case it should have the half life of the long lived parent,  $\text{Br}^{75}$ . This coincidence spectrum is very much like the singles spectrum. There is, however, one noteworthy difference. In the singles spectrum, the two neighbouring lines at 427.9 and 431.6 keV are roughly of equal intensities while in the coincidence spectrum, the lower energy line is about three times more intense than the higher energy one. This seems to show that the main contribution to this second gamma ray comes from electron capture (no 511 keV gamma ray emitted) rather than from positron decay. The details of this spectrum are shown in Figs. 3.10, 3.11 and 3.12.

Next the spectrum from the Ge(Li) detector was coincident gated with the strongest line, viz. 286.5 keV line from the NaI(Tl) counter. Since the NaI(Tl) crystal could not resolve the 286.5 and the 292.9 keV lines, this means that the energy selection window in the single channel analyzer associated with the NaI(Tl) detector was actually set on both lines. The lines observed

in this spectrum are the 140.9, 286.5, 292.9, 377.3, 431.6 keV and of course the 511 keV line. The intensity of the 286.5 keV line relative to the other lines was much smaller here than in the singles spectrum. The details of this spectrum are shown in Figs. 3.13 and 3.14.

The spectrum coincident gated by the 140.9 keV line from the NaI(Tl) counter was also studied and the lines observed in this case were the 286.5, 431.6 and the 511 keV lines. The details are shown in Figs. 3.15 and 3.16.

Finally the coincidence spectrum of the Ge(Li) detector with the 111.8 keV line from the NaI(Tl) detector was observed, and the only line appearing in this spectrum is the 511 keV line. The relative intensities of the different lines in the different coincidence spectra are presented in Table 3.2.

The information obtained in these coincidence measurements enabled the construction of the most probable decay scheme for Br<sup>75</sup>. This will be presented in a later chapter.

Table 3.2

Relative intensities of Gamma rays in coincidence spectra

Gamma Rays keV	Relative Intensities Gated with		
	140.9 keV	286.5 & 292.9 keV	511 keV
111.8	0.0	0.0	1.7
140.9	0.0	33.5	3.8
286.5	100.0	100.0	100.0
292.9	0.0	12.5	1.9
377.3	0.0	25.6	6.1
427.9	0.0	0.0	3.3
431.6	10.8	14.1	1.35
511.1	118.5	487.0	76.5

Figure 3.9- Circuit Diagram of charge-sensitive  
Pre-amplifier

FIGURE 3.9

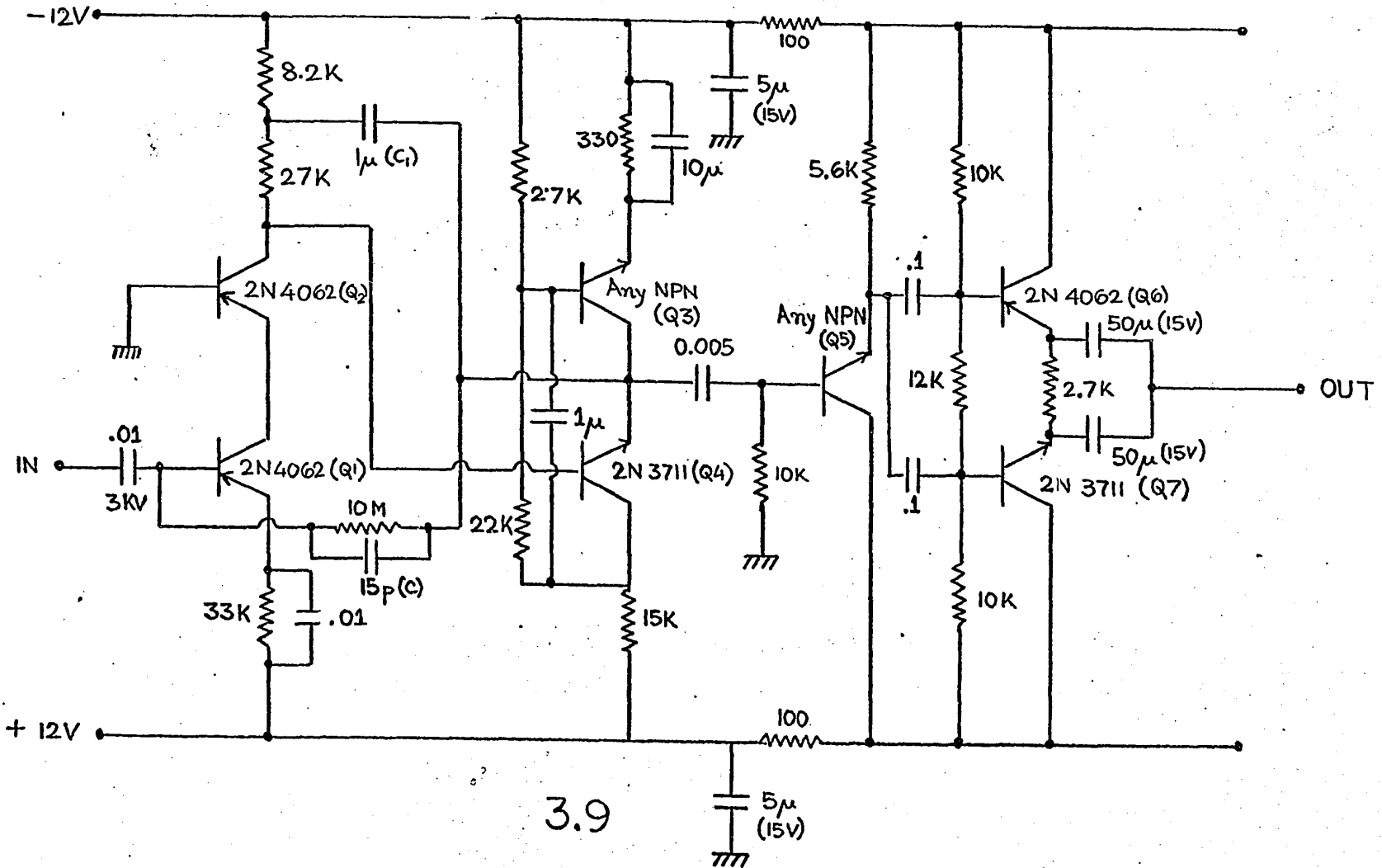


Figure 3.10- 25 c.c. Ge(Li) spectrum in  
coincidence with NaI(Tl) detector  
set on the 511 keV photopeak. All  
energies are in keV.

FIGURE 3.10

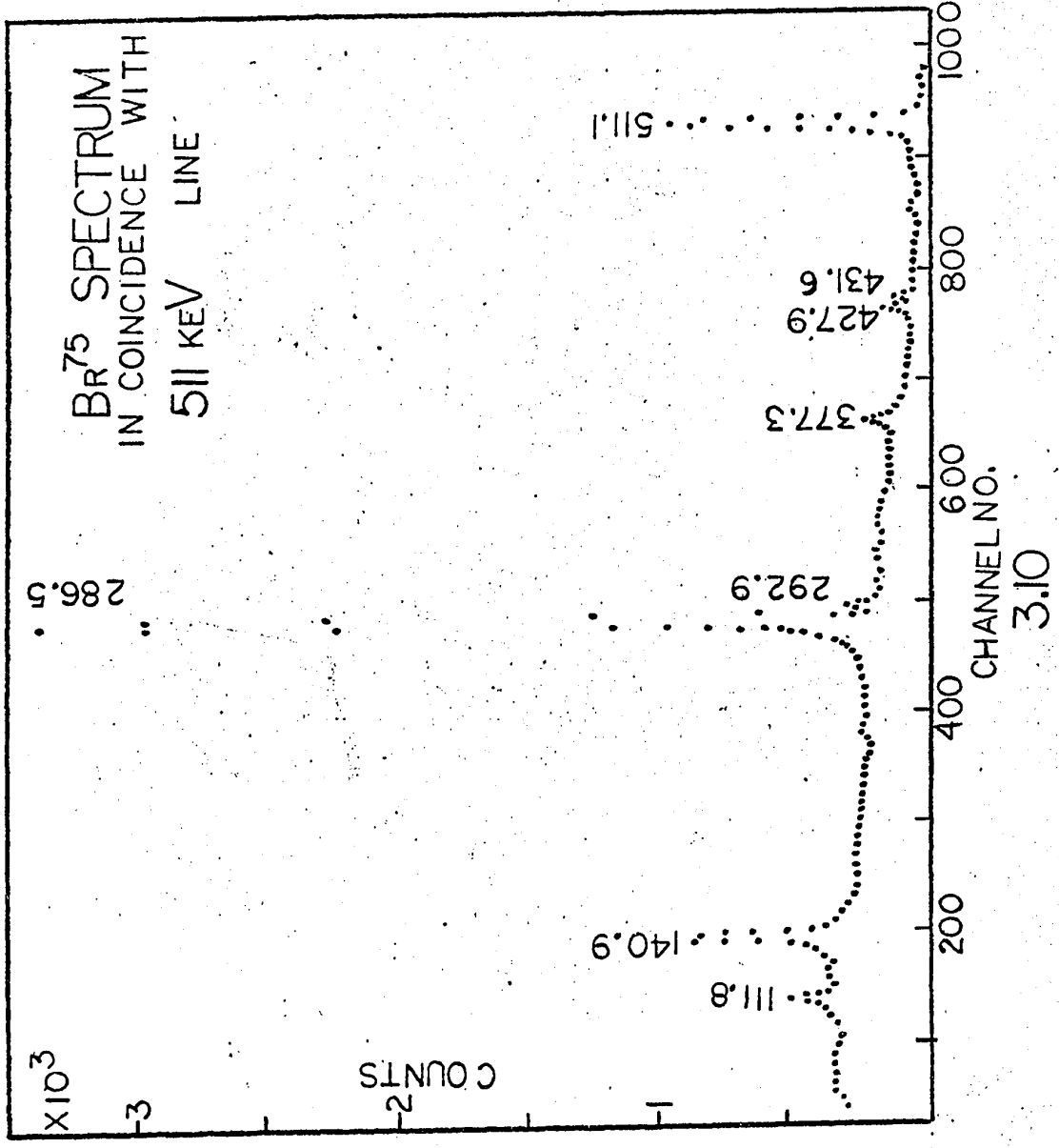
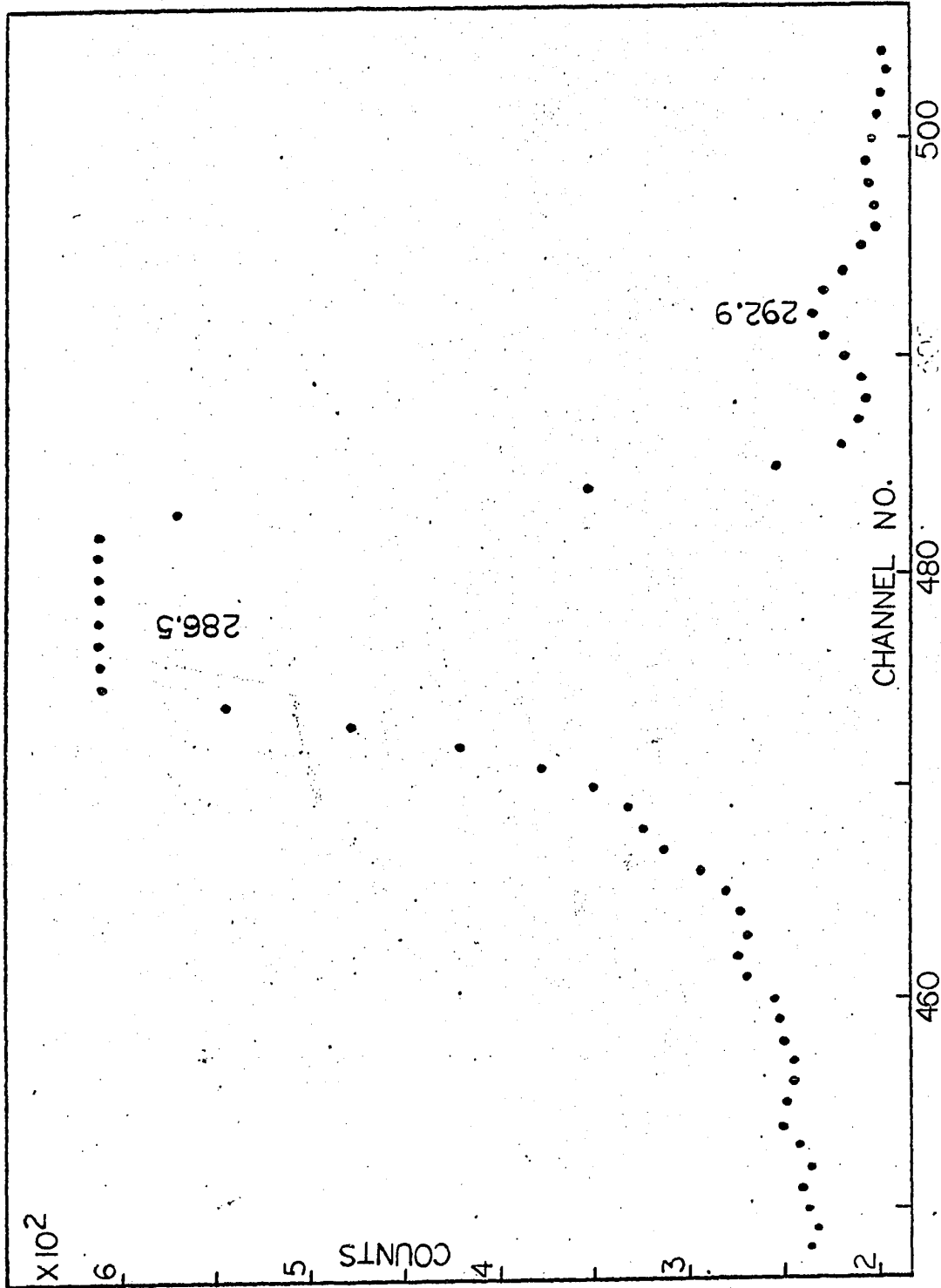


Figure 3.11- An expanded view of the doublet of lines at 286.5 and 292.9 keV in the spectrum in coincidence with the 511 keV line.



3.11

Figure 3.12- An expanded view of the doublet of lines at 427.9 and 431.6 keV in the spectrum in coincidence with the 511 keV line.

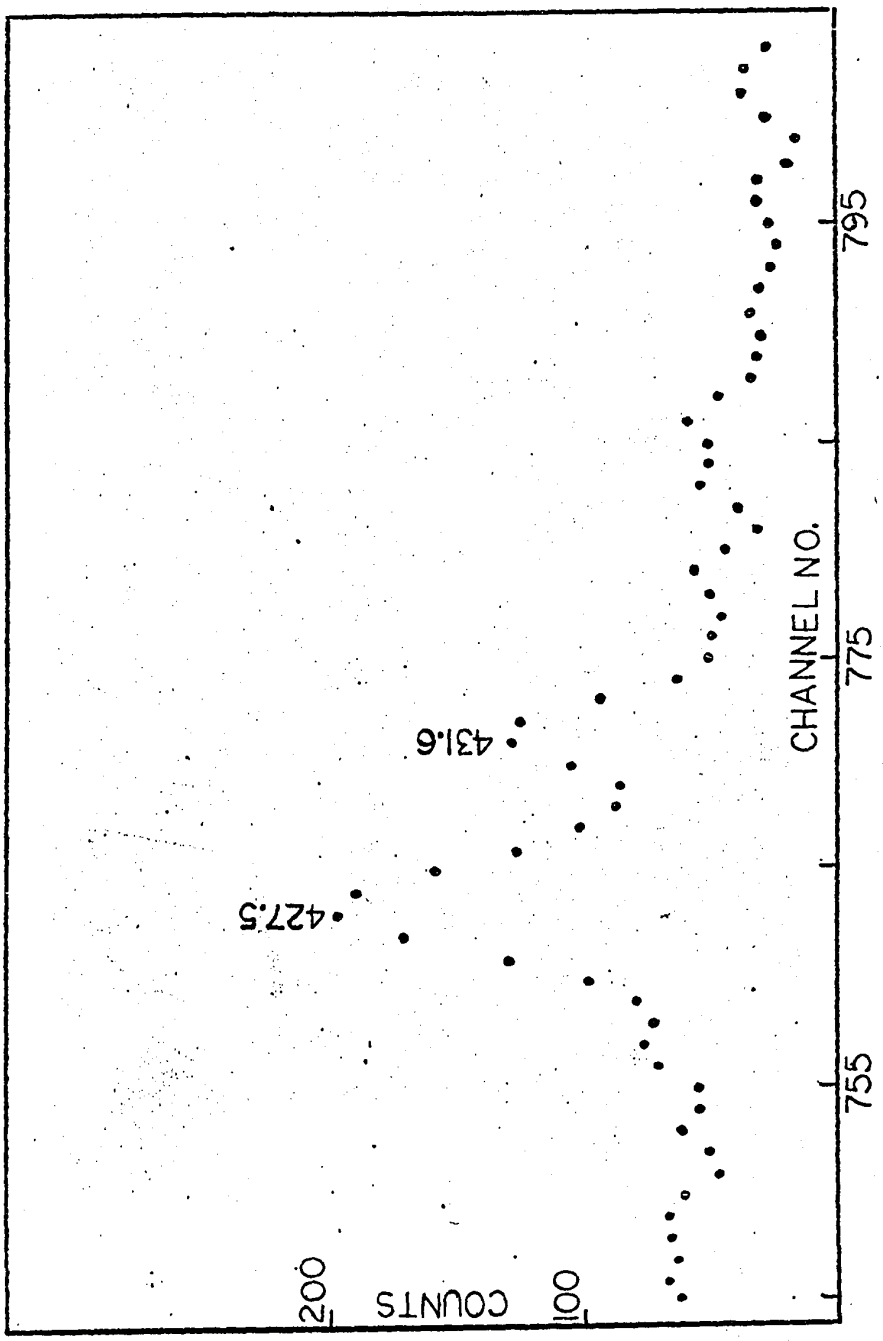


Figure 3.13- 25 c.c. Ge(Li) spectrum in coincidence with NaI(Tl) detector set on the 286.5 & 292.9 keV photopeak. All energies are in keV.

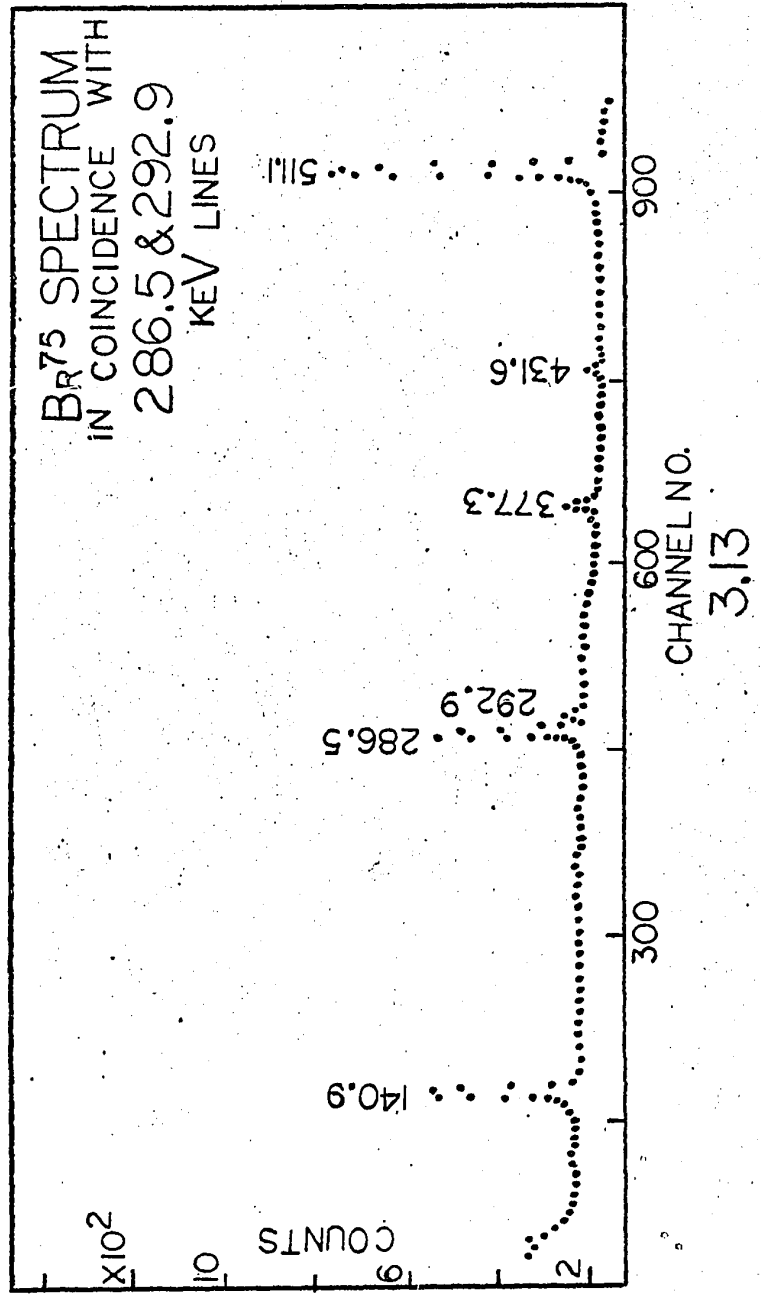
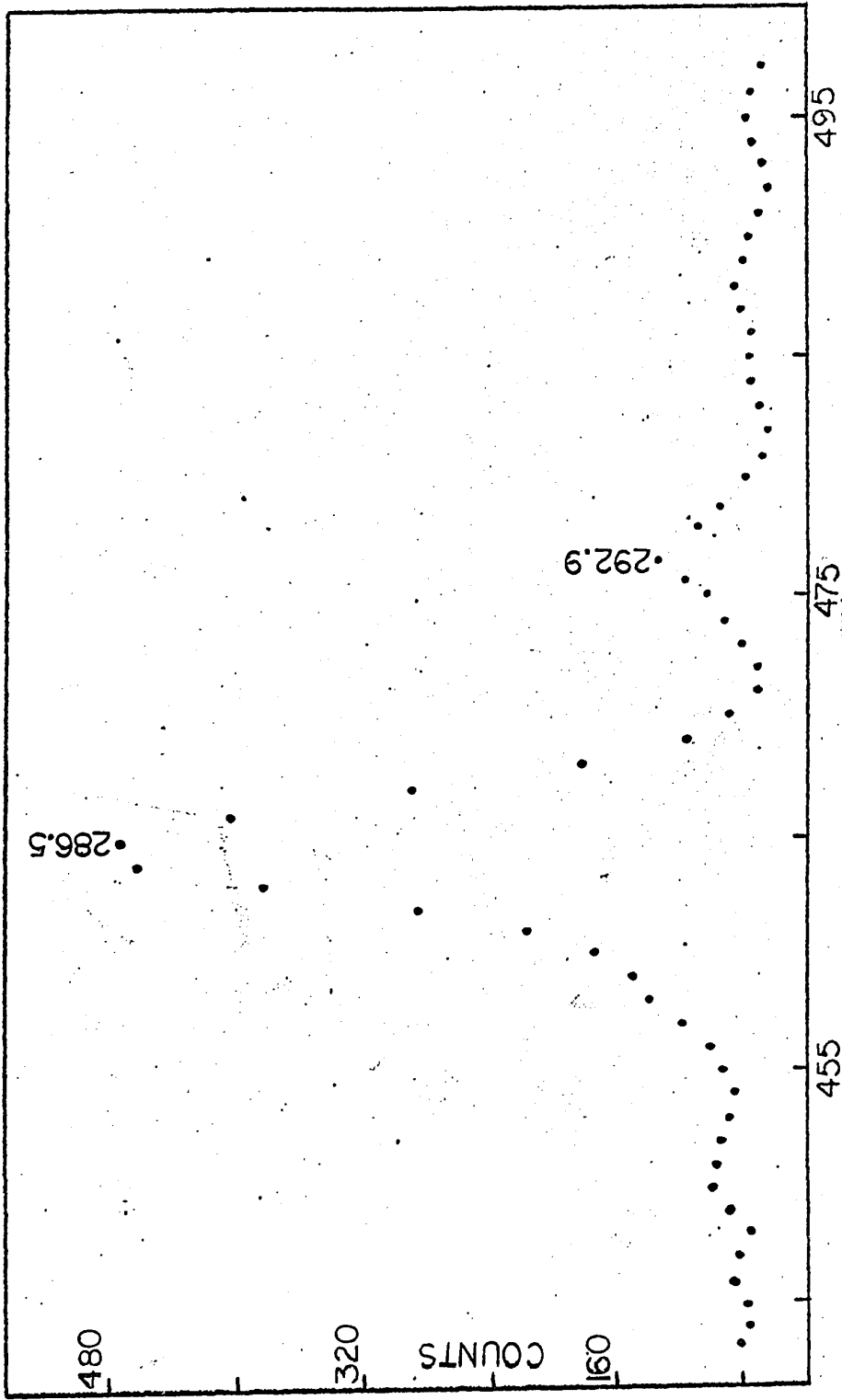


Figure 3.14- An expanded view of the doublet of lines at 286.5 and 292.9 keV in the spectrum in coincidence with the same two lines.



CHANNEL NO.  
3.14

Figure 3.15- 25 c.c. Ge(Li) spectrum in  
coincidence with NaI(Tl) detector  
set on the 140.9 keV photopeak.  
All energies are in keV.

BR<sup>75</sup> SPECTRUM  
IN COINCIDENCE WITH  
140.9 KEV LINE

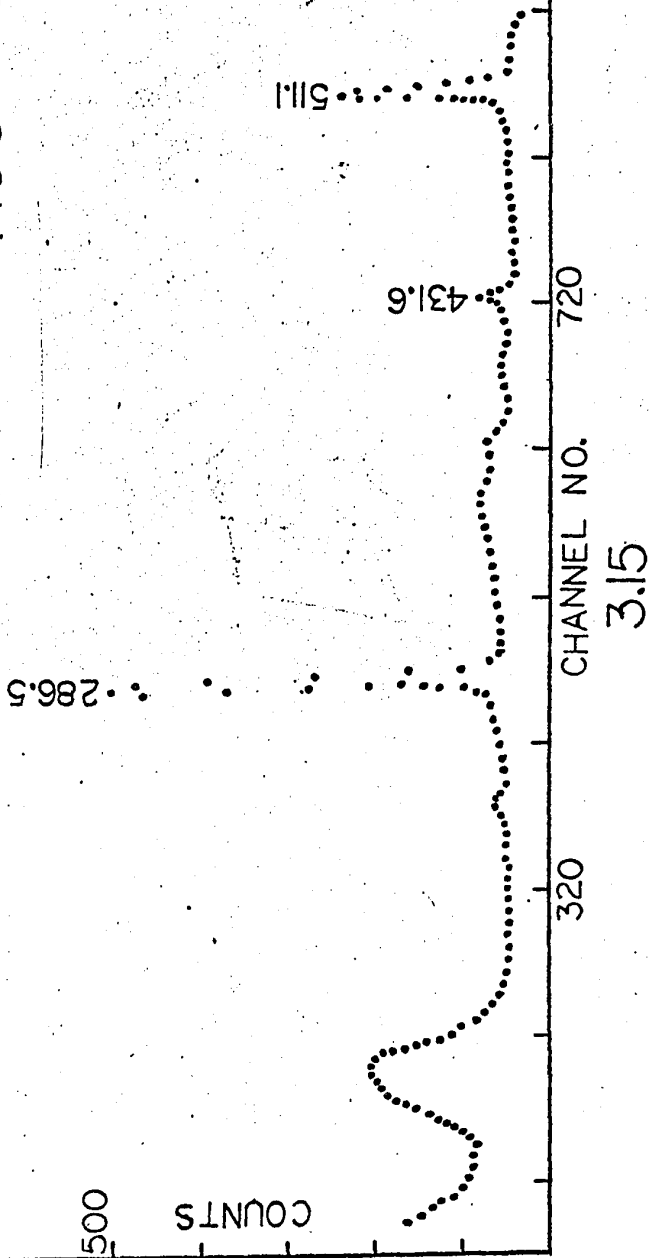
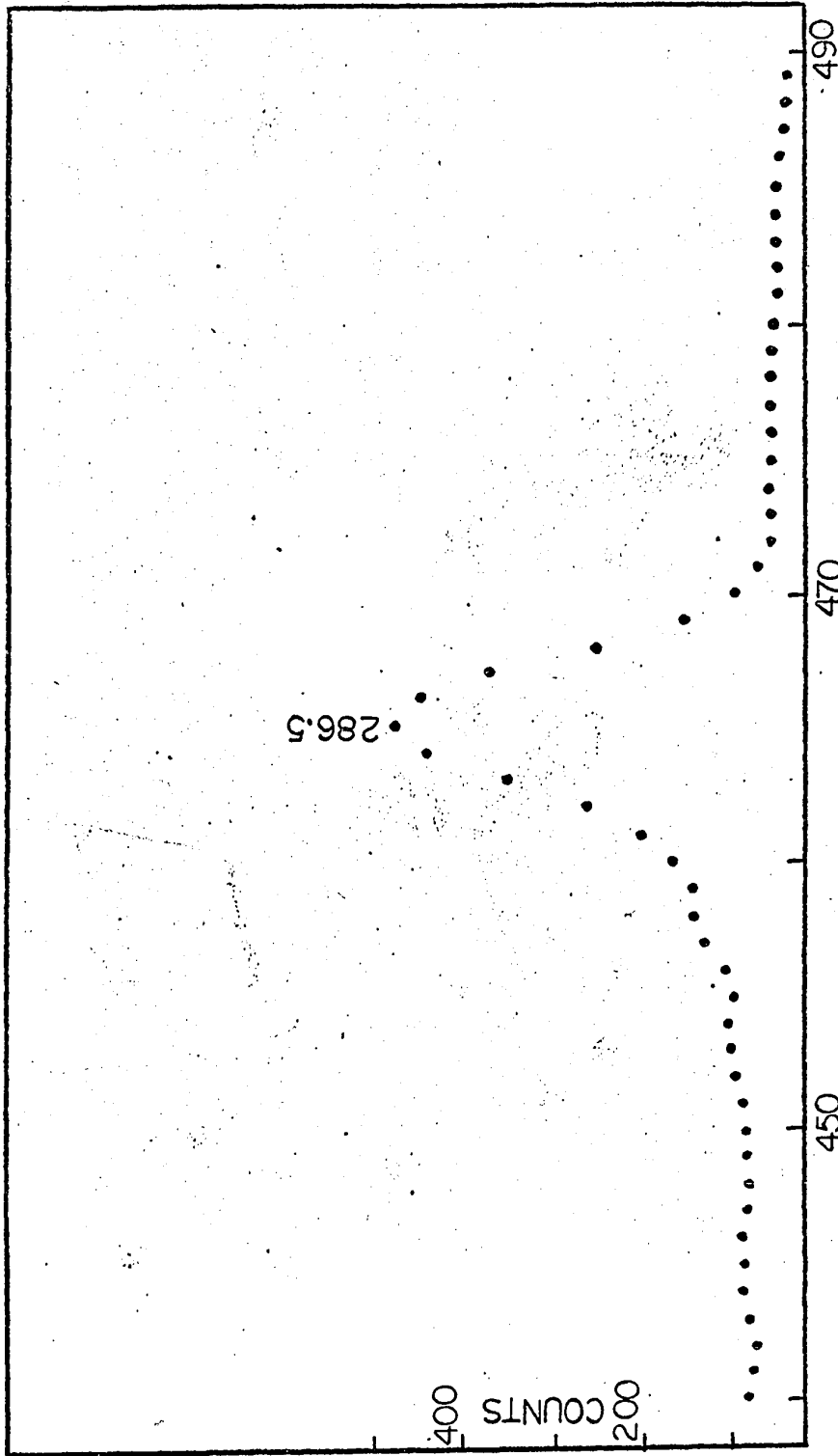


Figure 3.16- An expanded view of the 286.5 keV line in the spectrum in coincidence with the 140.9 keV line. The  $^{292}\text{Sg}$  9 keV line is absent.



CHAPTER IV

Beta rays from Br<sup>75</sup>

4.1 History

The first important work on the positron spectrum of Br<sup>75</sup> was done by Fultz and Pool (Fultz et al, 1952). Br<sup>75</sup> was produced by bombarding Selenium metal enriched in Se<sup>74</sup> with 7.3 MeV protons. The positron spectrum was examined in a 180° focusing magnetic spectrometer and was found to be quite complex. Fermi-Kurie plots of the spectrum revealed that it actually consisted of four beta branches having endpoint energies  $1.70 \pm 0.02$  MeV, 0.8 MeV, 0.6 MeV and 0.3 MeV and with relative intensities 46%, 20%, 15% and 19% respectively. These implied  $\log (ft)$  values of 5.6, 4.9, 4.7 and 4.7 for the branches in that order.

The other work on the positron spectrum was done by Baskova et al (Baskova et al, 1962). They produced Br<sup>75</sup> by bombarding Se<sup>74</sup> enriched to 41% as already reported in Chapter III. The positron spectrum was studied by a thin lens magnetic beta spectrometer. From the resultant Fermi-Kurie plot, they found three beta branches with endpoint energies  $1720 \pm 50$ , 1100 and 650 keV and relative intensities 80%, 15% and 5% respectively. Comparing this with the results of Fultz and Pool, it is seen that only one endpoint energy, viz. 1.72 MeV agree while the others are in

complete disagreement. They also carried out some beta-gamma coincidence experiments with a resolving time of 250 ns, and found that the 285 keV gamma ray was in coincidence with the 1720 keV beta ray.

#### 4.2 Target preparation

-----

For studying the beta rays from  $\text{Br}^{75}$ , thin and uniform sources had to be prepared.  $\text{Br}^{75}$  was produced as usual by bombarding  $\text{Se}^{76}$  isotope. The targets were prepared exactly as was done for gamma spectrometry. The isotope was wrapped up in an aluminium foil which was attached to the target holder. After bombardment, the active substance was taken out of the wrapping and dissolved in hot concentrated nitric acid. The excess acid was then boiled away. A couple of drops of this solution was then deposited on an aluminium backing about a quarter of a mil. thick. The solvent in the deposition was then evaporated. Drying at elevated temperatures in a heated oven quickens the process tremendously, but the deposition of the active substance on the backing material is usually quite non-uniform. An equally fast but more efficient way is to place the source in an airtight chamber for vacuum evaporation. The process of evaporation is extremely quick and the deposition on the backing material is also quite uniform. The average time for drying was about 10 mins. Alternately, the enriched

isotope could have been first deposited on the backing material and then bombarded. However this makes the backing material (aluminium) also highly radioactive, and as a result the positron spectrum of  $\text{Br}^{75}$  superimposes on a very high background.

#### 4.3 Positron spectrum from $\text{Br}^{75}$

-----

The positron spectrum from  $\text{Br}^{75}$  was studied by using the 5 mm Si(Li) detector (SIMTEC model K14). The source was placed inside the mini-chamber (described in Chapter II) and the continuous beta spectrum was recorded in the first 1024 channels of a TMC 4096 kicksorter. The energy calibration was done by using the electron internal conversion lines of  $\text{Bi}^{207}$ . A FORTRAN program was written to calculate the Fermi functions (Siegbahn, 1968) for  $\text{Se}^{75}$  (daughter nucleus) and also the ordinates for the corresponding Fermi-Kurie plots for allowed transitions. This program could also perform approximate separation of the different positron components in the spectrum. With the help of this program, the positron spectrum was analyzed.

$\text{Br}^{75}$  was produced via the (p,2n) reaction on  $\text{Se}^{76}$ . However a considerable amount of  $\text{Br}^{76}$  was also produced via the (p,n) reaction on  $\text{Se}^{76}$ . Fortunately  $\text{Br}^{76}$  has a relatively long half life and therefore its production would be weak in a relatively short bombardment. Besides,

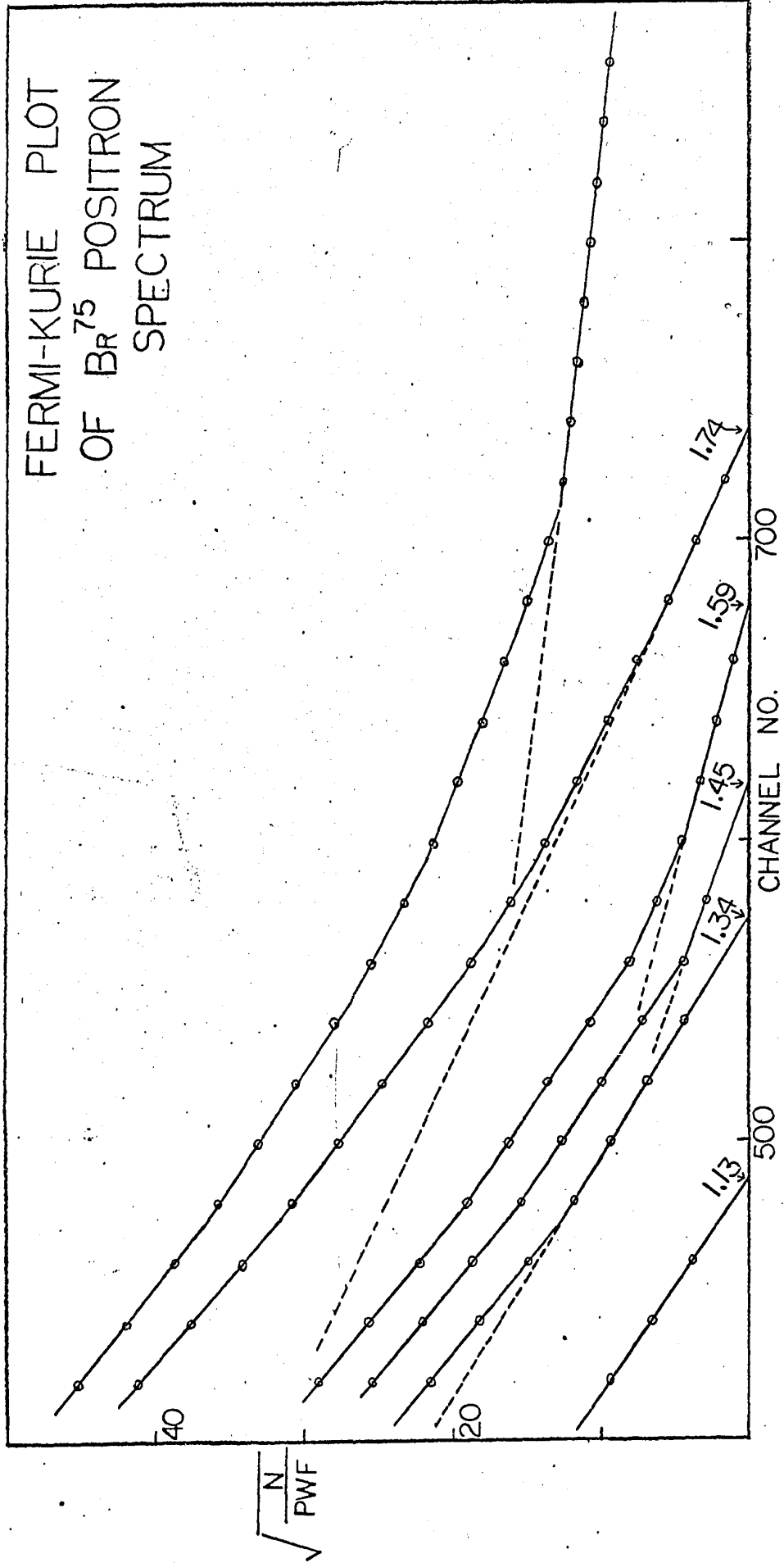
beta rays from  $\text{Br}^{76}$  have very high endpoint energies and can be distinguished as a general background. The mass difference between the ground states of  $\text{Br}^{75}$  and  $\text{Se}^{75}$  calculated from the semi-empirical mass formula (Seeger, 1961) is 3.02 MeV. This implies that the beta rays from the decay of  $\text{Br}^{75}$  can have a maximum energy of 2.01 MeV and the beta rays with higher endpoint energies must necessarily come from  $\text{Br}^{76}$  and other impurities.

The Fermi-Kurie plot of the beta spectrum obtained from the bombardment of  $\text{Se}^{76}$  with 20 MeV protons is shown in Fig. 4.1. The spectrum is not a simple one but is a superposition of several branches of positrons. The high energy portion ( $> 1.7$  MeV) is presumably due to beta rays from impurities, mainly  $\text{Br}^{76}$  decays. By extrapolating this high energy component down to the lower energy region and subtracting it from the spectrum, the beta spectrum from  $\text{Br}^{75}$  was obtained. The different components were separated by using standard techniques, and the resultant Fermi-Kurie plots are also shown in Fig. 4.1. The endpoint energies as determined from this diagram are 1.74, 1.59, 1.45, 1.34 and 1.13 MeV for the five branches. This energy determination is accurate to  $\pm 20$  keV.

The lower energy region could not be investigated, as the origin of the counts in this part of the spectrum is unknown. First, the thickness of the source as well as the backscattering of the detector have

Figure 4.1- Fermi-Kurie plot of the positron spectrum of  $\text{Br}^{75}$ . All energies are in MeV. In the ordinate,  $N$  represents the number of counts  $W$  the relativistic energy,  $P$  the momentum and  $F$  the Fermi function.

FERMI-KURIE PLOT  
OF  $Br^{75}$  POSITRON  
SPECTRUM



considerable smearing effects on the beta particles at low energy, and as a result the Fermi-Kurie plot curves upwards in this region. The other and the more serious one is the interference due to the gamma rays Compton scattered in the 5 mm detector. Although the Si(Li) detectors have negligible photoefficiency, the Compton efficiency is fairly high for low energy gamma rays. Since there are two intense gamma rays at 286.5 and 511 keV from the source, a lot of counts from gamma rays were superimposed on the beta spectrum.

#### 4.4 Beta-gamma coincidence studies

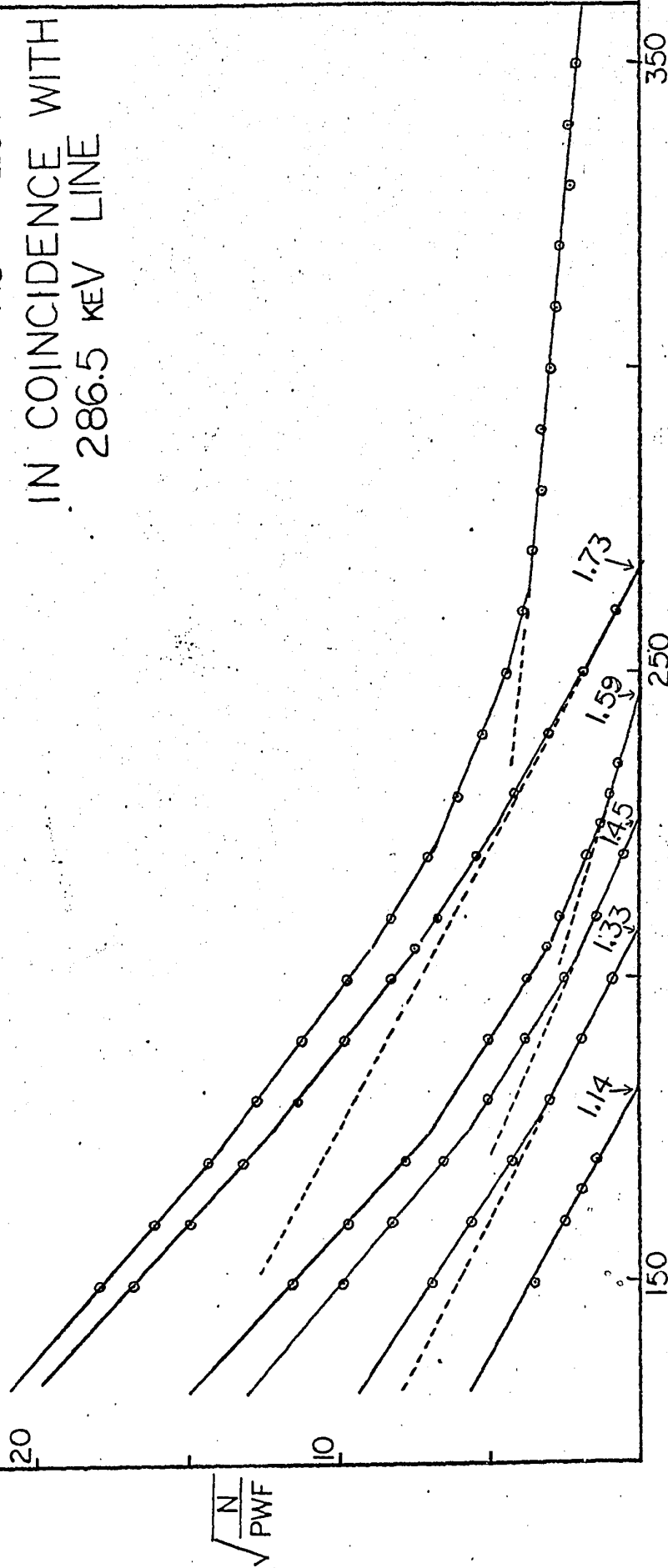
-----

In order to eliminate the high background beta activity from  $\text{Br}^{76}$  and other impurities, it was decided to study the positron spectrum in coincidence with the 286.5 keV gamma ray which comes from the decay of  $\text{Br}^{75}$ . The mini-chamber was used for this experiment. The beta particles were measured by the 5 mm Si(Li) detector while the gamma detector used was a 7.6 cm by 7.6 cm NaI(Tl) Harshaw detector placed outside the thin brass window (15 mil.) of the mini-chamber. The electronics set up was identical with the fast-slow system described in Chapter II. The resolving time in the fast coincidence unit was 75 ns. The positron spectrum recorded by the Si(Li) detector coincident gated by the 286.5 keV line from the NaI(Tl) counter was studied. The Fermi-Kurie plot of the resultant spectrum is

shown in Fig. 4.2. This spectrum also has a high energy background although with a much reduced intensity. This is because when the energy selection window is set on the 286.5 keV gamma ray, it is automatically set on a part of the Compton tail of the 511 keV annihilation gamma ray with which all positrons emitted are in coincidence. This results in a feedthrough of the high energy background. The endpoint energies of the different branches in this spectrum are 1.73, 1.59, 1.45, 1.33 and 1.14 MeV. These are identical with the endpoint energies obtained in the singles spectrum within the experimental accuracy.

Figure 4.2- Fermi-Kurie plot of the positron spectrum of Br<sup>75</sup> in coincidence with the 286.5 keV gamma ray. All energies are in MeV. In the ordinate, N represents the number of counts, W the relativistic energy, P the momentum and F the Fermi function.

FERMI-KURIE PLOT OF  
BR<sup>75</sup> POSITRON SPECTRUM  
IN COINCIDENCE WITH  
286.5 KEV LINE



250  
CHANNEL NO.  
4.2

CHAPTER V  
-----

Construction of the decay scheme of Br<sup>75</sup>  
-----

5.1 A summary of previous works  
-----

Elwyn et al (Elwyn et al,1958) applied a milli-microsecond time of flight technique to the study of (p,n) reactions on As<sup>75</sup> using 3 MeV protons. They observed five strong groups of neutrons with energies corresponding to the excitation of five energy states in the residual nucleus, Se<sup>75</sup>. They are the ground state,  $108 \pm 4$  keV,  $268 \pm 12$  keV,  $400 \pm 20$  keV and  $570 \pm 20$  keV states. Elwyn et al also pointed out that the 268 keV level they observed probably corresponds to the 286 keV level found by Butler et al (Butler et al,1957) while studying the same reaction.

From gamma ray measurements, ( described in Chapter III), Lobkowicz et al (Lobkowicz et al,1961) suggested a decay scheme as shown in Fig. 5.1. The gamma and beta spectroscopic measurements of Baskova et al (Baskova et al,1962) have led them to suggest a decay scheme with levels at 285, 905 and 1355 keV. The details of this scheme are also given in Fig. 5.1.

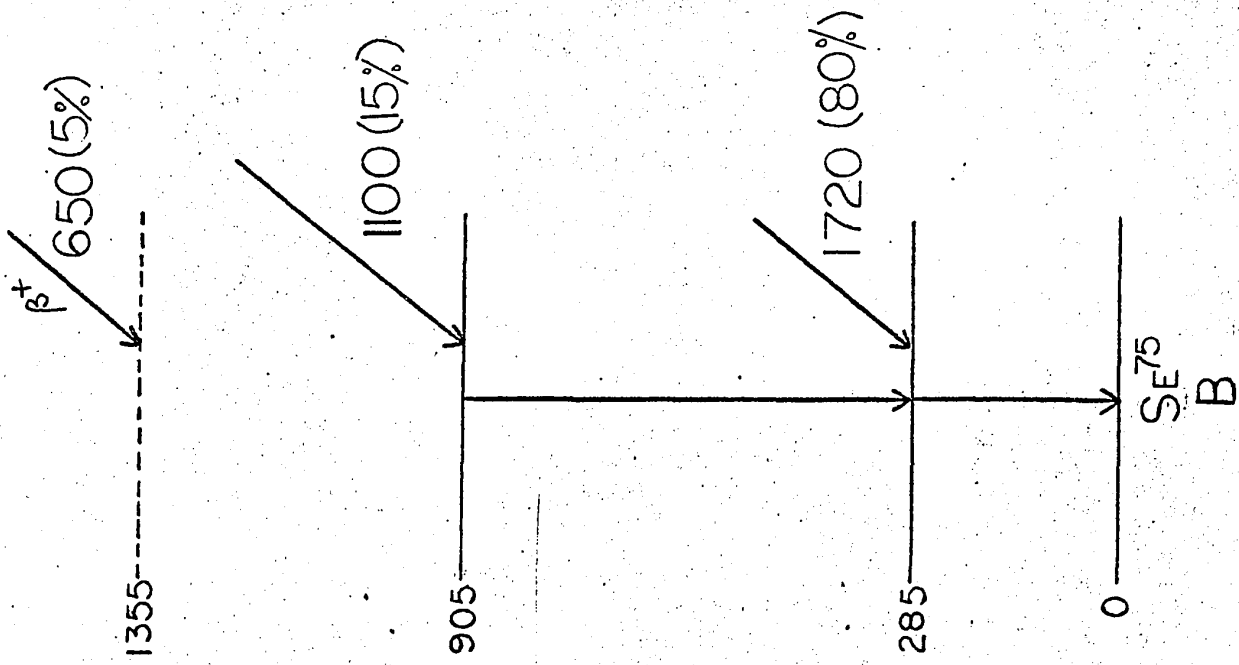
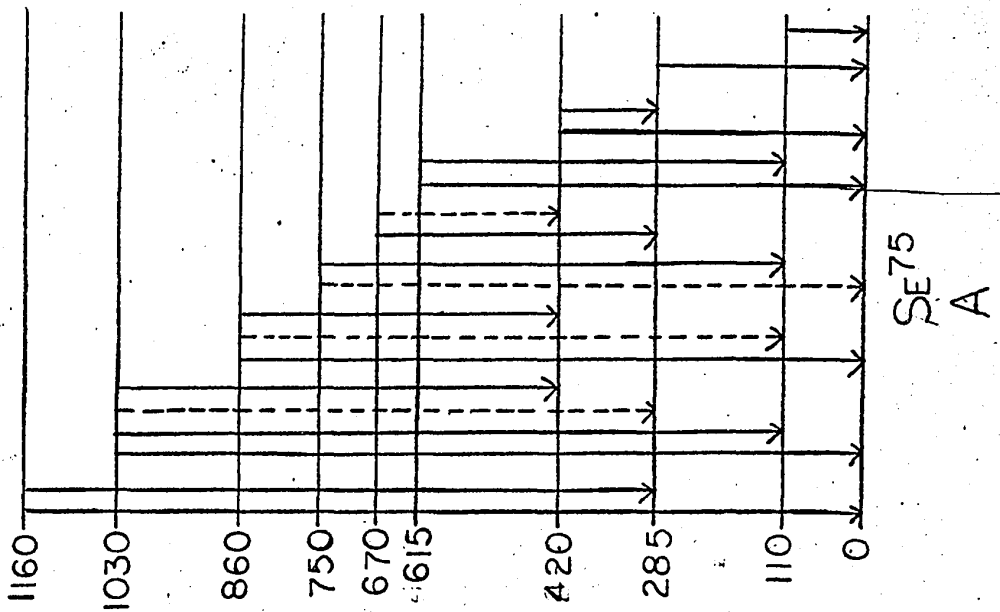
In the present work, seven gamma rays and five prominent branches of beta rays were observed. It is clear that neither of the two decay schemes suggested by the previous workers can quite accommodate the present results.

Figure 5.1-

A.- Decay scheme suggested by Lobkowitz et al

B.- Decay scheme suggested by Baskova et al

All energies are in keV.



In the remaining of this chapter, a decay scheme for  $\text{Br}^{75}$  will be constructed utilising the information obtained in the present experiments.

## 5.2 Construction of the decay scheme

Before discussing the possible decay scheme for  $\text{Br}^{75}$ , it is helpful to summarize some of the important results obtained from measurements described in Chapters III and IV. The seven gamma rays identified as coming from the decay of  $\text{Br}^{75}$  have energies 111.8, 140.9, 286.5, 292.9, 377.3, 427.9 and 431.6 keV. They are all in coincidence with the 511 keV positron annihilation gamma ray. This implies that the observed gamma rays resulted from the positron decay of  $\text{Br}^{75}$  and that none of them is from an isomeric state in  $\text{Se}^{75}$  with a life time much longer than 60 ns., which is the resolving time of the fast coincidence unit. The 111.8 keV line is in coincidence with the 511 keV annihilation gamma ray only and the 140.9 keV line is in coincidence with the 286.5 and the 431.6 keV lines apart from the 511 keV gamma ray. In the spectrum coincident gated simultaneously by the 286.5 and the 292.9 keV lines, there are five gamma rays at 140.9, 286.5, 292.9, 377.3 and 431.6 keV. Furthermore, from the positron measurements there are at least five branches of positron decay of  $\text{Br}^{75}$  to states in  $\text{Se}^{75}$ . There may be other weak branches of beta

decay not observed in the present work because of the background problem. Based on the semi-empirical mass formula given by Seeger (Seeger, 1961) the separation between the ground state of  $\text{Br}^{75}$  and the ground state of  $\text{Se}^{75}$  is 3.02 MeV. From this together with the energies of the five beta branches it is concluded that  $\text{Br}^{75}$  positron decays to at least five excited states of  $\text{Se}^{75}$  with excitation energies about 270, 400, 540, 640 and 850 keV. The accuracy of these values depends on the accuracy of the semi-empirical mass formula and also of the endpoint energy measurements which are accurate to  $\pm 20$  keV.

Consider the 111.8 keV line first. It is in coincidence with the 511 keV line only. Probably this is just the first excited state in  $\text{Se}^{75}$ . Since the positron branch to this state was not observed, this must be a weak branch. The assignment of the 111.8 keV line to the decay of the first excited state to the ground state agrees with the observations of Elwyn et al and Lobkowicz et al.

The 286.5 and 431.6 keV lines were observed in the spectrum in coincidence with 140.9 keV gamma ray. This implies that there are at least three excited states of  $\text{Se}^{75}$  involved which decay down to the ground state through a cascading process (The 431.6 keV line is also in coincidence with the 286.5 keV line). By comparing the intensities of the three lines in the singles spectrum, it is seen that the 431.6 keV line must be coming from the

highest level and the 286.5 keV line must come from the lowest level since the former has the lowest and the latter has the highest intensity. This would mean that the three excited states are at 286.5, 427.5 and 859.0 keV. This result is further substantiated by the results of the positron endpoint energy measurements, from which it was deduced that there should be levels at about 270, 400 and 850 keV. The conclusion that there are two states at 286.5 and 427.5 keV is in agreement with the works of Elwyn et al and Lobkowicz et al.

Thus far there are no ambiguities. In the spectrum jointly gated by the 286.5 and 292.9 keV lines, in addition to the gamma rays at 140.9 and 431.6 keV, three more lines at 286.5, 292.9 and 377.3 keV appear. The 431.6 keV line is also in coincidence with the 140.9 keV line while the 292.9 keV line is not in coincidence with the 140.9 keV line. This shows that the 431.6 keV line is really in coincidence with the 286.5 keV line and not with the 292.9 keV line. There could be three major ways of arranging the other three gamma rays.

First, it is assumed that there are two 286.5 keV lines in coincidence with each other as well as two 292.9 keV lines in coincidence with each other, and the 377.3 keV line is in coincidence with the 292.9 keV line(s). The different positions in which the 377.3 keV transition could be placed are shown in Figs. 5.2A, 5.2B, 5.2C and

5.2D. Since the 377.3 keV line is more intense than the 292.9 keV line in the singles spectrum, the scheme shown in Fig. 5.2A is the only acceptable one.

Alternately, the 377.3 keV line can be considered to be in coincidence with the 286.5 keV line(s), leaving the other aspects of the decay scheme unchanged. Again the 377.3 keV transition could be placed in any of the three possible places as shown in Figs. 5.3A, 5.3B and 5.3C. However the decay scheme shown in Fig. 5.3C is unacceptable because in the spectrum coincident gated simultaneously by the 286.5 and the 292.9 keV lines the yield of the 286.5 keV line is much greater than that of the 377.3 keV line, while this decay scheme demands that the yield of the 377.3 keV line should be at least as much as that of the 286.5 keV line. So only the decay schemes shown in Figs. 5.3A and 5.3B are the acceptable ones.

The remaining alternatives are shown in Figs. 5.4A, 5.4B and 5.4C. In Fig. 5.4A, the 292.9 and the 377.3 keV lines are both above the 286.5 keV line. There is no 286.5 keV line in coincidence with itself. So the levels are situated at 111.8, 286.5, 427.5, 579.4, 663.8 and 859.0 keV. There could be one objection to this scheme. According to this scheme, one should expect equal intensities of the 286.5 and the 292.9 keV lines in the spectrum coincident gated with these two lines together. In reality however, the 286.5 keV line is much more intense than the 292.9

keV line. However this apparent discrepancy can be explained in the following way. When the energy selection window of the single channel analyzer is set on the 286.5 and the 292.9 keV lines, the window is also set on that part of the Compton tail of the 511 keV line with which all other gamma rays are in coincidence. As a result there would be a feedthrough of all the gamma rays proportional their yields in the spectrum in coincidence with the 511 keV gamma ray. This yield is very high for the 286.5 keV line and the feedthrough in this case is actually greater than the true coincidence yield. For the other lines the feedthroughs are not that important as the yields are comparatively smaller. We shall estimate this feedthrough later in our intensity measurements (Appendix).

In Fig. 5.4B, the 292.9 keV line is on top of the 377.3 keV line, so that there is no level at 579 keV but an additional one at 956.7 keV. In Fig. 5.4C, the scheme shown is essentially the same as in Fig. 5.4B except that there are two 286.5 keV levels in coincidence with each other giving rise to a level at 573 keV.

Now the correct decay scheme has to be sorted out from the six possibilities, shown in Figs. 5.2A, 5.3A, 5.3B, 5.4A, 5.4B and 5.4C.

In order to resolve these uncertainties, a  $4\pi$  Ge(Li) detector to study the gamma rays from  $\text{Br}^{75}$  was used. A  $4\pi$  detector by definition is a detector which encloses

the radioactive source in all directions. This increases the efficiency of the detector considerably. But the main advantage of such a detector lies in the following. Consider a gamma ray source which emits two gamma rays that are in coincidence with each other. In an ordinary detector only one of them will be detected most of the time. However in a  $4\pi$  detector, the two gamma rays would enter the detector simultaneously, no matter in which directions they are emitted, and as a result, the detector would have a large probability of giving an output pulse equal to the sum of the two gamma rays. So, with this detector one can actually observe the levels of the nucleus under investigation. Of course, a lot of single gamma rays are still 'seen'.

The detector used was a RCA Victor  $4\pi$  detector (development model) which was used together with a Tennelec TC 130 pre-amplifier. The resolution obtained was 4.3 keV for  $\text{Co}^{57}$  (122 & 136 keV) lines and 5.6 keV for  $\text{Co}^{60}$  (1.173 and 1.332 MeV) lines. Gamma ray peaks at roughly 111, 141, 286, 378, 427, 511, 576, 664 and 859 keV were observed. By comparing this spectrum with the singles spectrum obtained with the 25 c.c. Ge(Li) detector, we concluded that the sum energy peaks were at 427, 576, 664 and 859 keV.

Now if the decay scheme shown in Fig. 5.2A is correct, a sum peak at 670 keV should be observed. However in the sum spectrum a strong line at 664 keV rather than any line at 670 keV is 'seen'. Hence this scheme is rejected.

The scheme in Fig. 5.3A can be rejected because a level was observed at 576 keV and not at 586 keV as predicted by this scheme. However, it may be argued that the 586 keV line was not seen because the 292.9 keV line is extremely weak. But it seems highly unlikely that there would be two 286.5 and 292.9 keV transitions in the same nucleus.

Let us consider the scheme shown in Fig. 5.3B. A strong line at 664 keV - the difference between the 950 and the 286 keV levels is observed. This means that the 286.5 keV transition between the levels at 573 and 286.5 keV should be quite strong, so that a reasonably strong sum peak at 573 keV should be observed. However the peak seen at about 578 keV is very weak and this is incompatible with our conclusions based on this decay scheme. Furthermore, no sum peak at 586 keV was observed.

The scheme shown in Fig. 5.4B can be rejected at once as it envisages no sum peaks around 575 keV and there is a definitely a sum peak at 576 keV.

There is very little to choose between the schemes shown in Figs. 5.4A and 5.4C. In the sum spectrum there is a weak line at 576 keV. Scheme 5.4A predicts a line at 579 keV while scheme 5.4C predicts a sum peak at 573 keV. So definite conclusions cannot be drawn as the line observed at 576 keV is close enough to either of the expected lines at 579 keV as in 5.4A or the 573 keV line

as in 5.4C. Both these decay schemes are in agreement with the results of the positron measurements, from which it was concluded that  $\text{Br}^{75}$  populates at least five levels in  $\text{Se}^{75}$  at energies about 270, 400, 570, 640 and 850 keV.

From the intensity measurements carried out on the different gamma-gamma coincidence spectra, the positron branching ratios to the different levels in  $\text{Se}^{75}$  can be calculated. When the detailed intensity calculations were carried out, some discrepancies such as negative branching ratios were obtained in the scheme 5.4C, while no such discrepancies were obtained in the scheme 5.4A. Therefore the scheme shown in Fig. 5.4A is accepted as the correct one. The results of the detailed branching ratio calculations are shown in Table 5.1 and the details of the method employed for such a calculation is given in the Appendix.

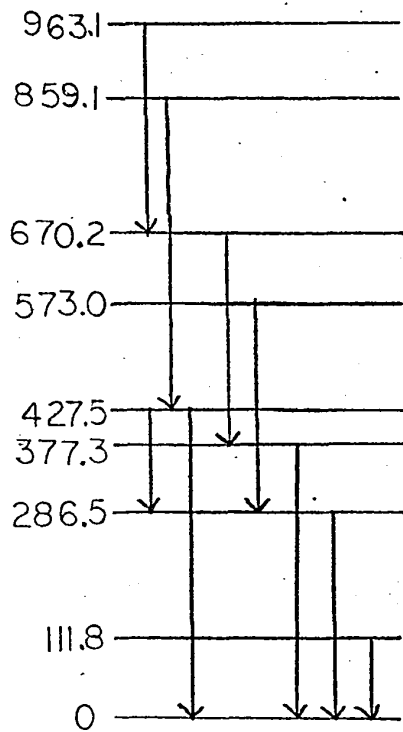
Branching ratio calculations showed that 90% of the total decay is by positron emission while electron capture accounts for the rest. The electron capture decays to the individual levels were also calculated and compared with the maximum theoretical values (Wapstra et al, 1959). Having already determined the endpoint energies of the positron branches, the half life and now the branching ratios, the  $\log (ft)$  values for the individual decay branches were computed (Verrall, 1966). The results are shown in Table 5.1. The final decay scheme is shown in Fig. 5.5.

Table 5.1

-----  
 Branching ratios and log(ft) values  
 -----

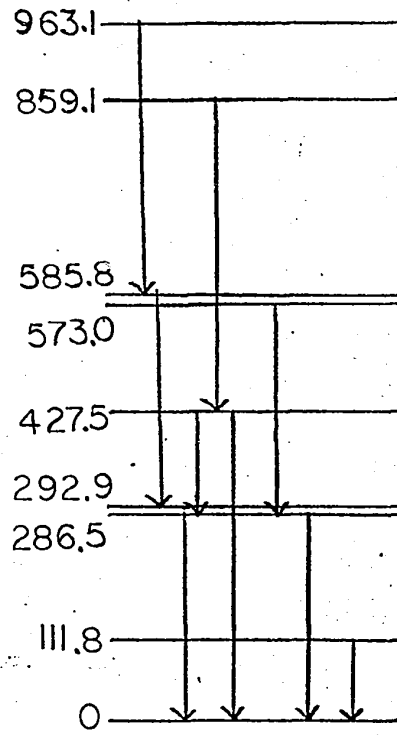
Energy levels in Se <sup>75</sup> key	% of positron decay	<u>Electron capture</u> Positron decay %	Threshold value %	log(ft)
0	0.0			
111.8	1.6	20	1515	7.0
286.5	84.2	0	20	5.1
427.5	5.4	20	25	6.2
579.4	1.8	42	40	6.4
663.8	5.7	5	47	5.8
859.0	1.3	280	120	6.2

Figure 5.2- Possible decay scheme. All energies  
are in keV.



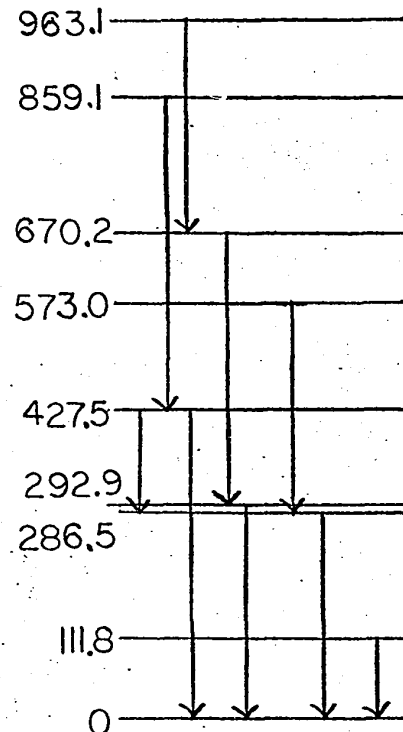
$Se^{75}$

A



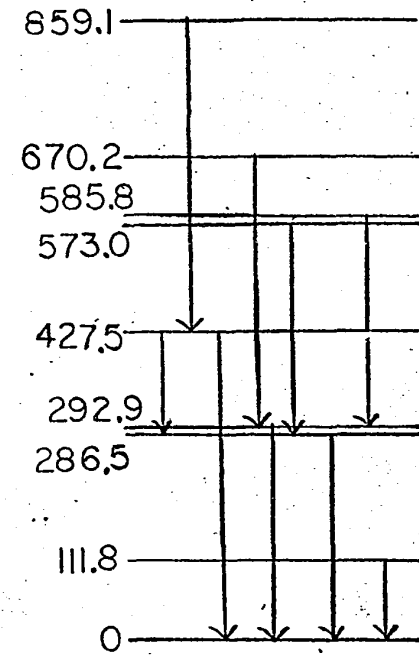
$Se^{75}$

B



$Se^{75}$

C

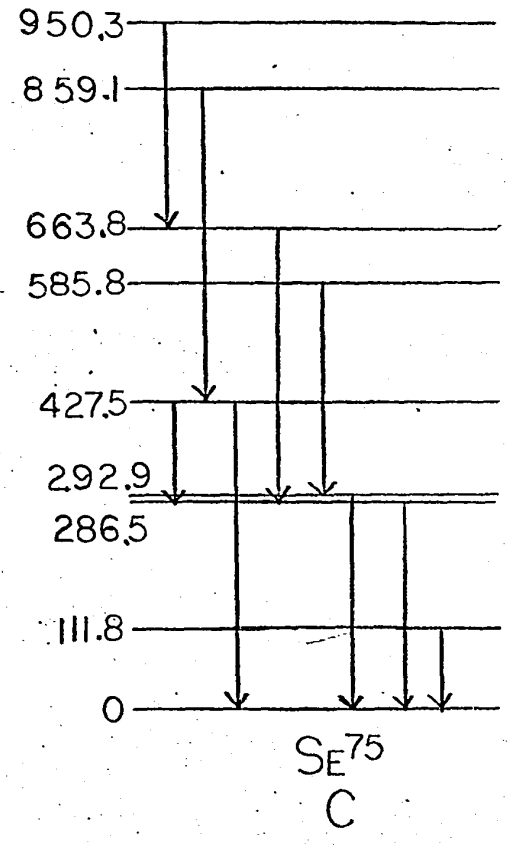
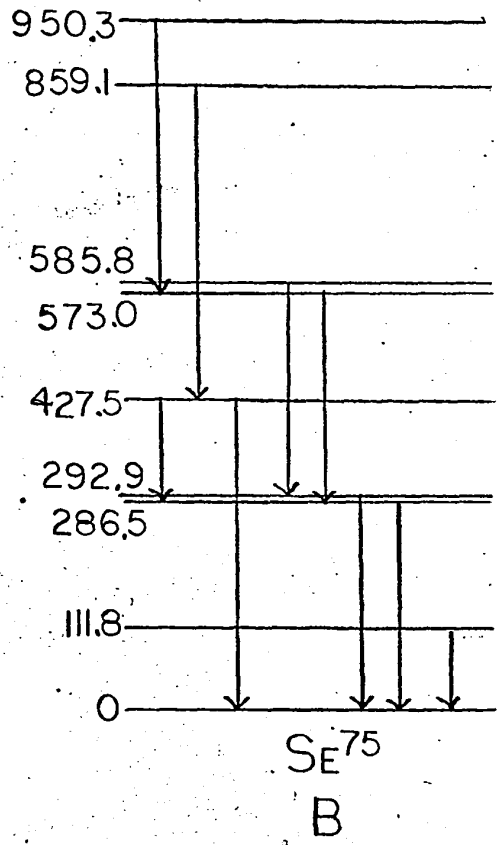
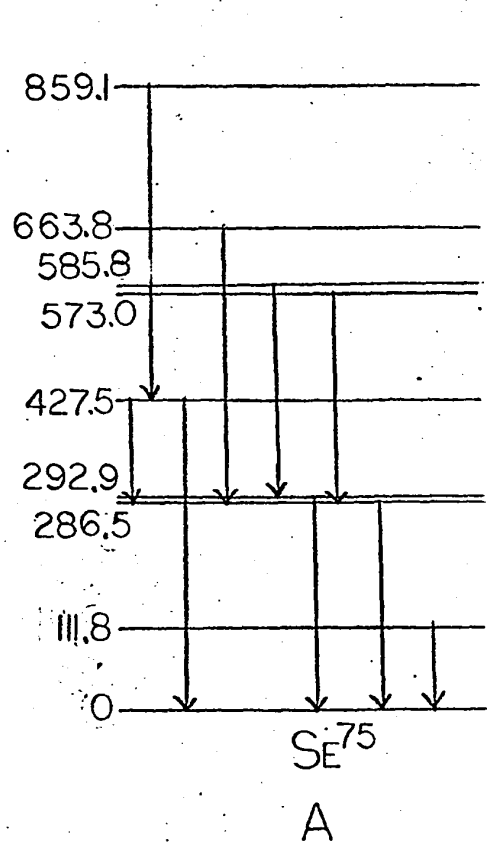


$Se^{75}$

D

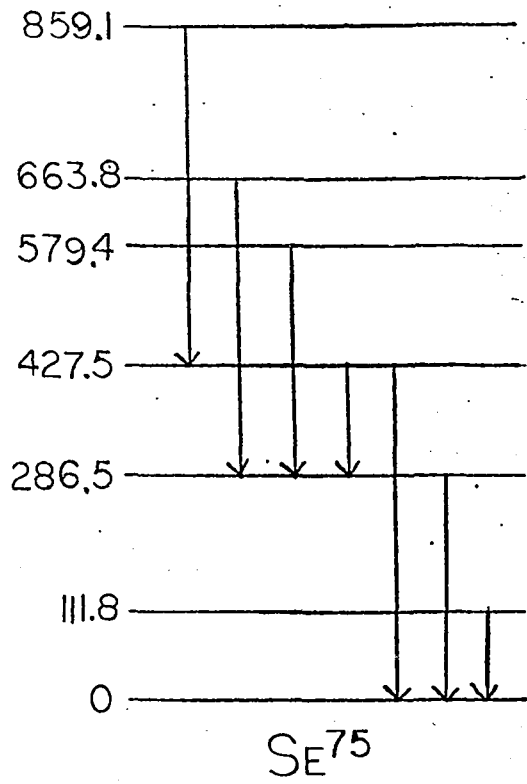
Figure 5.3- Possible decay schemes.

All energies are in keV.

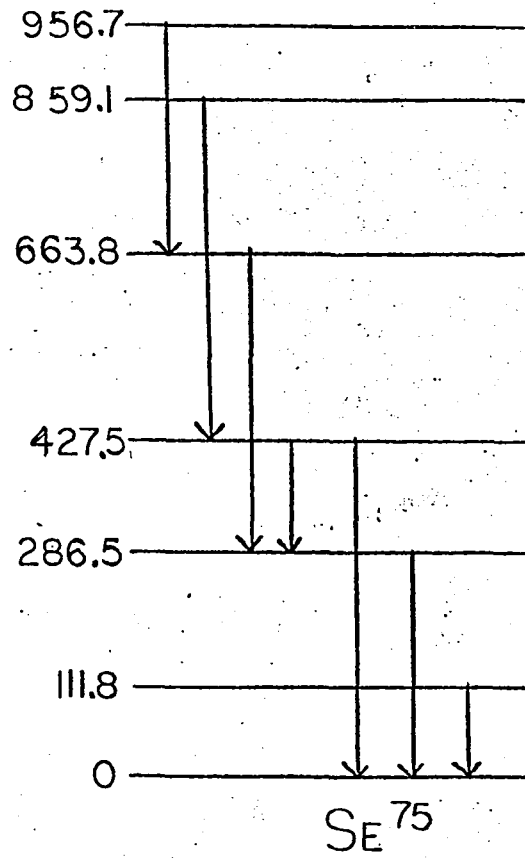


5.3

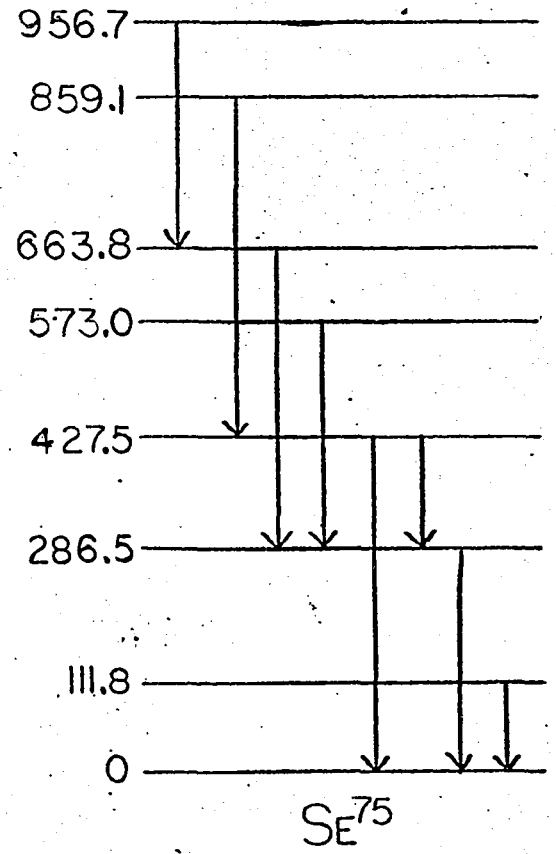
Figure 5.4- Possible decay schemes. All energies are in keV.



A

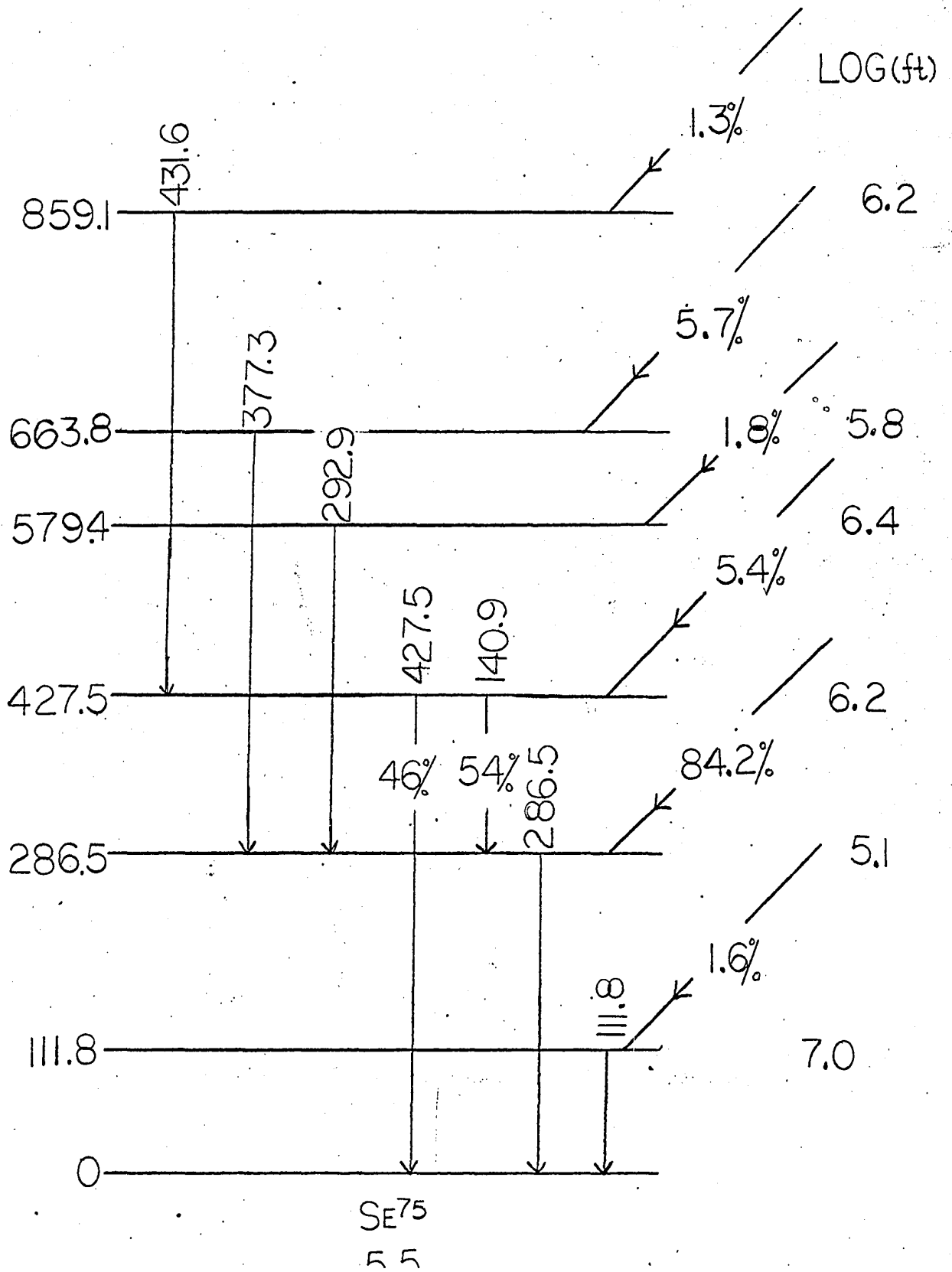


B  
5.4



C

Figure 5.5- Accepted decay scheme of  $\text{Br}^{75}$  with  
branching ratios and log (ft) values.  
All energies are in keV.



CHAPTER VI

---

Spins, Parities and Theoretical Discussions

---

6.1 Spins and Parities of the levels of  $\text{Se}^{75}$

---

The spin (J) and parity ( $\pi$ ) of the excited levels of  $\text{Se}^{75}$  are all unknown. The ground state spin and parity have been measured previously using microwave techniques (Lindgreen, 1964) and have been found to be  $\frac{5}{2}^+$ . The spin and parity of the parent state, viz. the ground state of  $\text{Br}^{75}$  are also unknown. However all other odd mass Bromine isotopes have ground state spin and parity  $\frac{3}{2}^-$ . Based on this nuclear systematic it is assumed that the spin and parity of  $\text{Br}^{75}$  ground state (g.s.) are  $\frac{3}{2}^-$ .

From the branching ratio calculations (Chapter V) it was found that 84% of the  $\text{Br}^{75}$  (g.s.) decay goes to the 286.5 keV state of  $\text{Se}^{75}$ . The log (ft) value of this transition is 5.1 which shows that the transition is of allowed type. Since the parent state has  $J^\pi = \frac{3}{2}^-$ , the 286.5 keV level can have  $J^\pi$  of any of the three values  $\frac{1}{2}^-$ ,  $\frac{3}{2}^-$  and  $\frac{5}{2}^-$ . The lifetime of the 286.5 keV level was measured in this laboratory by Muszynski (Muszynski, 1968) with a beta gamma delayed coincidence system. The half life of this level was found to be  $1.23 \pm 0.15$  ns. This represents a hindrance factor of roughly  $10^{-5}$  as compared to single

particle estimates for an electric dipole (E1) transition. This is typical of E1 transitions in this mass region (Perdrisat, 1968). This shows that the  $J^\pi$  of the 286.5 keV level has to be either  $\frac{3^-}{2}$  or  $\frac{5^-}{2}$ . The fact that this level exhausted 84% of the positron decay strength of  $\text{Br}^{75}$  indicates that some kind of similarity of nuclear structure exists between the two levels involved on the transition.

The level at 427.5 keV gamma decays to the ground state through two branches. There is a direct transition to the ground state which accounts for 46% of the decay while the rest cascade to the ground state through the intermediate state at 286.5 keV. The  $\log(ft)$  values for the positron decay to this level is 6.2 which shows that this transition is also allowed. So the  $J^\pi$  of this level has to be one of  $\frac{1^-}{2}$ ,  $\frac{3^-}{2}$  and  $\frac{5^-}{2}$ . If the  $J^\pi$  of this level is  $\frac{1^-}{2}$ , then the transition to the ground state would be a predominantly M2 or E3, while the transition to the 286.5 keV level would be either M1 or E2. As such the direct transition to the ground state would not be able to compete with the cascade transition through the 286.5 keV level. Since we observed roughly equal strengths for the two gamma decay branches, the possibility of  $J^\pi$  of  $\frac{1^-}{2}$  for this level can be ruled out. This leaves two possible  $J^\pi$  for the 427.5 keV level, viz. either  $\frac{3^-}{2}$  or  $\frac{5^-}{2}$ .

The  $\log(ft)$  value for the transition to the

579.5 keV level is 6.4, which indicates that this is also an allowed transition. So the possible  $J^\pi$  for this level are again  $\frac{1^-}{2}$ ,  $\frac{3^-}{2}$  and  $\frac{5^-}{2}$ . This level decays only to the 286.5 keV level and thence to the ground state. Similar argument applies to the 663.8 keV state whose positron branch decay  $\log (ft)$  is 5.8. The 859 keV state which decays to the 427.5 keV level and has a positron branch decay  $\log (ft)$  of 6.2 also has a possible  $J^\pi$  assignment of  $\frac{1^-}{2}$ ,  $\frac{3^-}{2}$  and  $\frac{5^-}{2}$ .

There are four possible combinations of spins for the 286.5 and the 427.5 keV levels. These are  $(\frac{3^-}{2}, \frac{3^-}{2})$ ;  $(\frac{3^-}{2}, \frac{5^-}{2})$ ;  $(\frac{5^-}{2}, \frac{3^-}{2})$  and  $(\frac{5^-}{2}, \frac{5^-}{2})$  for the two levels in that order respectively. In all the four cases, the 427.5 keV level would decay to the ground state by E1 and to the 286.5 keV state by M1 transitions. Since E1 transitions are usually hindered by several orders of magnitude, the E1 and M1 transitions from the 427.5 keV state could have roughly equal intensities as observed.

The 663.8 keV level can have either of the three spins  $\frac{5^-}{2}$ ,  $\frac{3^-}{2}$  and  $\frac{1^-}{2}$ . This level decays only to the 286.5 keV level. If its spin is either  $\frac{5^-}{2}$  or  $\frac{3^-}{2}$ , this state should decay to both the 286.5 and the 427.5 keV levels, irrespective of which one of the possible spin combinations these latter two levels have. If the 663.8 keV level is considered to have a spin of  $\frac{1^-}{2}$ , then transitions to both the 286.5 and the 427.5 keV levels

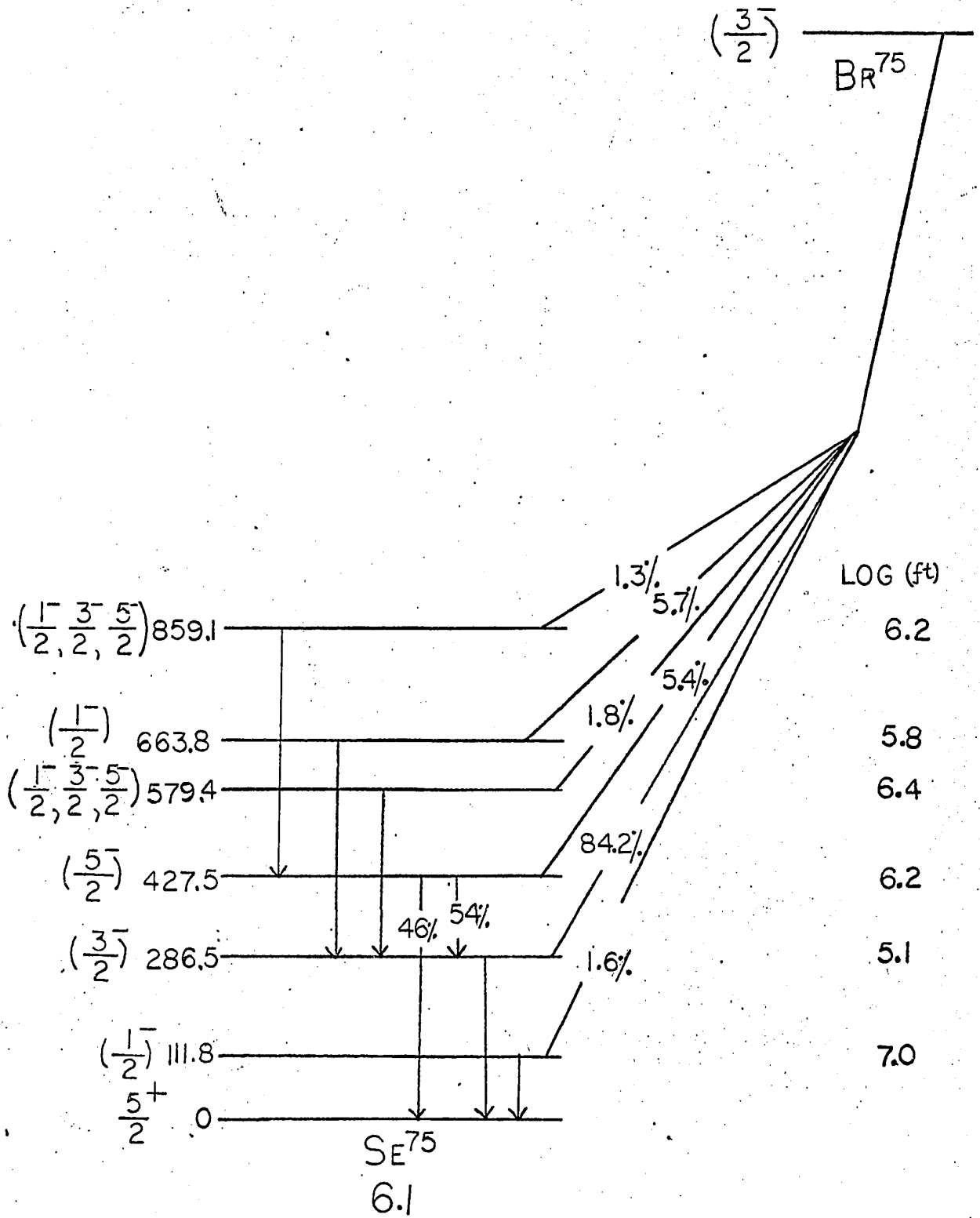
should be observed if the spins of these two states are either  $(\frac{3^-}{2}, \frac{3^-}{2})$  or  $(\frac{5^-}{2}, \frac{3^-}{2})$  or  $(\frac{5^-}{2}, \frac{5^-}{2})$  respectively. On the other hand, if these two levels have spins  $(\frac{3^-}{2}, \frac{5^-}{2})$  respectively, then the transition to the 286.5 keV level should be a M1 and energetically favoured while that to the 427.5 keV level would only be an E2. The M1 transition would be expected to dominate in this case and the 663.8 keV level should decay directly to the 286.5 keV level. So the most probable spins for the levels at 286.5, 427.5 and 663.8 keV are  $\frac{3^-}{2}$ ,  $\frac{5^-}{2}$  and  $\frac{1^-}{2}$  respectively.

The  $\log (ft)$  for the beta decay to the 111.8 keV level is 7.0 which means that it could be either an allowed or a first forbidden transition as there are frequent occurrences for large  $\log (ft)$  values for allowed transitions in this mass region. Since the  $\log (ft)$  value is too low for the beta transition to be a first forbidden unique one, the possible  $J^\pi$  values for this level are  $\frac{1^+}{2}$ ,  $\frac{3^+}{2}$  and  $\frac{5^+}{2}$  for a forbidden transition. On the other hand with so many allowed decay channels available, it seems highly unlikely that 1.6% of the transition should go through a forbidden decay. If indeed this is a forbidden transition, then  $\frac{5^+}{2}$  and  $\frac{7^+}{2}$  are the possible spins for this level because  $\frac{5^+}{2}$  is the lowest positive parity state that can occur in this region and this is the ground state. So the 111.8 keV level can only have a  $J^\pi$  of  $\frac{7^+}{2}$ , in which case the beta transition is first forbidden unique. Then

the  $\log (ft)$  value should be between 8 and 9 rather than 7. Moreover in all other odd mass neighbouring Selenium nuclei, the second positive parity state is usually situated at least  $\frac{1}{2}$  MeV above the first positive parity state. A  $J^\pi = \frac{7}{2}^+$  being situated only 111.8 keV above the ground state ( $\frac{5}{2}^+$ ) seems extremely unlikely.

There are quite a few allowed transitions with  $\log (ft)$  values of 7 or higher in this mass region. These are normally associated with some kind of selection rule violation in certain nuclear models. If this is the case, then the 111.8 keV level would have a  $J^\pi = \frac{1}{2}^-$ ,  $\frac{3}{2}^-$  or  $\frac{5}{2}^-$ . Furthermore, from the level scheme systematics of the odd mass Selenium isotopes ( $\text{Se}^{77}$ ,  $\text{Se}^{79}$ ,  $\text{Se}^{81}$  etc.), there is always a  $\frac{1}{2}^-$  state alternating with the lowest anomalous coupling state (the lowest positive parity state) as the ground state and separated by about 100 keV. It is highly probable that the first excited state at 111.8 keV in  $\text{Se}^{75}$  is a  $J^\pi = \frac{1}{2}^-$  state with the anomalous coupling state  $\frac{5}{2}^+$  as the ground state. However the assignment of a  $J^\pi = \frac{1}{2}^-$  to the 111.8 keV level would give rise to other problems. Its decay to the ground state would then be through an M2 transition, which in the single particle estimate, has a half life of the order of 1  $\mu\text{s}$  in this mass region for this energy. As the resolving time of the coincidence unit used was 60 ns. this gamma ray should not be observed in coincidence with the 511 keV annihilation gamma ray. Again

Figure 6.1- Suggested Spins and Parities of  
different levels of  $\text{Se}^{75}$ . All  
energies are in keV.



if this level does not have  $J^\pi = \frac{1}{2}^-$ , then there should be a  $\frac{1}{2}^-$  level in this region which would definitely be populated in the positron decay of  $\text{Br}^{75}$  ground state. It could be argued that this  $\frac{1}{2}^-$  state does not decay to the ground state ( $\frac{5}{2}^+$ ) by M2, but beta decays directly to a negative parity state in  $\text{As}^{75}$  as in the case of the corresponding  $\frac{1}{2}^-$  level in  $\text{Se}^{73}$ . However it is difficult to understand how the beta decay can compete with the M2 transition to the ground state of  $\text{Se}^{75}$ , since the single particle estimate for the half life of the M2 transition is of the order of 1  $\mu\text{s}$ . If this level is assigned a  $J^\pi = \frac{3}{2}^-$  or  $\frac{5}{2}^-$ , then there should be at least some higher levels decaying through this level to the ground state. But no other gamma rays were found to be in coincidence with the 111.8 keV line. So the position of the  $\frac{1}{2}^-$  state and its relation to the 111.8 keV level remain puzzling.

## 6.2 Theoretical discussions

The shell model description of  $\text{Se}^{75}$  is complicated. According to the simplest manifestation of this model, the last odd neutron in  $\text{Se}^{75}$  should be in the  $1g_{9/2}$  subshell and so the ground state spin should be  $\frac{9}{2}^+$ . This however is not the case with the ground state spin being  $\frac{5}{2}^+$ . This can be explained if it is assumed that  $\text{Se}^{75}$  has a proton configuration  $(2p_{3/2})^2 (1f_{5/2})^4 (1d)$  and a neutron configuration  $(2p_{3/2})^4 (1f_{5/2})^6 (1g_{9/2})^3$  with the three

neutrons in the  $1g_{9/2}$  subshell coupling to a spin  $\frac{5}{2}^+$  with seniority 3. The  $\frac{3}{2}^-$  level at 286.5 keV can be considered as having a neutron configuration  $(2p_{3/2})^3 (1f_{5/2})^6 (1g_{9/2})^4$  and the  $\frac{5}{2}^-$  excited level at 427.5 keV could have a  $(2p_{3/2})^4 (1f_{5/2})^5 (1g_{9/2})^4$  configuration for neutrons. A  $\frac{1}{2}^-$  excited level can be considered as either a  $(2p_{3/2})^2 (1f_{5/2})^6 (2p_{1/2}) (1g_{9/2})^4$  or a  $(2p_{3/2})^4 (1f_{5/2})^4 (2p_{1/2}) (1g_{9/2})^4$  configuration. The  $\text{Br}^{75}$  ground state can be considered as a proton configuration of  $(2p_{3/2})^3 (1f_{5/2})^4$  and a neutron configuration of  $(2p_{3/2})^2 (1f_{5/2})^6 (1g_{9/2})^4$ . The positron transition to the  $\frac{3}{2}^-$  level could occur by converting a proton in the  $(2p_{3/2})$  shell to a neutron in the same shell in which case this would be a Fermi transition. Alternately the  $\text{Br}^{75}$  ground state could be considered as having a configuration of  $(2p_{3/2})^4 (1f_{5/2})^3_{3/2}$  for the protons and a configuration of  $(2p_{3/2})^4 (1f_{5/2})^4 (1g_{9/2})^4$  for the neutrons. The positron decay to the  $\frac{5}{2}^-$  level in  $\text{Se}^{75}$  takes place when a proton in the  $(1f_{5/2})$  shell becomes a neutron in the same shell. The weak beta branch to this level can be explained on the basis of a small admixture of this particular configuration in the ground state wave function of  $\text{Br}^{75}$ . A detailed description on the basis of a shell model is known to be inadequate for nuclei in this region.

A better description of  $\text{Se}^{75}$  could be given in terms of couplings between the collective modes of motion and the single particle levels. The even-even

nuclei in this medium mass region exhibit typical vibrational spectra. Different states in  $\text{Se}^{75}$  can be considered as different modes of coupling between the extra-core neutron and the even-even core  $\text{Se}^{74}$ . The ground state ( $\frac{5^+}{2}$ ) can be considered as one of the states resulting from the coupling between a  $2^+$  phonon state of the core with a  $1g_{7/2}$ -neutron. The  $\frac{3^-}{2}$  and the  $\frac{5^-}{2}$  states could be generated by coupling a  $2^+$  phonon state to a  $2p_{1/2}$  neutron while the  $\frac{1^-}{2}$  state could be viewed as a result of coupling a 0 phonon core with a  $2p_{1/2}$  neutron. A coupling between a 0 phonon core and a  $2p_{3/2}$  neutron would also generate the  $\frac{3^-}{2}$  state. Calculations with this model would involve the solution of the Schrodinger equation with a Hamiltonian which includes the single particle, the pairing and the quadrupole terms using the BCS theory and the Random Phase Approximation. This requires lengthy numerical computations. Calculations along this line have been performed recently by Goswami et al (Goswami et al, 1968) on  $\text{Tc}^{99}$ ,  $\text{Rb}^{101}$  and  $\text{Ag}^{109}$ . Their results are rather encouraging.

CHAPTER VII

-----

The "107" keV gamma ray

-----

7.1 Introduction

-----

In Chapter III we noted that while studying the gamma rays subsequent to the decay of  $\text{Br}^{75}$  we observed a gamma ray of 107 keV with a half life of  $4.6 \pm 0.5$  mins.

This line cannot be ascribed to the decay of an isomeric state of  $\text{Se}^{75}$  as it fails to show the half life (106 min.) of the parent state. The other possible assignment for this line is to attribute it to an isomeric state in the parent nucleus itself viz.  $\text{Br}^{75}$ . This assignment seems all the more justified if we examine all other neighbouring odd mass Bromine isotopes.  $\text{Br}^{77}$  has an isomeric state at 108 keV with a half life of 4.2 mins.  $\text{Br}^{79}$  has a level at 210 keV with a half life of 4.8 sec., and  $\text{Br}^{81}$  has a level at 570 keV (although this is the second excited state) with a half life of 37  $\mu\text{s}$ .

However there is a probability that the 107 keV line actually arises from  $\text{Br}^{77}$  and not from  $\text{Br}^{75}$ . The target used has 86.1%  $\text{Se}^{76}$  and 4.4% of  $\text{Se}^{78}$ . The (p,2n) reaction on  $\text{Se}^{78}$  would produce  $\text{Br}^{77}$ . This isomeric state decays to the ground state, as already mentioned above, with a known half life of 4.2 min. and an energy of 108 keV

which are within the measured values of the present work. Also  $\text{Br}^{77}$  ground state has a half life of 57 hours so that we would not observe the gamma rays emitted subsequent to its decay to  $\text{Se}^{77}$ . However from the first glance at the intensity of the observed 107 keV line, it did not seem that all the contributions was from  $\text{Br}^{77}$  because the target contained only 4.4%  $\text{Se}^{78}$  contamination. In order to identify its origin properly we undertook the following studies.

## 7.2 Study of production threshold and yield

-----

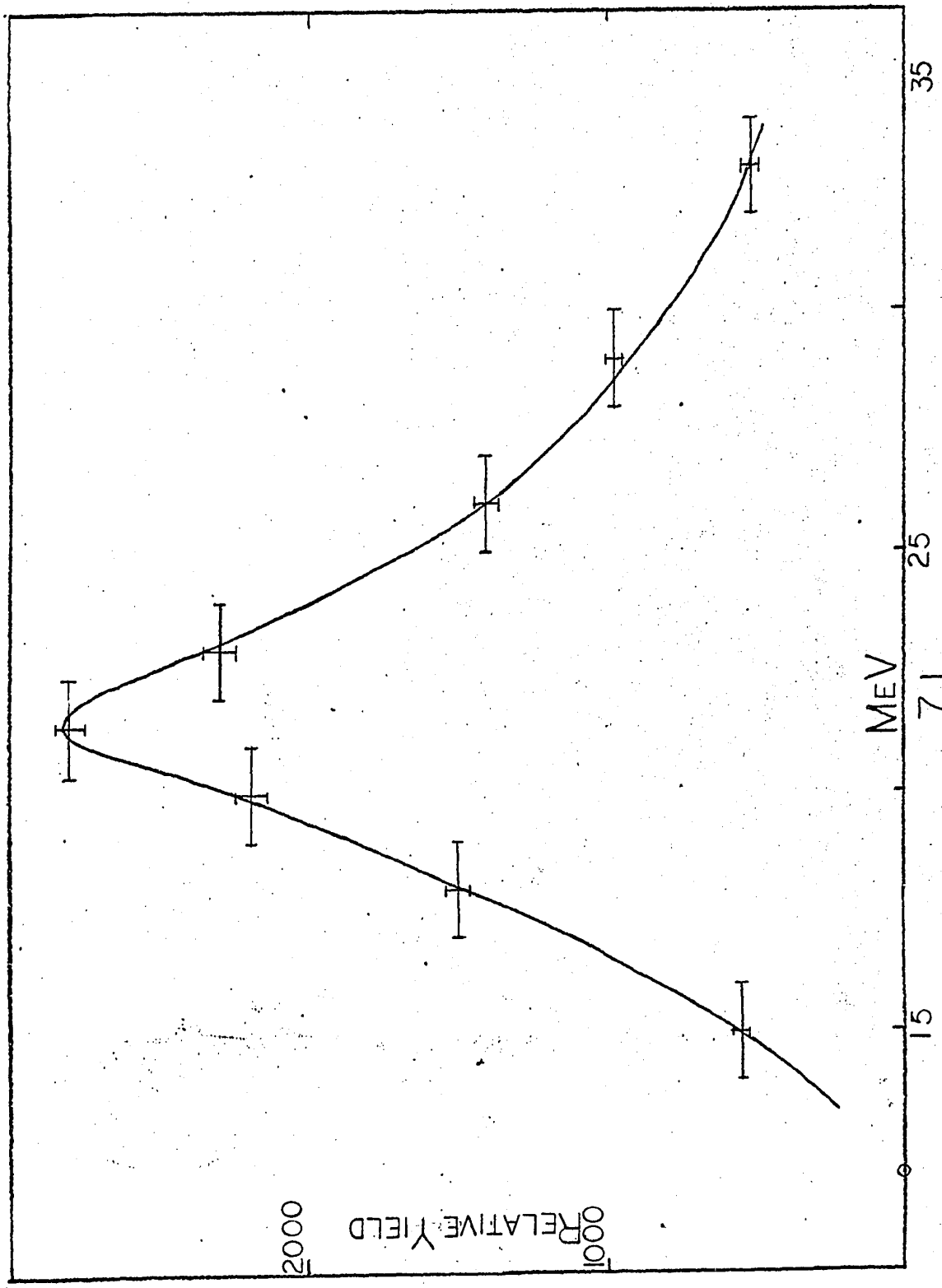
We performed a threshold and yield study of this 107 keV line to see exactly which  $(p, xn)$  reaction produced it. We prepared an enriched  $\text{Se}^{76}$  target by dissolving it in hot concentrated nitric acid and then boiled away the excess acid. A couple of drops of this solution was then deposited on an aluminium backing about a quarter of a mil. thick. The solution was then left to dry in a dessicator at room temperature. This slow drying process ensured that the solute was deposited more or less uniformly on the backing material.

Once the target was ready, we bombarded it with protons at different energies and calculated the yield of the 107 keV line. The same target was used in each bombardment using the same beam current viz. 1  $\mu\text{A}$  of protons and the bombardment lasted for the same interval of time

(20 seconds). Counting started exactly 5 mins. after the end of each bombardment and lasted for 10 mins. in each case. The position of the source with respect to the Ge(Li) detector was kept identical for each counting. After each counting of the yield, the source was allowed to die down over a period of 4 half lives of the long lived Br<sup>75</sup> ground state before the next bombardment was done to make sure that there was no significant activity left for the next bombardment.

All these precautions made sure that while calculating the relative yields, we would not have to make corrections for varying amount of source material, beam strength and geometry. The yields were calculated and have been plotted against the energy of bombardment in Fig. 7.1. The yield curve shows that no activity is produced at 12 MeV. In this context we should remember that the thresholds for (p,2n) reactions on Se<sup>76</sup> and Se<sup>78</sup> are respectively 13.7 and 14.5 MeV as calculated from the empirical mass Tables (Seeger, 1961). The maximum (p,n) cross-section should come at about 11 and 13 MeV for these two nuclei in that order. The 107 keV line is first noticed at 15 MeV, and the highest yield is obtained at 21.5 MeV. The thresholds for (p,3n) reactions on Se<sup>76</sup> and Se<sup>78</sup> are respectively at 25 and 23 MeV. As the peak cross-section for a (p,xn) reaction occurs just before the threshold of (p,(x+1)n) reaction we can positively say that the 107 keV line is being produced

Figure 7.1- Relative Yield of the 107 keV line  
against Energy of bombardment.



by the (p,2n) reaction.

### 7.3 Study of (p,2n) reaction on natural Selenium

We also studied the yield of the 107 keV line produced by the (p,2n) reaction on natural Selenium. We list below the compositions of both natural Selenium and the enriched isotope target we have been using.

#### Composition of Selenium

<u>Mass No.</u>	<u>Enriched</u>	<u>Natural</u>
74	< 0.2%	0.87%
76	86.1%	9.02%
77	2.0%	7.55%
78	4.4%	23.52%
80	5.9%	49.82%
82	1.6%	9.19%

Let us assume for the moment that the 107 keV line is produced from both  $\text{Se}^{76}$  and  $\text{Se}^{78}$ . Let  $\frac{\sigma_{107}}{76}$  and  $\frac{\sigma_{107}}{78}$  be the yields of the 107 keV gamma ray from unit quantities of  $\text{Se}^{76}$  and  $\text{Se}^{78}$  respectively. Since the 286.5 keV line is produced only from  $\text{Se}^{76}$  let  $\frac{\sigma_{286.5}}{76}$  be the yield of the 286.5 keV gamma ray produced from unit quantity of  $\text{Se}^{76}$ . We bombarded both the natural and enriched Selenium at 20 MeV

with 1  $\mu$ A of proton beam for 20 sec. and the yields of the 107 and 286.5 keV lines were recorded in both cases for 10 min. starting exactly 5 min. after the bombardment ended. We should note that the  $\sigma$ 's defined above are not directly proportional to the production cross-sections as they also include the life time factors of the two lines involved. We then have

i) Enriched Selenium yields

$$\text{Yield of the 286.5 keV line} = \frac{\sigma_{286.5}}{76} \times 86.1 \quad \text{----- (1)}$$

$$\text{Yield of the 107 keV line} = \frac{\sigma_{107}}{76} \times 86.1 + \frac{\sigma_{107}}{78} \times 4.4 \quad \text{----- (2)}$$

ii) Natural Selenium yields

$$\text{Yield of the 286.5 keV line} = K \times \frac{\sigma_{286.5}}{76} \times 9.02 \quad \text{----- (3)}$$

$$\text{Yield of the 107 keV line} = K \times \left[ \frac{\sigma_{107}}{76} \times 9.02 + \frac{\sigma_{107}}{78} \times 23.52 \right] \quad \text{--- (4)}$$

Although we have made the proton current, the bombarding and the recording times the same, we still have to consider the unequal source strengths resulting from the unequal amount of material used to prepare the two targets. The constant "K" represents this factor.

From eqns. (1) and (3) we obtained the value of K and then from eqns. (2) and (4) we solved for  $\frac{\sigma_{107}}{76}$  and  $\frac{\sigma_{107}}{78}$ . We found that the quantity  $\frac{\sigma_{107}}{76} \approx 0$  and in eqn. (2)  $\frac{\sigma_{107}}{78} \times 4.4$  contribute 98% of the total yield from the enriched

target. Hence we conclude that the 107 keV level is actually the first excited state of  $\text{Br}^{77}$  and not a hitherto unreported state in  $\text{Br}^{75}$  as we initially suspected.

#### 7.4 Conversion Electrons from the 107 keV level

-----

The 107 keV level has a comparatively long half life for an isomeric state of this energy. So this transition should have a high electron internal conversion ratio. Accordingly we undertook a study of the internal conversion coefficient to determine the multipolarity of the transition.

The sources for studying the electrons were prepared in an identical manner as that for the study of the yield curve. For electron study the sources have to be specially uniform and thin, a requirement not vital for gamma ray study. The backing material (aluminium) was of 1 mil. thickness which comes to  $6611 \text{ mg/cm}^2$ . The thickness of the deposited Selenium was about  $200 \text{ } \mu\text{g/cm}^2$ . The average loss of energy by an electron of 100 keV in  $200 \text{ } \mu\text{g/cm}^2$  of Selenium is less than 2 keV.

For measuring the conversion coefficient, the mini-chamber was used. The beta detector was the 1 mm Si(Li) detector. This detector has a very low gamma efficiency and hence was ideal for the study of low energy electrons. The source was placed in the mini-chamber facing the

electron detector. A vacuum better than  $10 \mu$  was always maintained inside the chamber. The gamma detector used was the 25 c.c. co-axial Ge(Li) detector placed outside the thin (15 mil.) brass window of the mini-chamber. The electron and the gamma spectra were recorded for the same time on two successive 1024 channel-groups of a 4096 channel TMC kicksorter. Thus any correction for timing was eliminated. The relative efficiencies of the gamma and the beta detectors were determined by measuring the conversion coefficient of the 570 keV line Bi<sup>207</sup> which is well known. We assumed that the efficiency of the charged particle detector remained fairly constant within the energy range. The efficiency of the gamma detector in this particular geometry was measured with standard sources and has been shown in Fig. 2.5.

The ratio  $\frac{\alpha_K}{\alpha_{L+M+N+\dots}}$ , the K-shell internal conversion coefficient to the L+M+N+... internal conversion coefficient was measured thrice. The absolute K, L+M+N+..., and total internal conversion coefficients,  $\alpha_K$ ,  $\alpha_{L+M+N+\dots}$ , and  $\alpha_{tot}$ , respectively, were measured twice. The results are presented in Table 7.1.

Table 7.1

## Internal Conversion Coefficients (Experimental)

Measurement No.	$\alpha_K$	$\alpha_{L+M+..}$	$\alpha_{tot}$	$\frac{\alpha_K}{\alpha_{L+M+..}}$
1				3.3878
2	5.45	1.55	7.00	3.52
3	5.49	1.50	6.99	3.64

The theoretical values (Sliv et al, 1968) for the different internal conversion coefficients are shown in Table 7.2 below.

Table 7.2

## Internal Conversion Coefficients (Theoretical)

Transition	$\alpha_K$	$\alpha_{L+M+..}$	$\alpha_{tot.}$	$\frac{\alpha_K}{\alpha_{L+M+..}}$
E1	$7.03 \times 10^{-2}$	$7.60 \times 10^{-3}$	$7.79 \times 10^{-2}$	9.25
E2	$6.97 \times 10^{-1}$	$9.90 \times 10^{-2}$	$7.96 \times 10^{-1}$	7.50
E3	5.65	1.55	7.20	3.64
E4	$4.44 \times 10^2$	$2.46 \times 10^1$	$4.69 \times 10^2$	$1.80 \times 10^1$
E5	$3.39 \times 10^2$			

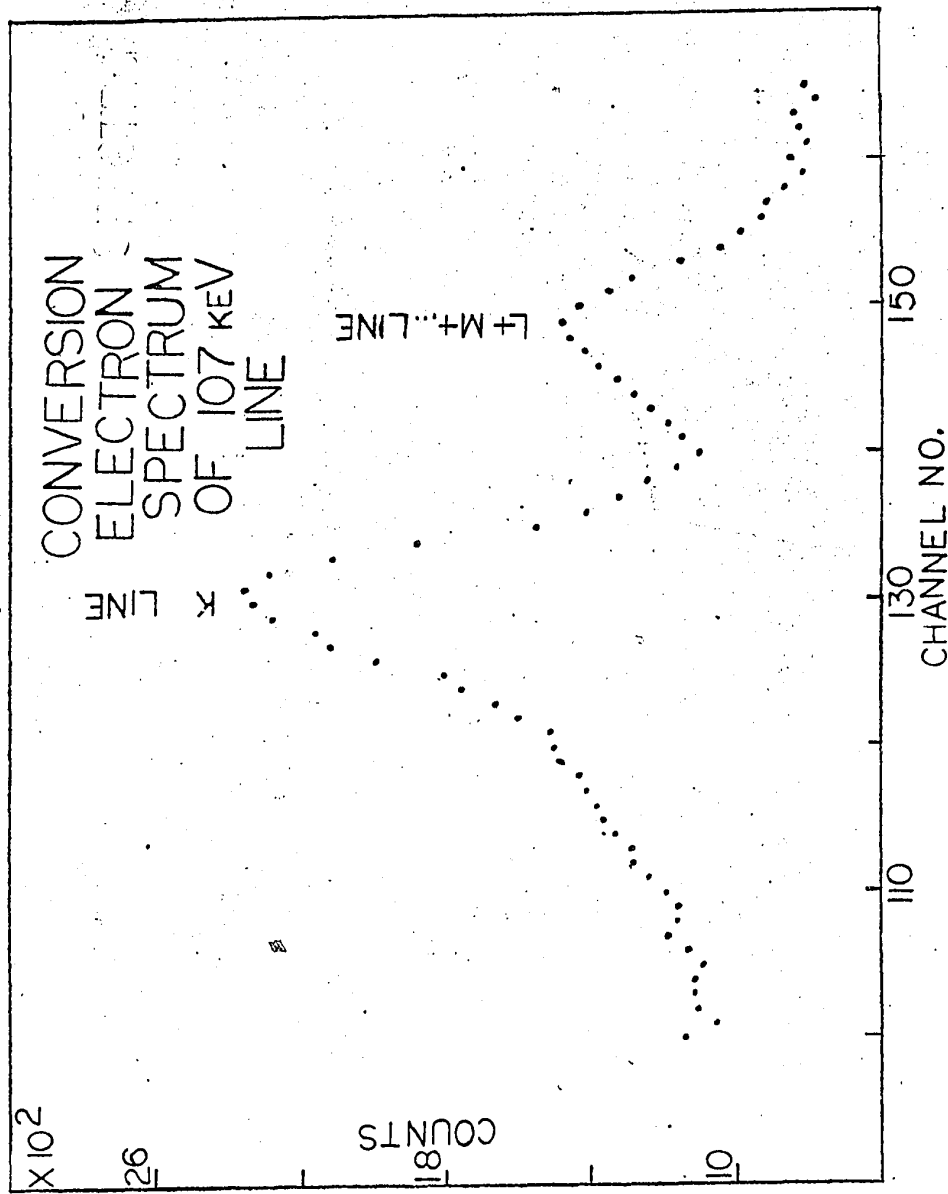
(contd.)

Table 7.2 (contd.)

Transition	$\alpha_K$	$\alpha_{L+M+..}$	$\alpha_{tot.}$	$\frac{\alpha_K}{\alpha_{L+M+..}}$
M1	$9.56 \times 10^{-2}$	$1.10 \times 10^{-2}$	$1.07 \times 10^{-1}$	8.70
M2	$9.48 \times 10^{-1}$	$1.36 \times 10^{-1}$	1.08	6.92
M3	8.65	1.72	$1.04 \times 10^1$	5.05
M4	$7.74 \times 10^1$	$1.28 \times 10^1$	$9.02 \times 10^1$	6.05
M5	$7.10 \times 10^2$			

From these values we see that the measured internal conversion coefficients are very close to those of a pure E3 transition. The ratio  $\frac{\alpha_K}{\alpha_{L+M+..}}$  has previously been reported by Thulin (Thulin, 1955) to be equal to 3.60. Our results confirm that measurement and also verifies the conclusion that the transition is a pure E3 one. The ground state spin being  $\frac{3}{2}^-$  the isomeric state must have a spin of  $\frac{9}{2}^+$ . If we examine the other odd mass Bromine isotopes, we find that all the isomeric states observed therein have spins  $\frac{9}{2}^+$  and decay by pure E3 transition to the ground states all of which have spins  $\frac{3}{2}^-$ .

Figure 7.2- Internal Conversion Electron spectrum  
of the 107 keV gamma ray recorded with  
1 mm Si(Li) detector.



7.2

CHAPTER VIII

Gamma rays from Br<sup>74</sup>

8.1 Introduction

In Chapter VI, a formalism which attempts to explain the level scheme of Se<sup>75</sup> in terms of couplings of an extra core neutron with the phonon states of the even-even core Se<sup>74</sup>, was discussed. Thus a knowledge of the level scheme of Se<sup>74</sup> would facilitate detailed calculations of the structure of Se<sup>75</sup> based on this formalism. It was with this view that a search for gamma rays following the positron decay of Br<sup>74</sup> was undertaken.

8.2 History of previous works

Temmer et al (Temmer et al, 1956) studied the gamma ray transitions in Se<sup>74</sup> by means of Coulomb excitations with alpha particles of energies up to 7 MeV. The gamma rays were detected by a 5 cm by 4 cm NaI(Tl) detector. They observed only one gamma ray at 634 keV and this they identified as coming from the decay of the first 2<sup>+</sup> state. Observations on other neighbouring nuclei showed that all even-even nuclei in this mass region exhibit typical vibrational spectra.

While studying the transmutations of Copper

by Nitrogen and Oxygen ions, Beydon et al (Beydon et al , 1957) observed a gamma ray of energy  $640 \pm 10$  keV with a half life of  $42 \pm 4$  mins. from  $\text{Br}^{74}$ . Butement et al (Butement et al, 1960) found a gamma ray of 635 keV with a half life of 26 min. following the positron decay of  $\text{Br}^{74}$ . Eichler et al (Eichler et al, 1962) observed the 635 keV gamma ray following the electron decay of  $\text{As}^{74}$  while examining the gamma rays from  $\text{Ga}^{74}$  and  $\text{As}^{74}$  for constructing the decay scheme of  $\text{Ge}^{74}$ . However the life time of the 635 keV transition was not studied. Gangrskii et al (Gangrskii et al, 1962) Coulomb excited the  $\text{Se}^{74}$  nucleus with 8.5 MeV alpha particles and found a level at  $1373 \pm 20$  keV. They concluded that this is the second  $2^+$  state of  $\text{Se}^{74}$ .

### 8.3 Gamma rays from the decay of $\text{Br}^{74}$

---

$\text{Br}^{74}$  was produced via (p,3n) reaction on  $\text{Se}^{76}$ . A target enriched in  $\text{Se}^{76}$  was bombarded in the McGill synchro-cyclotron with 1  $\mu\text{A}$  of proton current for 20 seconds. The threshold for (p,3n) reaction on  $\text{Se}^{76}$  is 25 MeV and that for (p,4n) reaction is 36 MeV. Since the maximum (p,3n) cross-section is obtained at about 1 MeV above the threshold for (p,4n) cross-section, the bombardment was done at 38 MeV.

The gamma rays were studied with the 25 c.c. co-axial Ge(Li) detector. The resolution obtained was 2.2 keV FWHM for  $\text{Co}^{57}$  (122 & 136 keV) lines and 3.0 keV for  $\text{Co}^{60}$

(1.17 & 1.33 MeV) lines. While producing  $\text{Br}^{74}$  via the (p,3n) reaction,  $\text{Br}^{76}$  and  $\text{Br}^{75}$  were also produced via the (p,n) and (p,2n) reactions respectively. However all the gamma rays from  $\text{Br}^{76}$  and  $\text{Br}^{75}$  as well as their half lives are well known and they could be easily separated from those of  $\text{Br}^{74}$ . Half lives of gamma rays upto 4 MeV were traced while searching for gamma rays following the positron decay of  $\text{Br}^{74}$ .

Two gamma rays with energies  $633.9 \pm 1$  keV and  $732.1 \pm 1$  keV were observed. The half life was found to be  $42 \pm 4$  mins. The half life curves are shown in Fig.8.1. The intensity of the 633.9 keV line was found to be 4.2 times that of the 732.1 keV line. This latter gamma ray has not been reported before.

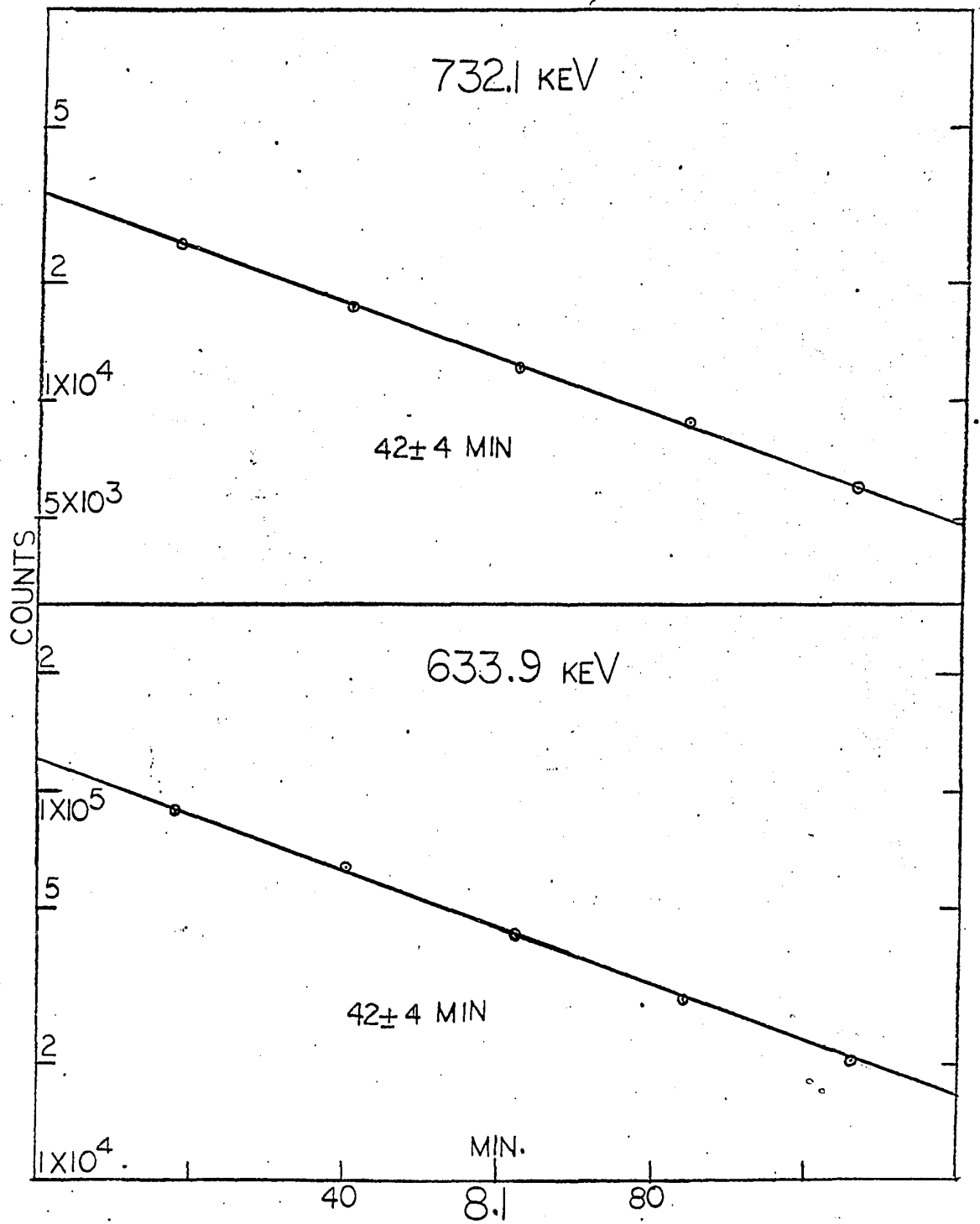
As other even-even Selenium isotopes have vib vibrational energy spectra, it is expected that  $\text{Se}^{74}$  would also display vibrational spectrum. So the ground state of  $\text{Se}^{74}$  would be a  $0^+$  state and the first excited state at 633.9 keV would be a  $\lambda = 2$  one-phonon state having a spin of  $2^+$ . The next group of excited states are expected to arise from the couplings of two  $\lambda = 2$  phonons and this multiplet should consist of three levels with spins  $0^+$ ,  $2^+$  and  $4^+$ . This second  $2^+$  state has been observed at  $1373 \pm 20$  keV by Gangrskii et al. This state should have a strong electromagnetic transition to the first  $2^+$  state and give rise to an approximately 738 keV transition, and this

probably corresponds to the 732.1 keV line observed in the present work. The  $0^+$  and  $4^+$  states, the other two members of the  $\lambda = 2$  phonon triplet, are expected to lie quite close to the second  $2^+$  excited state. This prediction seems justified if we examine the neighbouring even-even nuclei. In  $\text{Se}^{76}$ , the three states lie within 250 keV of each other. In  $\text{Se}^{78}$ , these three states lie within 200 keV of one another. Since no other gamma rays below 2 MeV have been found, except the two listed above, it seems that the  $0^+$  and  $4^+$  states in the multiplet are not populated in the positron decay from the ground state of  $\text{Br}^{74}$ . The spin of the ground state of  $\text{Br}^{74}$  is not known, but all other even mass Bromine isotopes have ground state spins of  $1^+$ , we assume that the spin of  $\text{Br}^{74}$  ground state is  $1^+$ . As such only the positron transitions to the ground state of  $\text{Se}^{74}$  ( $0^+$ ) and the two  $2^+$  states are allowed, while the transition to the  $4^+$  state is a second forbidden one. The transition to the second  $0^+$  state is an allowed one. However the transition to the ground state is much more favoured energetically. In  $\text{Se}^{76}$  only the  $2^+$  state in the two phonon multiplet is populated by positron decay from the ground state of  $\text{Br}^{76}$ . Less than 0.4% of the decay from  $\text{Br}^{78}$  ground state go to the two phonon multiplet in  $\text{Se}^{78}$ . The transition if any, from the second  $2^+$  state to the ground state would be retarded. A search was made for this gamma ray, but it was not observed. The absence of this cross-over transition

rendered further support to the collective vibrational model description of this nucleus.

It seems that it is difficult to populate too many excited levels of  $\text{Se}^{74}$  by positron decay of  $\text{Br}^{74}$ . Negatron decay from  $\text{As}^{74}$  ground state (spin  $2^-$ ) has only showed the 634 keV transition. A more suitable method would be to excite the levels of  $\text{Se}^{74}$  with direct reactions and then study the subsequent gamma rays. The spins and parities can be determined by analysing the corresponding angular distributions and performing coupled channel DWBA calculations.

Figure 8.1- Half life curves of the 633.9, and  
the 732.1 keV lines. The half life  
in each case is  $42 \pm 4$  min.



CHAPTER IX  
-----Summary  
-----

A 25 c.c. Ge(Li) detector was acquired for gamma spectroscopy measurements. Its absolute photopeak efficiencies for gamma rays of different energies with various source-detector geometries were determined utilising standard gamma ray sources of known strengths. The best resolutions obtained with this detector were 2.0 keV FWHM for Co<sup>57</sup> (122 & 136 keV) lines and 2.9 keV FWHM for Co<sup>60</sup> (1.17 & 1.33 MeV) lines. For gamma-gamma coincidence measurements a fast-slow coincidence system was set up with standard ORTEC modules. The resolving time of the system could be varied from 10 ns to 110 ns.

For charged particle (positrons and electrons) measurements, Si(Li) detectors were used. To house the detector for beta spectroscopic measurements, a special chamber called the "Mini-chamber" was designed and constructed. This chamber enabled the Si(Li) detector and the beta ray source to be kept in the same vacuum chamber without any intervening window while maintaining the detector at liquid nitrogen temperature. Provisions were also made so that a gamma ray detector could be placed outside a thin window of the mini-chamber for beta gamma coincidence experiments and internal conversion measurements.

Gamma rays subsequent to the positron decay of  $\text{Br}^{75}$  were studied. Seven gamma rays of energies 111.8, 140.9, 286.5, 377.3, 427.9 and 431.6 keV were observed. The half life of the ground state of  $\text{Br}^{75}$  was measured to be  $106 \pm 5$  mins. Different gamma-gamma coincidence experiments were performed using a 7.6 cm by 7.6 cm NaI(Tl) scintillation counter together with the 25 c.c. Ge(Li) detector.

The positron spectrum from the decay of  $\text{Br}^{75}$  ground state was recorded with a 5 mm Si(Li) detector and the endpoint energies of the different branches were determined with the help of a Computer program which did the Fermi-Kurie plots. The positron spectrum in coincidence with the 286.5 keV gamma ray was also recorded and the corresponding Fermi-Kurie plot was constructed.

The sum spectrum of the gamma rays from  $\text{Br}^{75}$  was also studied with a RCA  $4\pi$  Ge(Li) detector. Intensity measurements on the singles and the different coincidence spectra were performed and the results were utilised to construct the most probable decay scheme for  $\text{Br}^{75}$  and to determine the beta branching ratios. The endpoint energies of the different positron branches, together with the branching ratios and the half life of the decay, the  $\log(ft)$  values for the positron decays were determined. The possible spins and parities assigned to the different levels of  $\text{Se}^{75}$  are shown in details in Fig. 6.1.

Different theoretical descriptions of even-

odd nuclei in this mass region were considered. The latest formalism in terms of the coupling of a single particle to a  $2^+$  phonon even-even core was discussed. The qualitative agreements and disagreements of the experimental observations with the predictions of this formalism were also touched upon.

While studying the gamma rays from  $\text{Br}^{75}$ , an isomeric transition of 107 keV with a half life of  $4.6 \pm 0.5$  mins. was observed. This level was identified as the first excited state in  $\text{Br}^{77}$ . The internal conversion coefficient for this transition was measured using a 1 mm Si(Li) detector and the 25 c.c. Ge(Li) detector. A previous measurement was confirmed and supplemented and the multipolarity of the transition was uniquely determined as E3.

Gamma rays following the positron decay of  $\text{Br}^{74}$  to the levels of  $\text{Se}^{74}$  were also studied. Two gamma rays with energies 633.9 and 732.1 keV were observed with a half life of  $42 \pm 4$  mins. Only the 633.9 keV line has been reported previously. These lines correspond to the levels at 633.9 keV ( $2^+$ ) and 1366 keV ( $2^+$ ). Relative positron decay branching ratios were determined.

APPENDIX  
-----

An outline of the method used for calculating branching ratios from the intensity measurements on the singles and the different coincidence spectra for the decay scheme of  $\text{Br}^{75}$  (Fig. 5.5) is presented.

Let  $n_1$  and  $\epsilon_1$  be proportional to the strengths of the positron and electron capture decays, respectively to the 859.1 keV level in  $\text{Se}^{75}$ . (See Fig. A1). Also let  $(n_2, \epsilon_2)$ ;  $(n_3, \epsilon_3)$ ;  $(n_4, \epsilon_4)$ ;  $(n_5, \epsilon_5)$ ;  $(n_6, \epsilon_6)$  and  $(n_7, \epsilon_7)$  denote the same quantities for the levels at 663.8, 579.4, 427.5, 286.5, 111.8 and 0 keV respectively. Let  $\alpha$  be the fraction of the 427.5 keV level decaying directly to the ground state.

The yields of the different gamma rays in the different spectra are shown below. The relevant steps for branching ratio calculations are also indicated.

A. Spectrum in coincidence with the 511 keV gamma ray  
-----

	Gamma ray keV	Yield
1	111.8	$n_6$
2	140.9	$(1-\alpha)(n_1+n_4)$
3	286.5	$(1-\alpha)(n_1+n_4) + n_2+n_3+n_5$
4	292.9	$n_3$
5	377.3	$n_2$

	Gamma ray keV	Yield
6	427.5	$\alpha (n_1 + n_4)$
7	431.6	$n_1$
8	511	The counters were placed at right angles. So a lot of 511 were eliminated. The feedthrough is due to imperfect geometry.

From the intensities of the different gamma rays in this spectrum,  $n_1$ ,  $n_2$ ,  $n_3$  and  $n_6$  can be computed directly. The quantity  $\alpha$  can be determined from A2 and A6. Once  $\alpha$  is determined  $n_4$  and  $n_5$  can also be computed.

#### B. Spectrum in coincidence with the 286.5 keV gamma ray

When the energy selection window in the NaI(Tl) counter is set jointly on the 286.5 and 292.9 keV lines, it is automatically set on the Compton tail of the 511 keV gamma ray, which is in coincidence with all the other gamma rays. As a result a feedthrough of the different gamma rays would be obtained and this feedthrough for each gamma ray would be proportional to its yield when the energy selection window was set on the 511 keV gamma ray. Let  $\beta$  denote the area of the Compton tail included in the window and  $\gamma$  denote the area of the photopeak of the 511 keV gamma ray. Let  $Y_{511}^x$  denote the yield of the gamma ray at

x keV when the window is set on the 511 keV photopeak.

Then the feedthrough in this case for a gamma ray of energy x keV would be

$$\frac{\beta}{\gamma} Y_{511}^x$$

While computing the yields of the different gamma rays, it should be remembered that a different source was used and so a source strength factor  $k_1$  should also be considered. According to this decay scheme, the yields are:-

	Gamma ray keV	Yield
1	111.8	0
2	140.9	$k_1 \left[ (1-\alpha)(n_1 + \epsilon_1 + n_4 + \epsilon_4) + \frac{\beta}{\gamma} Y_{511}^{140.9} \right]$
3	286.5	$k_1 \left[ (n_3 + \epsilon_3) + \frac{\beta}{\gamma} Y_{511}^{286.5} \right]$
4	292.9	$k_1 \left[ (n_3 + \epsilon_3) + \frac{\beta}{\gamma} Y_{511}^{292.9} \right]$
5	377.3	$k_1 \left[ (n_2 + \epsilon_2) + \frac{\beta}{\gamma} Y_{511}^{377.3} \right]$
6	427.5	0
7	431.6	$k_1 \left[ (1-\alpha)(n_1 + \epsilon_1) + \frac{\beta}{\gamma} Y_{511}^{431.6} \right]$
8	511	$k_1 \left[ (1-\alpha)(n_1 + n_4) + n_2 + 2n_3 + n_5 + \frac{\beta}{\gamma} Y_{511}^{511} \right]$

C. From B3 and B4,  $k_1 \frac{\beta}{\gamma}$  can be calculated as  $Y_{511}^{286.5}$  and  $Y_{511}^{292.9}$  are already known. Then from B8,  $k_1$  and  $\frac{\beta}{\gamma}$

can be separately calculated. Once these two quantities are known,  $\epsilon_1$ ,  $\epsilon_2$ ,  $\epsilon_3$  and  $\epsilon_4$  can be easily obtained from the other equations.

### C. Singles spectrum

---

Again a source strength factor  $k_2$  has to be considered. The yields are:-

	Gamma ray keV	Yield
1	111.8	$k_2 (n_6 + \epsilon_6)$
2	140.9	$k_2 \left[ (1 - \alpha) (n_1 + \epsilon_1 + n_4 + \epsilon_4) \right]$
3	286.5	$k_2 \left[ (1 - \alpha) (n_1 + \epsilon_1 + n_4 + \epsilon_4) \right. \\ \left. + (n_2 + \epsilon_2 + n_3 + \epsilon_3 + n_5 + \epsilon_5) \right]$
4	292.9	$k_2 (n_3 + \epsilon_3)$
5	377.3	$k_2 (n_2 + \epsilon_2)$
6	427.5	$k_2 \alpha (n_1 + \epsilon_1 + n_4 + \epsilon_4)$
7	431.6	$k_2 (n_1 + \epsilon_1)$
8	511	$2k_2 (n_1 + n_2 + n_3 + n_4 + n_5 + n_6 + n_7)$

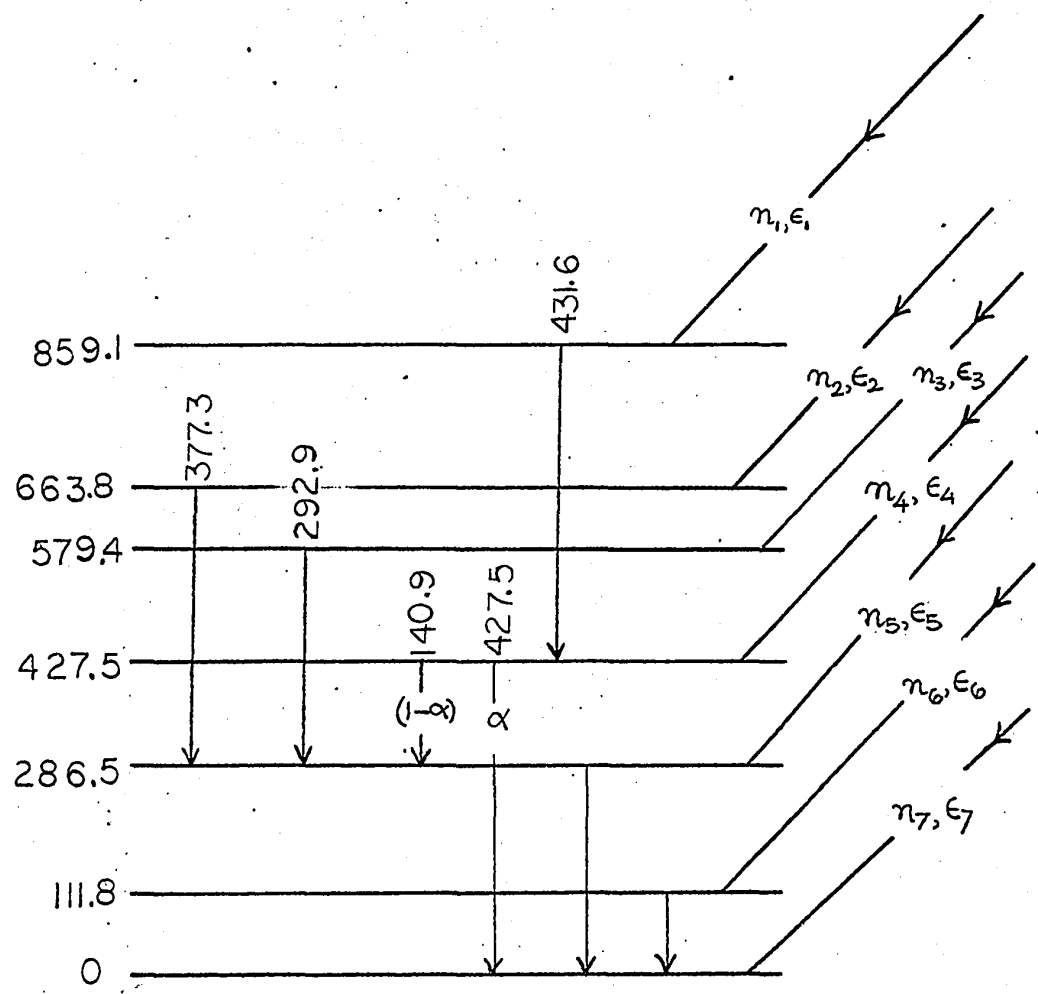
From each of the eqns. C2, C4, C5, C6 and C7  $k_2$

can be determined. These values can be checked for

consistency. Then  $n_7$ ,  $\epsilon_5$  and  $\epsilon_6$  can be determined from eqns.

eqns. C1, C3 and C8 respectively.

Figure A.1- Calculation of Branching ratios from intensity measurements. All energies are in keV.



$Se^{75}$

A.1

BIBLIOGRAPHY  
-----

1. Baskova, Vasilev, Chang & Shavtvalov- JETP; 14(1962) P. 1060
2. Beydon, Chaminade, Crut, Faraggi, Olekowsky & Papineau-  
Nucl. Phys.; 2(1957) P. 593
3. Buteмент & Boswell- J. Inorg. Nucl. Chem.; 16(1960) P. 102
4. Butler & Gossett- Bull. Am. Phys. Soc.; 2(Series 2)(1957)  
P. 230
5. De Shalit- Phys. Rev.; 122(1961) P. 1530
6. Eichler, O'Kelley, Robinson, Marinski & Johnson- Nucl. Phys.  
35(1962) P. 623
7. Elwyn, Landon, Oleksa & Glaso-- Phys. Rev.; 112(1958) P. 1200
8. Fultz & Pool- Phys. Rev.; 86(1952) P. 347
9. Gangrskii & Lemberg- JETP; 15(1962) P. 711
10. Goldhaber & Sunyer- Phys. Rev.; 83(1951) P. 906
11. Goswami & Nalcioglu--- Preprint; 1968
12. Goswami & Sherwood- Nucl. Phys.; 89(1966) P. 465'
13. Goulding- Nucl. Instr. Meth.; 43(1966) P. 1
14. Gurfinkel & Notea- Nucl. Instr. Meth.; 57(1967) P. /173
15. Houdayer, Mark & Bell- Nucl. Instr. Meth.; 59(1968) P. 319
16. Ikegami & Sano- Phys. Lett.; 21(1966) P. 323
17. Kisslinger & Sorensen- Rev. Mod. Phys.; 35(1963) P. 853
18. Kuchela- Ph. D. thesis (unpublished); McGill University  
1968.
19. Lederer, Hollander & Perelman- Table of Isotopes; John  
Wiley (Sixth Edition); 1967

20. Lessard- M.Sc. thesis (unpublished); McGill University  
1966
21. Lindgreen- Table of Nuclear Spins & Moments; Alpha, Beta  
& Gamma Ray Spectroscopy, North Holland; Edited by  
Siegbahn; 1964
22. Lobkowicz & Marmier- Helv. Phys. Acta.; 34(1961) P. 85
23. Mayer- Nucl. Instr. Meth.; 43(1966) P. 55
24. Muszynski- M.Sc. thesis (unpublished); McGill University  
1968
25. Perdrisat- Rev. Mod. Phys.; 38(1966) P. 41
26. Seeger- Nucl. Phys.; 25(1961) P.1
27. Siegbahn- Alpha, Beta & Gamma ray Spectroscopy; North  
Holland; 1968
28. Sliw & Band- Table of Internal Conversion Coefficients;  
Alpha, Beta & Gamma ray Spectroscopy; North Holland; 1968
29. Temmer & Heydenburg- Phys. Rev.; 104(1956) P. 967
30. Thulin- Arkiv. Fysik.; 9(1955) P. 137
31. Verrall, Hardy & Bell- Nucl. Instr. Meth.; 42(1966) P. 258
32. Wapstra, Nijgh & Van Lieshout- Nucl. Spectroscopy Tables;  
North Holland; 1959
33. Woodward, McCowan & Pool- Phys. Rev.; 74(1948) P. 870